Experimental Investigations of Combustion Chamber Heat Transfer in a Light-Duty Diesel Engine

Dahlström, Jessica

2016

Document Version:
Publisher's PDF, also known as Version of record

Experimental Investigations of Combustion Chamber Heat Transfer in a Light-Duty Diesel Engine

Experimental Investigations of Combustion Chamber Heat Transfer in a Light-Duty Diesel Engine

by Jessica Dahlström

LUND
UNIVERSITY

Thesis for the degree of Doctor of Technology
Thesis advisors: Prof. Öivind Andersson, Ass.Prof. Martin Tunér
Faculty opponent: Sebastian Verhelst

To be presented, with the permission of the Faculty of Engineering of Lund University, for public criticism in the M:B lecture hall at the Department of Energy Sciences on Friday, the 3rd of June 2016 at 10:00.

Organization
LUND UNIVERSITY

Department of Energy Sciences
Box 118
SE–221 00 LUND
Sweden

Document name
DOCTORAL DISSERTATION

Date of disputation
2016-06-03

Sponsoring organization

Author(s)
Jessica Dahlström

Title and subtitle
Experimental Investigations of Combustion Chamber Heat Transfer in a Light-Duty Diesel Engine

Abstract
This work concerned experimental studies of heat transfer in a light-duty diesel engine. Combustion is affected by several parameters, such as pressure, engine speed, mass of injected fuel and in-cylinder gas flow. These parameters are in turn affected by the combustion chamber geometry and fuel spray characteristics. At high load the exhaust heat was increased more than at high engine speed. Swirl was found to speed up the combustion event and increased heat loss to the piston cooling, but had no measurable effect on exhaust heat loss. Exhaust gas recirculation (EGR) diverts part of the exhaust gas and mixes it with intake air. The recirculated gas acts as a heat sink and reduces in-cylinder temperatures and thus, heat losses. The air-fuel ratio is another important factor. More air resulted in faster combustion while also increasing exhaust gas temperature. Altering the combustion chamber geometry affected both in-cylinder gas flow and mixing. A more open and shallow design was found to redistribute heat losses from cooling media to exhaust. The original injectors were proven to have a higher fuel flow than the two other configurations, but faster combustion and less heat in the exhaust was mainly found with the injectors with fewest holes.

Hot exhaust gases could be more useful than hot cooling media, because that heat may be extracted and used to improve engine efficiency. This reduces fuel consumption, and consequently emissions of greenhouse gases, which contribute to global warming. The world energy demand is still increasing, and more natural resources are being used. Higher efficiency requires less fuel, and thereby reduces the impact on environment and humanity.

The work was performed in a 4-cylinder light-duty diesel engine. Temperatures and mass flow measurements were performed in cooling media and exhaust gas. From these calculations were executed to find out the heat fractions emitted to each medium. Two combustion chamber geometries and three injectors were tested and compared with respect to their impact on combustion and heat losses.

Key words
heat transfer, internal combustion engine, compression ignition, diesel combustion

Classification system and/or index terms (if any)

Supplementary bibliographical information

Language
English

ISSN and key title

ISBN
978-91-7623-828-8 (print)
978-91-7623-829-5 (pdf)

Recipient's notes

Number of pages
137

Price

Security classification

Experimental Investigations of Combustion Chamber Heat Transfer in a Light-Duty Diesel Engine

by Jessica Dahlström

LUND
UNIVERSITY

A doctoral thesis at a university in Sweden takes either the form of a single, cohesive research study (monograph) or a summary of research papers (compilation thesis), which the doctoral student has written alone or together with one or several other author(s).

In the latter case the thesis consists of two parts. An introductory text puts the research work into context and summarises the main points of the papers. Then, the research publications themselves are reproduced, together with a description of the individual contributions of the authors. The research papers may either have been already published or are manuscripts at various stages (in press, submitted, or in draft).

Funding information: The thesis work was financially supported by Volvo Car Corporation and the Swedish Energy Agency.

Faculty of Engineering, Department of Energy Sciences

ISBN: 978-91-7623-828-8 (print)
ISBN: 978-91-7623-829-5 (pdf)
ISRN: LUTMDN/TMHP-16/1117-SE
ISSN: <0282-1990>

Printed in Sweden by Tryckeriet i E-huset, Lund University, Lund 2016

To my family:
Joacim, Joel, Alve and Leo

Contents

List of publications

This thesis is based on the following publications, referred to by their Roman numerals:

I **Effects of Spray-Swirl Interactions on Heat Losses in a Light Duty Diesel Engine**

J. Dahlström, Ö. Andersson, M. Tunér, H. Persson
ASME Proceedings, 10.1115/IMECE2015-53606

II **Experimental Comparison of Heat Losses in Stepped-Bowl and Re-Entrant Combustion Chambers in a Light Duty Diesel Engine**

J. Dahlström, Ö. Andersson, M. Tunér, H. Persson
SAE Technical Papers 2016-01-0732

III **Experimental Comparison of Heat Losses in a Light Duty Diesel Engine with Various Injector Geometries**

J. Dahlström, Ö. Andersson, M. Tunér, H. Persson
Draft

Other publications

IV **Reducing the Cycle-Cycle Variability of a Natural Gas Engine Using Controlled Ignition Current**

P. Tunestal, B. Johansson, **J. Dahlström**
SAE Technical Papers 2013-01-0862

V **Experimental Evaluation of a Novel High Frequency Ignition System Using a Flow-Reactor Set-up**

A. Schönborn, P. Tunestal, B. Johansson, **J. Dahlström**
SAE Technical Papers 2013-01-2564

Acknowledgements

There are so many people who, in their own ways, have helped me come this far. I would like to express my gratitude to my main supervisors during my two projects: Per Tunestål and Öivind Andersson. They are completely different personalities, but are both very helpful and knowledgeable. It has been an honour to work with such a supportive supervisor as Öivind, who also shares my love of books. Thank you for rewarding discussions about Stephen King novels and suggesting other interesting authors to read. I will definitely read more Neil Gaiman from now on!

I want to say a big thank you to my former and present fellow PhD students: Mehrzad for helping me getting settled with my first engine, Ashish for great cooperation with the same engine and lots of fun private discussions. Ida, Hadeel, Mengqin, and Maja for being great colleagues and standing up for equal rights. You made going to work so much more fun and you've got Girl Power! I would also like to thank Prakash and Helgi.

Thank you Pablo for working so hard to make our common test cell functional and the great cooperation on our engine. Another thank you goes to Håkan at Volvo Cars for being patient and helpful with all our questions regarding the engine. And of course a big thank you to our fantastic team of technicians, especially Mats, Tommy, Anders and Tomas. Without your help this work would have been impossible to finish!

At last I want to thank my family for all your love and support. I would not even have been able to get my Master of Science, let alone a PhD, without all the help with babysitting and taking children to their various activities! So thank you Gun-Britt and Janne for being the most supportive parents and grandparents anyone could wish for! To my husband Joacim and our sons Joel, Alve and Leo I want to say that I am so privileged to have you in my life. Through ups and downs, we always come out stronger as a family than ever before. I love you so much!

Populärvetenskaplig sammanfattning på svenska

Detta arbete handlade om att studera värmeförlusterna i en dieselmotor, och hur de påverkas när olika förbränningssystemparametrar ändras. Förbränningen i cylindern påverkas t.ex. av hur högt trycket är, hur snabbt motorn arbetar, hur mycket bränsle som sprutas in och hur gasen rör sig i cylindern. Dessa saker påverkas i sin tur av formen på förbränningsrummet, det slutna utrymme där förbränningen sker, och hur bränslesprayen ser ut och beter sig under insprutningen. Vid hög last, då motorn får arbeta hårt med mycket bränsle, ökade energin i avgaserna mer än vid hög hastighet. Swirl, en roterande gasrörelse runt cylinderaxeln, snabbade upp förbränningsförloppet och ökade värmeförlusterna till kolvkylningen något, men hade ingen mätbar effekt på avgasenergin. Exhaust gas recirculation (EGR) innebär att en del av avgaserna förs tillbaka och blandas med den luft som sugs in i cylindern. Dessa gaser deltar inte i förbränningen som syret i luften gör, men absorberar en del av värmen som frigörs vid förbränningen vilket sänker temperaturen i cylindern och minskade värmeförlusterna generellt. Mängden luft i förhållande till mängden bränsle är en annan viktig faktor. Ökad luftmängd gav snabbare förbränning, samtidigt som avgasenergin ökade. Ändring av förbränningsrummets form påverkar både hur gasen rör sig i cylindern och hur väl bränsle och luft blandas. En grundare och mer öppen design visade sig kunna omfördela värmeförluster från kylmedier till avgaser. Originalinsprutarna visade sig i de flesta fall ge högre bränsleflöde än de två andra varianterna, vilket resulterade i snabbare förbränning och mindre värme i avgaserna.

Är det då bättre med varma avgaser än varm kylvätska? Svaret är ja, för värmeenergi i avgaserna kan tas tillvara och användas för att göra motorn effektivare. Effektivare motorer minskar bränsleförbrukningen, och därmed också utsläpp av ämnen som kan vara skadliga för miljön, exempelvis växthusgaser som bidrar till den globala uppvärmningen. Världens energibehov ökar ständigt, vilket leder till större utnyttjande av våra naturtillgångar. Genom att energieffektivisera krävs mindre bränsle, därmed minskas även påverkan på naturen och i förlängningen oss människor.

Arbetet bedrevs genom experiment i en 4-cylindrig dieselmotor avsedd för personbilar. Temperaturer och massflöden uppmättes i motorns kylmedier och avgaser. Med hjälp av dessa beräknades hur mycket energi som avgavs till respektive medium. Olika parametrar som kan påverka förbränningsförloppet varierades för att se vilken inverkan de hade. Två olika kolvgeometrier och tre insprutare med olika antal hål testades och jämfördes.

Experimental Investigations of Combustion Chamber Heat Transfer in a Light-Duty Diesel Engine

Chapter 1

Introduction

The world energy consumption is increasing, although the sources of energy are limited. New technologies must be developed to achieve a sustainable world community where humans, animals and plants can live together without endangering each other. Still today the largest part of the consumed energy comes from oil. 2013 this part was 39.9% while the second largest energy source was natural gas at 15.1% [25]. The natural gas part has stayed at almost the same percentage since the 1970's, while the oil part has receded from 48.3% to its current value. The increase in energy consumption is largely due to the developing countries increasing their standard of living, OECD countries only increased their energy consumption slightly during this period and although they still are the major users, their part of the total consumption decreased from 60.3% to 39.1% between 1973 and 2013 [25].

The increase in fossil fuel consumption unfortunately also results in increased emissions of greenhouse gases such as carbon dioxide (CO_2), which contribute to global warming. Emissions of CO_2 have become an important measure of how environmentally friendly a product is, but also methane is considered a very aggressive greenhouse gas. To a very high extent this concerns the internal combustion engine (ICE). In 2013 just over 23% of the world energy consumption was used by the transport sector, so there is an indisputable need to reduce fuel consumption. Along with that, the emissions legislations become increasingly stringent which is an important focus area for engine research and development. There are different paths to increase engine efficiency, and thereby decrease fuel consumption and emissions. To increase efficiency measures must be taken to reduce engine losses, and that forms the basis for this work.

1.1 Engine heat loss

One of the greatest contributors to engine energy losses is heat loss. Almost one third of the heat released during combustion is lost to cooling media and exhaust gases, thus

dominating the ICE energy balance. Where the ICE heat losses are found are discussed in more detail in Chapter 2. Many attempts have been made to study and understand the causes of these heat losses and what amendments could be done, mainly through simulations but also through experimental work. The processes affecting heat losses to the walls are complex. Large-scale gas motions, local turbulence levels, spray-wall interaction, heat release as well as other parameters all play a role. This complexity means that the problem needs to be broken down to be able to systematically develop an understanding of the system. So far, a significant part of the work concerning heat transfer in internal combustion engines has been concentrated on new combustion concepts such as homogeneous charge compression ignition (HCCI) and partially premixed combustion (PPC), which show promising results regarding reduced heat transfer. The development of diesel engines is mainly towards higher specific power, resulting in more released heat per unit displacement volume. This is usually achieved through downsizing, which results in higher mechanical efficiency, but at the same time also higher combustion temperatures that increase heat losses. However, there is still room for improving heat transfer characteristics also in conventional diesel combustion (CDC).

1.2 Objective

Many engine parameters have been studied regarding their effect on heat transfer to the combustion chamber walls, but there are still areas which have yet to be examined. This work concerns the effects of different combustion chamber and spray parameters on heat transfer in CDC mode. Few examples can be found in the literature regarding interactions between spray parameters and in-cylinder flow patterns. In this area mainly numerical simulations have been published. The drawback with these is that it is difficult to know if the models recreate realistic conditions with respect to turbulence and combustion. In this project empirical studies are used to find out how different combustion system parameters and their interactions affect heat losses in a light duty (LD) diesel engine.

1.3 Method

In order to analyse engine heat transfer experimentally, a number of thermocouples and flow meters were installed in a Volvo LD diesel engine. The engine was operated at different conditions while varying combustion chamber geometry and spray parameters. The energy balance was set up to find out how much heat was lost to the cooling media in different parts of the engine, and heat release calculations were performed based on in-cylinder pressure measurements.

1.4 Contributions

The presented work has contributed to the understanding of how piston bowl geometry, swirl, different spray parameters, and interactions between these contribute to the combustion chamber heat transfer characteristics. It was also established how speed, load, rail pressure, EGR, and λ affect heat transfer. The main conclusions are the following:

- It was found that applying different injection strategies did not generate much differences in heat transfer, so the injection strategy can be optimised to suit other purposes like reducing emissions or noise.
- The parameter sweeps showed that load has greater importance for heat losses than speed. Rail pressure affects combustion duration and thus the portions of the heat going to the various losses. Swirl seems less important for heat transfer than most previous research shows. EGR lowers temperature and prolongs combustion, rearranging heat losses from piston to cylinder head cooling. Increasing λ reduces combustion duration and thus puts the heat losses earlier in the cycle.
- A wider and shallower piston bowl geometry, here the stepped-bowl, reduced combustion duration and usually increased exhaust losses.
- Injectors with different numbers of holes gave different combustion durations, shorter for less holes and longer for larger hole numbers. Larger number of holes increased exhaust heat loss.

Chapter 2

Heat transfer and heat losses

In internal combustion engines fuel is fed to the system, and then the fuel energy is converted to work on the piston. In the ideal case all of this heat released in the process would be converted to useful work. Why then is the engine efficiency usually only 30-40%? The aim of this chapter is to sort out the most important factors that reduce engine efficiency, and describe the theory behind heat transfer losses which is the focus of this work. This will serve as a background and base for the literature study presented in Chapter 3. One important factor affecting heat transfer in engines is the bulk flow, which is also described and discussed.

2.1 Engine energy balance

One of the first to investigate engine efficiency was Sadi Carnot, who presented his method to theoretically calculate efficiency in 1824. His closed cycle analysis assumes that the working fluid is restored to its original state after going through the intermediate steps. He defined a reversible and an irreversible cycle, and also showed that the reversible cycle was impossible. His thesis states that the maximum efficiency of a heat engine depends on the temperature difference between the beginning and the end of the expansion (power) stroke [12]. This is nowadays known as Carnot efficiency, and can be expressed as Equation (2.1), where W is work, Q_H is supplied heat, T_C and T_H denote the temperatures of the cold and hot fluid, respectively.

$$\eta_{Carnot} = \frac{W}{Q_H} = 1 - \frac{T_C}{T_H} \tag{2.1}$$

Unfortunately this maximum efficiency is not possible to achieve in reality. During the engine cycle there are several processes where heat is lost in different ways, which is demonstrated in the diagram in Figure 2.1. Describing where the heat goes in the

engine is facilitated by defining a mean effective pressure, MEP, relating the engine power and torque to the piston displacement. Starting from the top, FuelMEP denotes the chemical energy content of the fuel. FuelMEP is defined by Equation (2.2), where m_f is the fuel mass, Q_{LHV} is the lower heating value and V_D is the piston displacement.

$$FuelMEP = \frac{m_f Q_{LHV}}{V_D} \tag{2.2}$$

The fuel is then burned, and the chemical energy is converted to heat. The heat generated by the combustion process can be denoted Q_{in}, and then the heat mean effective pressure, QMEP, can be defined according to Equation (2.3).

$$QMEP = \frac{Q_{in}}{V_D} \tag{2.3}$$

Part of the fuel is left unburned or not fully oxidised, ending up as unburned hydrocarbons (HC) and carbon monoxide (CO) in the exhaust. This lost heat, Q_{CL}, can be expressed as Combustion Loss MEP, CLMEP, as described by Equation (2.4).

$$CLMEP = \frac{Q_{CL}}{V_D} = FuelMEP - QMEP \tag{2.4}$$

Now that heat has been extracted from the fuel, it needs to be converted into mechanical work through a thermodynamic cycle. This indicated work, W_i, can be calculated by integrating the in-cylinder pressure p over the in-cylinder volume V. Dividing W_i by V_D will give in the indicated mean effective pressure, IMEP, see Equation (2.5).

$$IMEP = \frac{W_i}{V_D} = \frac{1}{V_D} \oint p dV \tag{2.5}$$

There are two versions of IMEP: IMEP_g and IMEP_n. The former results from integrating only over the compression and expansion strokes, and the latter from integrating over the complete engine cycle, four strokes. During this process some of the heat will be transferred to the cylinder walls and cooling media, denoted Heat Transfer MEP (HTMEP) in Figure 2.1. There will also be a portion of the heat lost to the exhaust gases, EXMEP.

During the gas exchange (exhaust and intake strokes) some work is also performed when the combusted gases are replaced with fresh air and in some cases also fuel. This can also be expressed as a mean effective pressure denoted PumpMEP (PMEP). As stated in Equation (2.6) this is the difference between IMEP_g and IMEP_n. In Equation (2.6) p_{exh} is the exhaust pressure and p_{in} is the intake pressure. Usually p_{in} is lower than p_{exh}, resulting in negative work during gas exchange.

$$PMEP = IMEP_g - IMEP_n = p_{exh} - p_{in} \tag{2.6}$$

Finally the work on the piston is transferred to the output shaft, and then frictional forces must be overcome. The engine output can be described as break mean effective pressure, BMEP, defined by Equation (2.7) where P is the engine power, N denotes engine speed and n_T is the stroke factor. The friction can also be described by a mean effective pressure, FrictionMEP (FMEP).

$$BMEP = \frac{P}{V_D \frac{N}{n_T}} \tag{2.7}$$

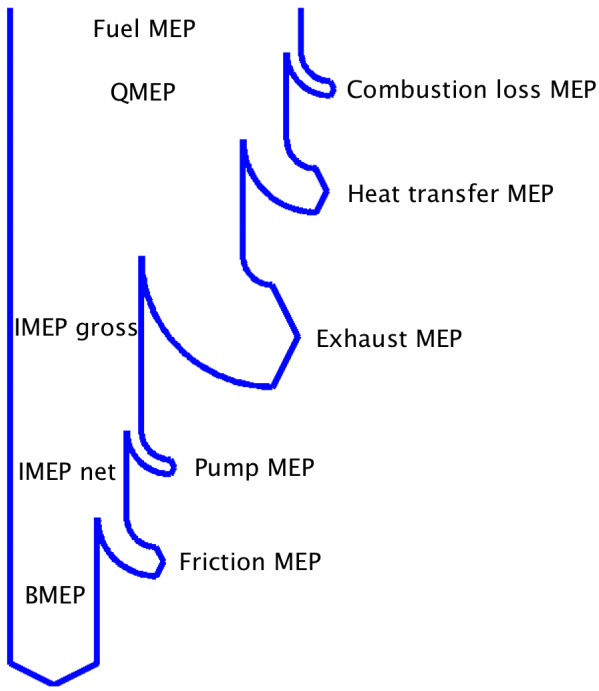

Figure 2.1: Sankey diagram showing the energy flow from fuel via the different steps in the engine cycle to useful work from the engine [26].

As Figure 2.1 shows, heat transfer is one of the major causes for loss in the IC engines, and thus reducing heat transfer should increase engine efficiency. Figure 2.2 shows common proportions of the different heat losses in CI and SI engines. In CI engines pumping losses are negligible compared to in SI engines, which are often throttled. Combustion losses are also lower in CI engines because they are always operated globally lean, as opposed to the often stoichiometric conditions in an SI engine. The throttling required in SI engines can even result in too little oxygen to burn all the fuel, which greatly impairs combustion efficiency. Throttling also impairs gas exchange, *e.g.* how efficiently the burned gas can be replaced by a fresh charge. CI engines are not limited by knock, which also gives them an advantage over SI engines because they can have

a higher compression ratio which improves efficiency. Another explanation is the fact that CI engines only compress air instead of a fuel-air mixture, and air has a higher γ value than fuel. γ is the ratio of specific heats and is described by Equation (5.9) in Chapter 5. However, there is still a considerable amount of energy lost to heat transfer in both engine types, affecting both engine performance, efficiency and emissions.

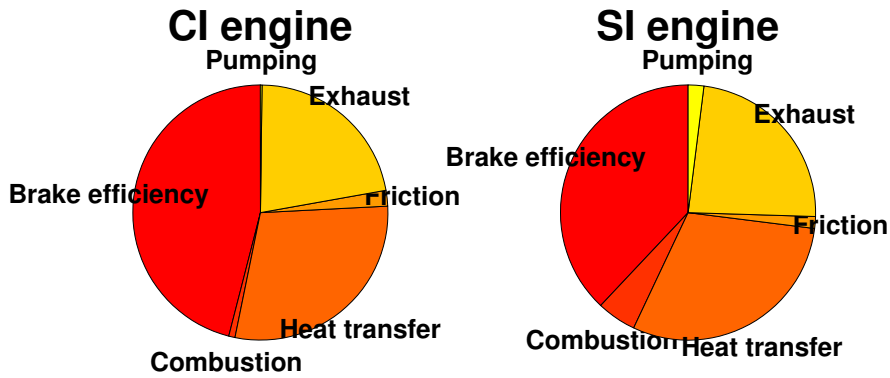

Figure 2.2: Proportions of fuel energy disappearing to losses, and what is left for work on the piston. The chart on the left shows a typical distribution for a CI engine, and the chart on the right shows the corresponding values for a typical SI engine.

2.2 Basic heat transfer theory

Heat transfer is the exchange of energy from a hot body to a colder body, and occurs through conduction, radiation and convection [51]. These will be described i section 2.2.1, 2.2.2 and 2.2.3, respectively.

2.2.1 Conduction

Heat conduction is heat diffusing through solids or static fluids through molecular movement, or electron movements in metals. Conduction can be described by Equation (2.8), also known as Fourier's law. q is the transferred heat, k is the thermal conductivity, and $\partial t/\partial n$ is the temperature gradient along the surface normal.

$$q = -k\frac{\partial t}{\partial n} \tag{2.8}$$

At the surface the fluid velocity is zero so only conduction can occur.

2.2.2 Radiation

Thermal radiation is emitted by a body due to its high temperature, and consists of electromagnetic waves, also called photons. Heat exchange through radiation does not need a media between the surfaces, and is actually maximum without any media in between [51]. Equation (2.9) is called the radiation equation, where σ is the Stefan-Boltzmann constant $5.67 \cdot 10^{-8} W/m^2 \cdot K^4$. The equation describes the heat flux from one black body at temperature T_1 to another at temperature T_2, without any heat absorbing material in between [23].

$$q = -\sigma(T_1^4 - T_2^4) \tag{2.9}$$

2.2.3 Convection

Convection occurs when a fluid flows along a body. The heat exchange between the surfaces of the fluid and the solid affects the macroscopic motion of the fluid. Convection can be natural due to density variations in the fluid, or forced by *e.g.* a pump or fan. The predominant heat transfer phenomenon in the engine cylinder is forced convection. Heat transfer in a fluid occurs through a combination of molecular heat conduction and inner energy transport via macroscopic motion. The inlet air stream produces fluid motion in the cylinder, which is enhanced and in some cases transformed by the oscillating motion of the piston and different combustion chamber properties. This will be further discussed in section 2.4.

To describe convection, a heat transfer coefficient, h_c, is introduced as in Equation (2.10). Here t_w is the wall surface temperature and t_∞ is the fluid temperature far from the wall.

$$q = -h_c(t_w - t_\infty) \tag{2.10}$$

Consider a solid body surrounded by a flowing fluid at a higher temperature than the body. Both in the body and in the fluid a temperature field results from the temperature difference. However, at the surface of the body the fluid velocity is always zero, and as mentioned above heat transfer can only occur by conduction. The heat flow, $\dot{Q}$, per unit area, A, can be described by Equation (2.11).

$$\frac{\dot{Q}}{A} = q = -k_f \left(\frac{\partial t}{\partial y}\right)_{y=0^+} = \left\{-k \left(\frac{\partial t}{\partial y}\right)_{y=0^-}\right\}_{body} \tag{2.11}$$

Then the heat transfer coefficient h_c in Equation (2.10) can be written as Equation (2.12).

$$h_c = \frac{q}{t_w - t_\infty} = \frac{-k_f \left(\frac{\partial t}{\partial y}\right)_{y=0^+}}{t_w - t_\infty} \tag{2.12}$$

h_c is a complex non-constant entity depending on the geometry of the body, the flow field and the physical properties of the fluid [51]. To determine h_c both the flow and temperature fields in the fluid need to be analysed. For this, the continuity equation, Navier-Stokes equations and the energy equation (first law of thermodynamics) are needed.

The continuity equation, Equation (2.13), expresses the conservation of mass. ρ is the density of the fluid, τ and u, v, w are the velocity components in the x, y, and z directions, respectively.

$$\frac{\partial \rho}{\partial \tau} + \frac{\partial(\rho u)}{\partial x} + \frac{\partial(\rho v)}{\partial y} + \frac{\partial(\rho w)}{\partial z} = 0 \tag{2.13}$$

The special case of steady, incompressible and two-dimensional flow yields Equation (2.14)

$$\frac{\partial u}{\partial x} + \frac{\partial v}{\partial y} = 0 \tag{2.14}$$

Equation (2.13) implies that the sum of the mass in the volume element $dxdydz$ and the net in- and outflowing mass is constant, and can, thus, be said to make up a system.

The heat transfer theory can be expanded to three dimensions, describing the Navier-Stokes equations and so on. However, that is beyond the scope of this work which focuses on experimental investigations.

2.3 In-cylinder heat transfer

Analysing heat losses in engines presents a need for a properly working heat transfer model. As mentioned in section 2.2, the exact mathematical description of heat transfer from an unsteady, turbulent flowing gas to a cylinder wall is quite complicated. Conditions are difficult to measure and the influencing factors may still be insufficiently known. Several attempts have been made over the years to find empirical models of the heat transfer coefficient h_c to describe engine heat losses and how they depend on in-cylinder pressure and temperature. Common examples are the heat transfer correlations of Nusselt, Eichelberg, Annand, Woschni, and Hohenberg, which have been used for calculating instantaneous average heat transfer coefficients. Nusselt first attempted to describe in-cylinder heat transfer in 1923, based on experiments in a spherical combustion vessel [37]. The next important contribution came 1939 when Eichelberg

published his formula for estimating instantaneous heat transfer, which has been used extensively for predicting heat transfer in large-scale two- and four-stroke engines [59].

Annand's heat transfer model, originally published in 1963, is confined to heat transfer during the compression and expansion stroke, thus excluding the gas exchange period. He considered it unreasonable to expect that the radiation factor during the combustion and expansion processes could be accurately calculated. With the knowledge of those days, its variation with crank angle also seemed impossible to predict. Annand concluded that the best that could be done was to empirically determine an average factor for the entire combustion-expansion phase [5]. The correlation was based on thermocouple measurements in the cylinder head only, but has been used to estimate instantaneous heat fluxes for the whole combustion chamber. The compression stroke heat transfer is assumed entirely convective, while during the expansion stroke both convective and radiative heat transfer is included [5]. Annand's model is given by Equation (2.15), where the first term on the right hand side corresponds to heat transfer due to convection and the second term is the radiative contribution. B is the cylinder bore, a is a constant varying with charge motion intensity and geometry and Re is the Reynolds number defined by Equation (2.19). In this case the characteristic velocity v is the mean piston speed $\bar{S}_p$, and the characteristic length L is set equal to B. k and μ are the thermal conductivity and dynamic viscosity, respectively, as in section 2.2. A is defined as the surface area exposed to heat transfer. The constant c before the radiation term is zero during compression [5]. With normal combustion, $0.35 \leq a \leq 0.8$ and $b = 0.7$, a increases with charge motion intensity [5, 23].

$$\frac{q}{A} = \frac{ak}{B} \left(Re\right)^b \left(T - T_w\right) + c\left(T^4 - T_w^4\right) \tag{2.15}$$

The gas properties are evaluated based on the average in-cylinder charge temperature, $\bar{T}_g$, defined by Equation (2.16). p is the in-cylinder pressure, V is the volume, m is the charge mass, M is the molecular weight and $\widetilde{R}$ is the universal gas constant.

$$\bar{T}_g = \frac{pVM}{m\widetilde{R}} \tag{2.16}$$

As indicated above, the effects due to differences in geometry and flow pattern are integrated in the proportionality constant a.

In 1967, Woschni published a new heat transfer model. Similar to Annand, he assumed that the convective heat transfer obeys the law in Equation (2.17), where Nu is the Nusselt number, described by Equation (2.18) and Re is the Reynolds number [57]. The constant C and exponent m are determined experimentally.

$$Nu = CRe^m \tag{2.17}$$

The Nusselt and Reynolds numbers are described by Equations (2.18) and (2.19), respectively [23]:

$$Nu = \left(\frac{h_c L}{k} \right) \tag{2.18}$$

$$Re = \left(\frac{\rho v L}{\mu} \right)^m \tag{2.19}$$

L and v are a characteristic length and velocity, and the exponent m is a constant. The density, viscosity and conductivity of the gas can be expressed as functions of pressure, resulting in Equation (2.20) where w is the local average in-cylinder gas velocity.

$$h_c = C L^{m-1} p^m w^m T^{0.75-1.62m} \tag{2.20}$$

Because the gas velocity is not known, it is approximated by the mean piston speed, $\bar{S}_p$. Thus, for a motored engine where gas velocity is only affected by piston motion, it can be written as Equation (2.21).

$$w = C_1 \bar{S}_p \tag{2.21}$$

However, in the fired case h_c shows a dependence on the pressure difference between the fired and the motored case, $(p - p_m)$. This should be multiplied with the cylinder volume, V, and related to the weight of the charge through the ideal gas law. To take this into account, Woschni added a second term to w which resulted in Equation (2.22) [57].

$$w = \left[C_1 \bar{S}_p + C_2 \frac{V_d T_r}{p_r V_r} (p - p_m) \right] \tag{2.22}$$

V_d is the displaced volume, p is the instantaneous cylinder pressure, and p_r, V_r, and T_r are the pressure, volume, and temperature of the working gas at some reference point. This could be *e.g.* inlet valve closing or start of combustion. The constants C_1 and C_2 are determined empirically to adapt the model to the current engine. Woschni finally arrived at Equation (2.23). He later used this to determine the heat transfer coefficients for different parts of the piston in a diesel engine [58].

$$h_c = C B^{-0.2} p^{0.8} T^{-0.53} w^{0.8} \tag{2.23}$$

The Hohenberg heat transfer model presented in 1979 [24] applies to diesel engines. Hohenberg states that for the compression phase the result of Woschni's equation is too low, which is somewhat compensated by the combustion term being too high [24]. Hohenberg starts with Woschni's Equation (2.23), and the general heat transfer equation. His expression is described by Equation (2.24), where A is the corrected cylinder wall area from Equation (2.26) and T_g is the gas temperature.

$$\dot{Q} = h_c A \left(T_g - T_w\right) \tag{2.24}$$

The main differences between Woschni's and Hohenberg's final models are the expression for the in-cylinder gas velocity, w, and the replacement of the cylinder bore, B, with the diameter $\bar{D}$ of a spherical volume corresponding to the cylinder volume. $\bar{D}$ is defined by Equation (2.25), where V_c is the cylinder volume and C is a constant different from the C in Equation (2.23). The term $B^{-0.2}$ was assumed to describe the effect of the cylinder diameter on mass flow close to the wall. Hohenberg argued that since the cylinder volume changes periodically with crank angle, a constant has only limited use in describing this effect.

$$\bar{D}^{-0.2} = C V_c^{-0.06} \tag{2.25}$$

Hohenberg's model also accounts for the effect of the piston top land by adding 30% of the top land area to the combustion chamber surface according to Equation (2.26).

$$A = A_{comb.chamber} + 0.3 A_{topland} \tag{2.26}$$

Equation (2.26) is plugged into Equation (2.24) and Equation (2.25) is used to substitute B in Equation (2.23). The final expression for h_c then becomes Equation (2.27). The constants C_1 and C_2 were determined experimentally for various DI diesel engines.

$$h_c = C_1 V_c^{-0.06} p^{0.8} T^{-0.4} \left(\bar{S}_p + C_2\right)^{0.8} \tag{2.27}$$

All of these heat transfer correlations have their benefits and disadvantages, and it is not generally established that one is better than the other. However, Woschni's model is widely used and acknowledged and was chosen for the heat release calculations in this work, for more details see Chapter 5.

2.4 In-cylinder flow and turbulence

The in-cylinder fluid flow strongly affects the combustion process in both SI and CI engines. It affects mixing, flame speed, and also heat transfer. The intake port geometry directs the jet flow to create a certain bulk flow pattern in the cylinder when interacting with the cylinder walls [23]. Fluid flow and turbulence are also influenced by valve timing and the shape of the combustion chamber. The latter will be discussed further in Chapter 3.

If the bulk flow rotates around an axis perpendicular to the cylinder axis, this is known as tumble. This is the predominant flow pattern in SI engines. In CI engines the bulk flow often rotates around an axis parallel to or coinciding with the cylinder axis, known

as swirl. The third bulk flow pattern is squish, which is a result of two surfaces moving towards each other so the fluid between them is pushed out [26]. The flow in an engine cylinder is unsteady and may vary substantially from cycle to cycle. It is characterised as irregular and random, and is usually defined using the mean velocity and different length scales. If the speed of the fluid motion in a cylinder is measured many times, the turbulence can be defined as the difference between the individual measurements and the mean velocity, $\bar{U}$, defined by Equation (2.28) [26]. N is the number of cycles and $\Delta\theta$ is the crank angle interval within which the samples are averaged to calculate the mean velocity.

$$\bar{U}(\theta, i) = \frac{1}{N} \sum_{\alpha=\theta-\frac{\Delta\theta}{2}}^{\alpha=\theta+\frac{\Delta\theta}{2}} U(\alpha, i) \tag{2.28}$$

The size of the largest eddies is limited by the system boundaries, and the smallest are limited by molecular diffusion. A measure of the largest eddies is the *integral scale*, l_I, meaning that two velocity measurements separated by a distance $x \gg l_I$ will show no correlation while a separation $x \ll l_I$ will be correlated [23]. The integral length scale is defined as the integral of the autocorrelation coefficient of the velocity at two adjacent points with respect to the distance between them, as shown by Equation (2.29), where R_x is the autocorrelation coefficient.

$$l_I = \int_0^\infty R_x dx \tag{2.29}$$

R_x is defined in Equation (2.30), where N_m is the number of measurements, and u is the fluctuating velocity component [23]. At very small distances R_x will be 1, while gradually reducing to 0 at large distances.

$$R_x = \frac{1}{N_m - 1} \sum_{i=1}^{N_m} \frac{u(x_0)u(x_0 + x)}{u(x_0)u(x_0)} \tag{2.30}$$

Within this large scale flow, there are smaller eddies of different sizes resulting from the breakdown of larger eddies. Dissipation of energy to heat occurs in the smallest eddies, with sizes indicated by the *Kolmogorovscale*, l_K. It is defined by Equation (2.31), using the kinematic viscosity, ν, and the dissipation per time and mass unit, ε.

$$l_K = \left(\frac{\nu^3}{\varepsilon}\right)^{1/4} \tag{2.31}$$

The *microscale*, l_M, describes the most energetic eddies and can be derived from the second order derivative of the auto correlation coefficient at zero separation as Equation (2.32) [26].

$$l_M = -\frac{2}{\left(\frac{\partial^2 R_x}{\partial x^2}\right)} \tag{2.32}$$

The importance of flow patterns and turbulence for the combustion process differs between SI and CI engines, even between different types of SI and CI engines. In an SI engine the main purpose is to wrinkle and stretch the flame front to enhance and speed up combustion. Engines with conventional diesel combustion (CDC) also use bulk flow and turbulence to enhance fuel and air mixing and prevent overly rich zones which are well known to produce soot. In addition, the spray itself generates fluid motion when injected. In this work different combustion chamber geometries are investigated using different swirl levels, to find out how these interact with the spray. This interaction is anticipated to influence heat transfer, and the literature study presented in Chapter 3 reveals that this has not been widely studied before.

Chapter 3

Review of the field of heat transfer

As demonstrated in Chapter 2, heat transfer in internal combustion engines is a complicated topic. Nevertheless, researchers all over the world put great effort into theoretical as well as experimental studies of the mechanisms behind and effects of in-cylinder heat transfer. This is a very important aspect of engine development, due to its effect on the integrity of engine parts, engine performance, emissions, turbocharger design, and ancillary cooling equipment. In the literature reports can be found concerning insulated combustion chambers, effects of turbulence and both combustion chamber geometry and spray parameters, to name just a few examples. These and other interesting views on heat transfer will be reviewed in this chapter to find out what has been done, and where there are perspectives missing in the literature.

3.1 Low heat rejection engines

One way of reducing heat losses and trying to increase efficiency is designing low heat rejection (LHR) engines, where a ceramic coating is applied to the combustion chamber walls to minimise heat transfer. Over the years, both experimental and simulation work has been performed. However, reports concerning the effect of thermal barrier coatings on engine performance are contradictory and results depend on the type of engine as well as test conditions [22]. Cooling water loss is much lower in LHR engines compared to other engines [1], because the coat works as an insulator preventing heat from being conducted through the combustion chamber wall to the cooling media. Instead most of the heat stays inside the cylinder, resulting in increased exhaust temperatures [54, 22, 52]. Also volumetric efficiency decreases as the hotter walls and residual gas decrease the density of the intake air [54, 22, 52], but this problem can be overcome through increased boost pressure from the turbocharger [52]. The main benefits have been

improved fuel economy and thermodynamic efficiency, and increased engine power and brake torque [10, 22, 52, 35, 44, 41, 2, 1]. Brake torque and power increased between 1 and 8%. Specific fuel consumption was reported to decrease 5-20%, the highest numbers at high load conditions. Brake thermal efficiency was found to increase 10-15%. Several authors report that the heat balance indicates that some of the heat wasted in conventional engines can be utilised to increase brake power in the coated engines. This seems especially beneficial for LHR engines operated with biodiesel, eucalyptus oil, and other renewable fuels [35, 41, 2, 1]. This is an important research area for adapting world energy consumption to more sustainable energy sources and prevent further climate change. An additional benefit with ceramic coatings is that they show better wear characteristics than conventional materials. However, just like conventional combustion systems LHR engines need the correct combination of injector parameters and combustion chamber design to achieve high efficiency engine operation [13].

In some cases emissions have been found to improve. Lower CO, HC [54, 35, 2] and soot emissions [54] have been reported, as well as lower NO_x [35, 44, 2]. On the other hand, increased NO_x emissions due to the increased temperature [54] have also been reported. There are also discrepancies in the literature regarding unburned hydrocarbons (HC) and soot emissions, which in some cases have been found to increase compared to uncoated engines, [54, 10, 2]. One explanation could be quenching effects due to the porous and rough surface of the coating [10].

However interesting insulated combustion chambers may be, the focus of this project is reducing heat losses through altering combustion system parameters, not the combustion chamber materials. It would be too much to include both, and the coating technology is yet too far from application in a production engine. Also, as mentioned above, test results are contradictory. As the following sections will show there is evidence of great improvements being feasible in CDC, which are also much easier to apply to a production engine in the near future. Then the heat losses could be directed to the exhaust gases, where the heat could be recovered by turbo charger and other waste heat recovery (WHR) systems.

3.2 Heat transfer models

Analysing heat losses in engines presents a need for a properly working heat transfer model. Many different factors affect heat transfer, even varying from one part of the cylinder to another. Several attempts have been made to find mathematical models that describe how heat losses depend on in-cylinder pressure and temperature. Some examples are the heat transfer correlations of Annand, Hohenberg, Woschni, Nusselt and Eichelberg, described in section 2.3. These are used for calculating instantaneous average heat transfer coefficients. Different heat transfer correlations lead to varying heat loss predictions. Predicted combustion behaviour also changes with different heat transfer coefficients. A large heat transfer coefficient results in too much heat loss, and improper characteristic velocity causes incorrect heat loss to the cylinder wall. The piston is in a downward and upward motion, so the instantaneous velocity changes across

the crank angle range. Instantaneous piston speed is minimum at TDC and BDC, and maximum in the middle of the stroke. In spite of this, heat losses are greatest around TDC. This can be explained by the large scale gas motion, which is enhanced by the piston motion and thereby also increases convection. The increased pressure also causes a temperature rise, which in turn increases heat losses because of the larger temperature difference between the gas and the combustion chamber walls, as stated by Equation (2.10).

Different heat transfer coefficient models use different characteristic length and velocity scales as well as different temperature exponents. These differences lead to substantial variations in heat flux predictions between models. Correct tuning of constants is necessary before using the models in engine simulation [6]. Much has happened since the third quarter of the 20^{th} century, and the work to improve these old models and adapt them to todays combustion systems is ongoing.

A heat transfer model including heat transfer through cylinder walls, taking into consideration heat transfer through cylinder head, piston crown, cylinder liner and valves is discussed in [31]. Studies of heat transfer through the engine to the coolant revealed that 20-35% of the fuel energy is transferred to the coolant. The primary heat transfer mechanism in a fast-running combustion engine is convection from cylinder gases to surrounding areas. However, especially in case of sooting flames heat transfer due to radiation should also be taken into consideration because of the very high in-cylinder temperature during combustion [31, 43]. Nowadays the radiant fractions are usually small. For all cases investigated in [47] radiant fractions were less than 0.5%.

When the heat release occurs later, towards the expansion stroke, combustion related pressure increase is reduced. This could result in underestimation of the combustion-generated convection. This occurs in basically all heat transfer equations in which combustion-induced pressure change is used as a measure of combustion-generated convection (*e.g.* Woschni and Hohenberg) [21]. A modified calculation approach for determining the transient wall heat losses describes the increasing turbulence during combustion using the differential speed between the burned fraction expansion velocity and the unburned cylinder mass penetration velocity into the flame. Opposite to the original approach, this is considered in a modified characteristic velocity and combustion term. The method was found to determine the wall heat losses in the piston top land area, also considering any occurring leakage [21]. As mentioned in section 2.3 the experimental work of Hohenberg showed that heat transfer in the piston top land gap was only about one third of the combustion chamber heat flux due to lower temperature and gas velocity in this area. Bargende has used the same approach, but reduced Hohenberg's factor to 0.25 [8]. The suggested equation is derived from the differential form of the first law of thermodynamics for the piston top land and describes enthalpy flow. Until the end of the high-pressure phase enthalpy flows out of the piston top land volume back into the combustion chamber, reduced by the blow-by mass flow into the crankcase. To account for the enthalpy leakage the specific enthalpy should be calculated using the gas temperature in the piston top land instead of the averaged in-cylinder temperature [21]. Several reports conclude that different heat transfer equations give very different results in the high-pressure phase depending on engine type, load, and

speed. According to [56], the results of the Woschni equation during the gas exchange phase are too low compared with measurements and 3D-CFD simulations. Considerable improvement was achieved replacing average piston speed with in-cylinder flow velocity. To achieve a more exact and detailed description of the heat transfer in the combustion chamber during the high-pressure phase, geometry-dependent flow parameters such as velocity distribution, swirl, and turbulent kinetic energy need to be considered.

Although research in heat transfer models has been ongoing for decades, the equations widely used today are the ones developed in the 1960s and -70s with slight modifications. Efforts have been made to find out if one is better than the other, but the general conclusion is that their respective results differ so much it is difficult to say that one is preferred over another. Tuning and modifications with respect to geometry and flow parameters should still be done for each engine.

3.3 Engine size effects

In order to reduce fuel consumption and emissions, engine efficiency must increase. This is particularly important for light duty engines, which are still lagging behind heavy duty engines regarding efficiency. An interesting question is what role heat transfer may have in this. However, there are few examples in the literature addressing this issue. One conclusion is that the surface to volume ratio of the combustion chamber could be part of the explanation. Heat generation is proportional to the combustor volume, while heat loss is proportional to surface area. The surface to volume ratio is inversely proportional to the characteristic dimension of the combustion chamber. Thus, heat transfer rate increases as chamber dimension decreases [46]. Reduced scale also increases the water jacket temperature gradient and conduction heat loss [46]. Tests have showed that LD engines experience increased heat transfer losses due to high swirl ratio and less favourable combustion chamber design [28]. Energy balance calculations show that the differences in gross indicated efficiencies between LD and HD engines are due to increased combustion losses (higher HC and CO) and heat transfer [28] for the LD engines. The few results found in literature, together with indications of increasing recent interest in this issue implies that this is a research area with considerable room for improvement.

3.4 Speed and load effects

Speed and load have been proven to have a significant effect on heat transfer. When engine speed increases there is less time for heat exchange, so the engine could be considered more adiabatic [39]. On the other hand turbulence increases linearly with engine speed, which in general increases convective heat losses [4]. These are two competing phenomena, so the question is which one has the largest effect on heat transfer. The mean piston temperature has been found to increase almost linearly with increasing engine speed as well as with engine load [30]. Peak heat transfer coefficients

have been found to increase with engine load but only moderately with engine speed [33]. The convective heat transfer coefficient consists of several factors, as described in section 2.2.3. One factor is the thermal conductivity, k. k varies depending on the gas composition, which in turn changes with fuel/air ratio, ϕ. The load condition determines ϕ, and thus also k. For higher speed under constant load the increase was found to be marginal due to combustion deterioration, reduced peak pressure and temperature. This was also found valid for measured heat flux values. Increasing engine load and speed also retarded the peak angle [33]. Although it was not explicitly mentioned, increased turbulence with engine speed could be one explanation for the presented results. Similar results were found by [45], who states that heat transfer increases slightly with load, while the coefficient increases with speed. Their conclusion is that this is the result of the turbulence increasing with speed. Increased heat transfer rate and -coefficient at higher speed was also found by [36], and a significant increase in heat transfer loss at medium and high load was demonstrated by [50].

The mean heat transfer coefficient during the exhaust stroke was found to be higher than during the intake stroke, for all engine loads and speeds [33]. It was also discovered that the two exhaust phases, blowdown and displacement, could be distinguished by a heat flux variation minimum marking the transition between them. At lower engine speeds the transition period was found to be longer than at higher speed [33]. During the exhaust stroke the peak heat flux point was transferred from displacement to blow-down stage as engine speed increased [34]. Increasing engine speed under constant load reduced the temperature oscillation amplitude, more for higher load. At lower engine speed, the displacement phase was found to be longer than blowdown and vice versa [32].

In DI engines, there is always a risk of producing soot due to the nature of the diffusion flame. Soot particles radiate heat, and could thereby contribute to the heat losses. Studies of this radiative heat loss can also be found in the literature. The authors of [16] found that radiation heat flux as well as the ratio of radiant to total heat flux reduce with increased engine speed and compression ratio. Reduced engine speed on the other hand results in lower wall heat losses. The kinetic energy of the injection pulse was assumed instantaneously converted to turbulent kinetic energy. This causes a rapid increase in convection velocity, which was believed to have a more significant effect at low engine speed when swirl and squish flows are less important. Reduced engine load was found to decrease the combustion-induced turbulence, resulting in reduced convective heat transfer [16]. The two-colour method is a measurement technique used by the authors of [43] at various load conditions. This technique can exhibit changes in radiation heat flux while changing the engine load. The signal shape was found to differ significantly for different loads, even though the peak magnitude remains almost the same. This showed that soot radiant emission is load dependent. Increased engine speed showed no effect on peak radiation heat flux [43]. An increase in radiant heat flux with engine load was also found by [42]. The radiation heat transfer due to soot formation varies during the engine cycle, which is evidence of temperature changes that were found to indirectly affect heat transfer rates according to [50].

The results found in the literature are pointing in more or less the same direction. Both load and speed have an effect on heat losses, but the effect of speed seems to be the most important one. Both theory and experimental results suggest that one of the main factors behind this is enhanced in-cylinder flow and turbulence. In DI engines the effect of radiation heat loss due to soot should be taken into account, especially at higher load. Higher load demands a larger amount of fuel, which increases the fuel/air ratio and could thus easily result in more soot.

3.5 Effects of temperature, pressure and combustion phasing

In addition to the increase in heat loss due to turbulence discussed in section 3.4, high in-cylinder temperatures lead to high combustion chamber wall heat fluxes during combustion. High wall temperatures also have other disadvantages, such as causing high thermal stress and fatigue cracking, as well as impairing the lubricating oil film. Removing heat is thus critical to avoid engine failure and reduced durability [36].

In section 2.3, discussing different heat transfer models, the heat transfer coefficient was found to be proportional to pressure and inversely proportional to temperature, see *e.g.* Equations (2.23) and (2.27). Also more recent experimental work has confirmed these relations [17]. This is a good argument for using EGR, which decreases both peak pressure and temperature. Higher temperature and pressure at medium and high loads than at low load can partly explain the higher heat transfer loss at these conditions found by [50]. They also found that heat transfer tends to increase with combustion duration, so prolonged combustion can be part of the explanation when higher heat transfer loss occurs at low and medium loads [50]. Highly dilute operation reduces flame temperatures and could be another way of minimising heat transfer losses.

In CDC, later combustion phasing also delays and reduces heat flux [19]. As injection timing is advanced, the radiant heat transfer peaks increase in magnitude and occur earlier. By injecting fuel later, peak radiation will be reduced [43]. As discussed in the literature, late combustion phasing may reduce heat losses to the walls, but on the other hand the heat is then lost to the exhaust gases instead. There are both good and bad aspects of hot exhaust gases. On one hand engine efficiency could suffer from unused heat, on the other hand the heat could be used in auxiliary systems such as turbo chargers and waste heat recovery systems. From this point of view it is important to look at the whole system to avoid suboptimation.

3.6 Combustion chamber geometry effects

The combustion chamber may look very different depending on the engine type and size. Naturally, the shape is important for the flow pattern and thus, also has an

effect on heat transfer. Several studies have been done concerning the heat transfer characteristics of different bowl geometries. Numerical simulations of a LD engine proved that a stepped-bowl piston, with less surface area compared to a conventional piston, was beneficial for reducing wall heat transfer and reducing fuel consumption [15]. The stepped-bowl also improved mixing so oxygen could be used more efficiently, which in turn also reduced soot formation. This was done by targeting the first injection at the upper bowl portion, and the second directed below to mix with air not taking part in the first injection's combustion process. The conventional bowl forces second injection fuel to mix with combustion products from the first injection, resulting in more soot. Another research group optimised a chamfered, re-entrant bowl with low swirl and an 8-hole nozzle [49]. It resulted in a more uniform equivalence ratio field in the bowl than for the wide re-entrant bowl. A lean region along the liner was found useful for preventing heat loss to the coolant. It may also reduce oil contamination by fuel and soot [49]. Another geometry that has been investigated is a lip-less shallow dish combustion chamber [20, 29]. The heat transfer coefficient was reduced through restricting the in-cylinder gas flow using a zero swirl port. To counteract inadequate fuel-air mixing, a micro multi-hole injector was adopted creating a highly dispersed fuel spray. Moving the combustion area to the combustion chamber centre reduced temperature gradients near the combustion chamber wall. Tapering the piston bowl reduced heat loss due to strong squish flow from the sidewall to the squish area, further reducing cooling heat loss [20]. This work focused on PCCI (Premixed Charge Compression Ignition) combustion, where most of the cooling losses occur along the cylinder sidewalls and squish region, due to this reversed squish flow. The tapered shallow-dish cavity, gradually changing the cross-sectional opening area from cavity to squish region, suppresses this reversed squish flow [29].

The heat transfer characteristics of the stepped-bowl investigated by [15] were also compared to the tapered, lipless piston in [20, 29] and two more conventional re-entrant geometries using CFD simulations by Fridriksson *et al.* [18]. At all load conditions, the conventional re-entrant diesel geometry showed considerably lower thermodynamic efficiency and higher heat losses than the more shallow and open geometries. At high load the shallow, open piston bowls experienced more heat transfer in the bowl, while the more conventional types showed more bowl-lip heat transfer. Also a shallower, more open version of the conventional bowl showed improved performance at all load cases [18]. A low surface-to-volume ratio may be assumed to provide low heat transfer due to reduced heat transfer area, but [18] found that this is not always the case. Before the start of spray-driven combustion, the surface-to-volume ratio directly influences heat transfer with higher surface-to-volume ratio providing larger heat flux. After this point, other combustion parameters and turbulence have more influence. The study included the geometries used in Papers I, II and III in this work.

For some combustion concepts, an open bowl shape has been proven to increase engine efficiency. The explanation found was that heat transfer losses decrease significantly with reduced bowl depth and increased squish height [48, 14]. The authors attributed this to the decreased surface-area-to-volume ratio and decreased bowl depth. Heat transfer losses were reduced for both low and high load cases [14].

Accurate heat transfer calculations are difficult due to different combustion chamber shapes, as well as variations in timing and valve lift which affect flow velocities and directions as stated by [36]. During combustion the chemical composition and temperature changes, and so does heat transfer by gaseous and soot-emitted radiation and convection. Heat transfer was found to increase with compression ratio, and decrease with larger bore [36]. This is consistent with the previously discussed effects of pressure, section 3.5, and engine size, section 3.3. A higher compression ratio increases in-cylinder pressure, and larger engines have a more favourable surface-to-volume ratio.

In general, researchers seem to agree that a shallow bowl with low surface-to-volume ratio is the best choice for reducing heat transfer. However, the geometry always must be matched to the prevailing conditions such as bulk flow pattern and spray parameters, which are discussed next.

3.7 Spray effects

The injector nozzle-hole orientation and number of holes have a documented effect on heat transfer through the combustion chamber walls [13]. These parameters are matched to the specific combustion chamber geometry and require optimisation. At equal rail pressure larger holes result in shorter injection duration compared to smaller holes. The impingement area of the burning spray has also been found to be of importance for the heat loss characteristics. A smaller impingement area is favourable for reducing heat loss [13, 20, 27, 40, 55] because of the hot flame heating the wall. The heat transfer coefficients at different locations in the combustion chamber could vary significantly due to the flame arriving at different times [33]. Flame spread and impingement on the wall have been found to dramatically increase heat-transfer. Modelling and measurements proved it to be around ten times higher than the pre-impingement level [27]. High injection velocity resulted in increased vapour penetration speed, and thus earlier flame arrival. Bulk flow, liquid penetration length and vapour penetration speed had significant effect on heat transfer due to the effect these parameters have on flame spread [27].

Reduced injection duration can be achieved with larger hole size, which increases the rate of heat release (RoHR). This generally improves efficiency, but the effect can be offset by increased heat transfer losses [13] and soot. Injector nozzle hole orientation may reduce heat loss by moving the flame away from the walls, thus directly affecting convective heat transfer. As the spray plume is moved away from the cylinder axis, a large amount of air remains unutilised near the cylinder axis, which results in richer regions and smoke formation [13]. The effect of injection duration has also been studied. Reduced injection duration can be achieved with larger holes and increases the rate of heat release (RoHR), which is also associated with increased combustion chamber wall heat transfer. Efficiency is generally improved, but the effect can be offset by increased heat transfer losses [13]. The number of injector holes was also found to affect heat transfer. However, the effect seems to differ between different combustion chamber geometries. For an open chamber geometry the heat transfer rate was found

to increase with 8 holes and decrease with 12 holes, as compared to the 6-hole baseline case. With the 12-hole injector, the combustion performance was compromised slightly, while the overall performance was improved. This was believed to be due to improved mixing and flame-wall interactions. In the 12-hole case, the rate of heat release suffered slightly, which could be due to increased spray plume-to-plume interaction [13]. CFD and experimental results have shown that multiple injections greatly improve BSFC compared to single injection. This was explained by reduced wall heat loss due to improved in-cylinder temperature distribution. Very little of the after-injection flame mass was found to reach the cylinder walls [38]. Using the same multiple injection strategy, IVC timing was retarded to decrease the effective compression ratio. This improved BSFC despite increased wall heat loss, mainly due to utilising heat energy resulting from the increased effective expansion ratio [38]. Another experimental study found that wall surface temperature, and temperature drop due to interaction with liquid fuel sprays are important parameters influencing the spray-wall interaction [30]. Increasing temperature drop with increasing rail pressure was shown due to locally intensified spray-cooling. The wall film mass was reduced by increased air entrainment with higher injection pressure [30]. Injection pressure also plays a major role for combustion development as confirmed by modelling and experimental work. High injection pressure was found to result in increased impact area and greater spray jet momentum, which significantly increased wall heat transfer. Increased mixture stratification with overly lean areas in the centre of the combustion chamber was also detected at higher injection pressures [40]. Another experimental study investigated how surface heat flux follows the rate of temperature change [55]. Spray impingement increased the peak heat flux value as well as caused the peak to occur sooner. CFD simulations have also found that impingement of a burning spray increases the turbulent kinetic energy compared to other regions, which in turn increases heat flux into the piston [53].

At some distance from the nozzle the spray will reach a stagnation point. Where this occurs depends on ambient density and the state of the spray [55, 38]. At lower in-cylinder density the spray arrived at the stagnation point sooner than at higher density. A combusting spray was also found to arrive sooner than an evaporating spray. Low injection pressure and ambient density resulted in combustion starting after the spray impinged on the wall. At increased ambient density, combustion started before impingement due to lower spray velocity and shorter ignition delay. When increasing injection pressure combustion again started at impingement [55]. It has been established that spray penetration is affected by swirl, as greater air entrainment into the jet due to swirl would reduce radial penetration [40]. Increased impact area and greater spray jet momentum led to significantly increased wall heat transfer, mixture stratification, and delayed ignition timing [40]. Experiments with multi-orifice nozzles with very small orifices have been tested in conventional diesel combustion [29]. They were proven to produce a highly dispersed spray which can promote air entrainment under low swirl conditions. The nozzles had weak spray penetration, which led to decreased overall load performance. With this highly dispersed spray, the high temperature area causing cooling losses is along the side walls of the piston cavity. However, this area is reduced compared to conventional sprays [29]. In conclusion, burning spray impingement on combustion chamber walls should be avoided to reduce heat losses. Both the high flame

temperature and increased turbulent kinetic energy contributes to a larger heat transfer coefficient.

3.8 Flow effects

The most thoroughly investigated form of in-cylinder gas flow affecting heat transfer is swirl. In general, most studies have found that low swirl levels provide lower heat loss [9, 18, 39, 40]. However, different geometries respond differently to swirl ratio changes, which may be due to variations in the combustion chamber gas velocity fields. Reduced rotational motion in the bowl area has been found to reduce convective heat flux. With higher swirl, increased gas movement primarily occurs in the outer combustion chamber region, where spray momentum is largest at the end of injection. Increased gas motion late during the expansion has also been found to greatly increase heat transfer. CFD simulations have shown that for CDC bowl geometries, reduced swirl reduces heat loss. The same study also found that other, more open, piston geometries gave rise to increased heat losses as near-wall fluid velocity was unchanged or even increased as the swirl level decreased. The effect was more pronounced at higher load, where considerable peak heat flux differences were detected [18]. A tapered piston, simulated under extremely low-swirling conditions, indicated that heat losses could be reduced by using a multi-, micro-hole injector, and a swirl ratio reduced to almost zero [18]. Experiments have shown that increased charge motion at high swirl and injection pressure significantly changed the mixture structure and composition at the walls [40]. Increasing the swirl ratio resulted in higher peak heat release rates, and more fuel mass was premixed to overly lean conditions in the squish volume. Increasing injection pressure resulted in overly lean mixture near the nozzle as well as in the squish volume [40]. With high swirl ratios, wall heat transfer was found to increase significantly, which slightly delayed ignition timings predicted by CFD modelling. Experimental measurements instead indicated advanced ignition at high swirl levels [40]. On the other hand, an experimental study in both CDC and LTC mode found that in CDC mode the RoHR was not strongly affected by swirl level when CA50 was controlled [19]. The mean surface temperature was seen to increase with increasing swirl. The diffusion flame of CDC, with much higher local temperatures, caused much greater heat flux magnitude and duration compared to LTC concepts. The main reason was considered to be that LTC strategies had lower in-cylinder temperatures compared to CDC [19]. Experimental work concerning instantaneous heat transfer in a diesel engine showed that during the intake stroke swirl velocity and turbulence increased with engine speed. This caused increasing local heat transfer coefficients, but lower speed also increased heat transfer coefficient instabilities. During the exhaust stroke similar turbulence intensity and instabilities were found for all engine speeds [33]. HCCI simulations in a HD engine have also shown that heat transfer increases during the compression stroke due to increased in-cylinder fluid velocity, generating the highest heat transfer rate. A smaller peak value was also found during the exhaust stroke, because at exhaust valve opening, the high pressure difference between cylinder inlet and outlet increases the gas velocity. Thus, the heat transfer rate reaches high values [7]. A study of the effects of

boost pressure on cylinder wall heat flux revealed that heat flux peaks were increased up to 30 % by turbo- or supercharging. This could be explained by an intensified flow field turbulence level, caused by the increased pressure drop across the inlet valve. The convection part of the total heat transfer was also found to increase, which is supported by the greater heat flux during compression [16].

As touched upon above, the heat flux can vary significantly at different locations in the combustion chamber. Another CFD study, which focused on swirl and clearance height, confirms that heat transfer increases with swirl due to higher tangential velocities. The increase or decrease of the clearance height was not found to significantly change the in-cylinder flow structure, and was thus not an important parameter for heat transfer to the cylinder walls of DI diesel engines [39]. Transient heat flux measurements in a diesel engine also resulted in the conclusion that spatial non-uniformities of fluid flow and combustion caused different temperature histories at different points in the cylinder head [31].

The in-cylinder gas motion also plays a role in emission formation. When the increased swirl ratio resulted in overly lean conditions in the squish volume, this also resulted in greater HC and CO emissions. The mixture distribution in the bowl was generally enriched, resulting in lower HC and CO emissions. These competing effects led to a complex emissions behaviour. HC emissions initially increased with swirl, even as CO was reduced [40]. Locally rich areas in CDC, not found in LTC, also lead to soot formation which may have a negative impact on heat flux. Soot radiation is not expected to be present in LTC [19].

3.9 EGR effects

EGR can also be used as a means to reduce heat loss. CFD simulation found that significant heat loss reduction could be obtained with increased EGR. This was probably due to the increased charge mass, requiring more heat to increase the charge temperature [13]. In experimental work, increasing the EGR rate above 50 % suppressed smoke emissions and improved BSFC in CDC mode. Using a two-colour method the flame temperature was determined to less than 2000 K, and both BSFC and BSNO$_x$ emissions were simultaneously improved [38]. Another research group used experiments to conclude that the heat transfer coefficient does not vary significantly with EGR, since by increasing the EGR rate both temperature and pressure reduce. With decreasing temperature, convective heat transfer was reduced as a result of charge temperature reduction and thus reduced temperature difference [17].

3.10 Spray-swirl interaction effects

Very little can be found in the literature regarding interactions between the fuel spray and swirl. A CFD study found that increasing the swirl level decreases the peak heat

flux at locations under the spray axis and delays flame arrival times. At locations mid-way between sprays, both parameters show the opposite behaviour [27]. Perini *et al.* [40] performed both experimental and simulation work, which to some extent gave different results. Higher injection pressure gives stronger jet penetration, and could in theory be more strongly affected by higher swirl levels. Modelling suggested that it would result in more air entrainment into the jet and thus leaner mixture close to the nozzle and near the bowl rim. However, experiments showed that the fuel jets were not deflected as much as anticipated, which resulted in larger spray impingement areas and increased wall heat transfer. It was also concluded that low swirl places the richer mixtures in the squish volume, whereas at higher swirl the fuel is more confined to the bowl. Both behaviours result in rich areas, which advance ignition. Both experiments and simulations confirm a critical ignition timing dependency on in-cylinder spray-flow field interactions at very low loads, as well as on mixing and heat transfer. It is also concluded that a more detailed understanding of how the jet-to-jet behaviour changes due to different spray impingement and tangential velocities affect the overall combustion characteristics.

The lack of research in this particular area suggests that this is a research area in need of development. The work presented in this thesis is therefore aimed at studies of how heat transfer is affected by combinations of different swirl levels and spray parameters, as well as combustion chambers with different design characteristics.

Chapter 4

Experimental Setup

There are many ways of performing experimental work with engines. The engine and equipment used is very important for the kind of results and the nature of the data acquired. This chapter will shed some light on the equipment used to generate the results presented in Chapter 6.

4.1 Test engine

Experiments were performed in a 4-cylinder light-duty diesel engine with Denso injectors. Engine specifications are presented in Table 4.1. In order to set up the engine energy balance, temperature and mass flow measurement equipment was installed. All cylinders were instrumented with thermocouples for measuring temperature differences in the cooling system.

Table 4.1: Engine specifications

Displaced volume [l]	2.0
Stroke [mm]	93.2
Bore [mm]	82
Connecting rod [mm]	147
Compression ratio [-]	15.8
No. of injector holes	8
Fuel	Diesel

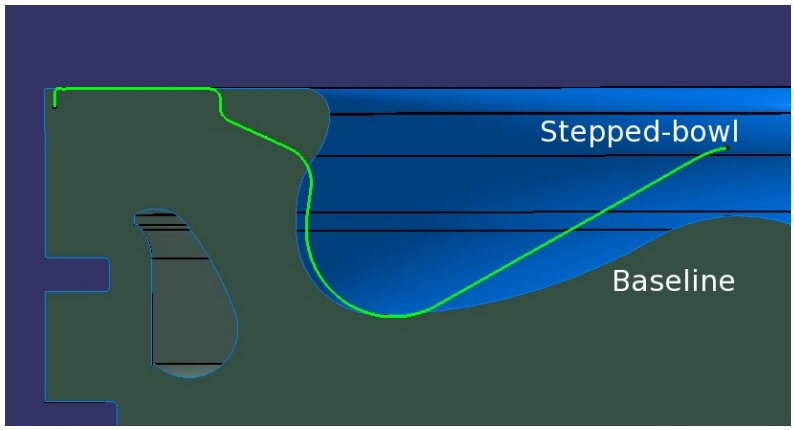

Figure 4.1: Piston geometries, the stepped-bowl design is outlined in the drawing of the baseline piston.

4.2 Baseline geometry

All of the measurement campaigns were to some extent performed with the baseline, re-entrant CDC piston depicted in Figure 4.1. It is fairly conventional CDC design, but with the bowl made shallower and wider to improve air utilisation and reduce the heat losses and heat load on the piston. This is a Euro 6 piston. Compared to the Euro 5 piston from the same manufacturer it is lightweight with reduced compression height, longer and lighter connecting rod and smaller piston pin diameter. The oscillating mass is thus reduced by 20 % and balancer shafts are not needed. The design includes a cooled ring carrier for optimal cooling performance [11].

4.3 Stepped-bowl

The experimental work was based on CFD simulations performed by Helgi Fredriksson. The results presented in reference [18] concerns heat transfer characteristics of four different piston designs, including the baseline geometry and a so called "stepped-bowl" developed by Ford for heavy duty engines [49]. The baseline bowl has a good soot-NO_x trade-off over the whole load range, but the stepped-bowl was found to be almost as good. The stepped-bowl also demonstrated the lowest heat losses, even though it did not have the best thermodynamic efficiency. In the late cycle, the stepped-bowl had considerably lower heat flux than the baseline bowl. This was probably a result of the high-temperature gases being located in the centre in the stepped-bowl, rather than at the cylinder liner surface as for the baseline case late in the cycle. The baseline piston also demonstrated a lot of heat transfer at the bowl-lip, which the other piston did not. At full load and high swirl the stepped-bowl had the lowest in-cylinder temperature,

which along with the lower surface-to-volume ratio explained its low heat flux. In Fredriksson's study the stepped-bowl did not seem to be as affected by different swirl levels as other pistons. When the swirl level was reduced, heat losses were relatively unchanged. As mentioned above, the different combustion chamber velocity fields in the pistons could be part of the explanation [18].

Why then is this stepped-bowl design so beneficial in terms of heat transfer? Andersson and Miles [4] have tried to explain this. One feature of the stepped-bowls is splitting the fuel spray, so part of it is directed upward toward the cylinder head and the rest downward into the bowl. The penetration of the upper portion of the jet into the squish volume will then be impeded, and less soot will be generated near the cylinder walls. Heat loss to the cylinder liner is thereby also reduced. As also mentioned by Fridriksson *et al.* the stepped-bowl also has an improved surface to volume ratio, which reduces heat losses to the piston surfaces [4].

4.4 Measurement systems

The information needed from the experimental work demanded precise measurements of temperatures in the cooling media, as well as the corresponding fluid flows. The cooling water flows up from the engine block to the cylinder head through channels on the inlet side, and returns to the engine block through channels on the exhaust side. The cylinder head was equipped with T-type thermocouples in all cooling channels for cylinder 3 and 4, the other cylinders only had one on the inlet and one on the exhaust side. Figure 4.2 shows the thermocouple positions viewed from the exhaust side.

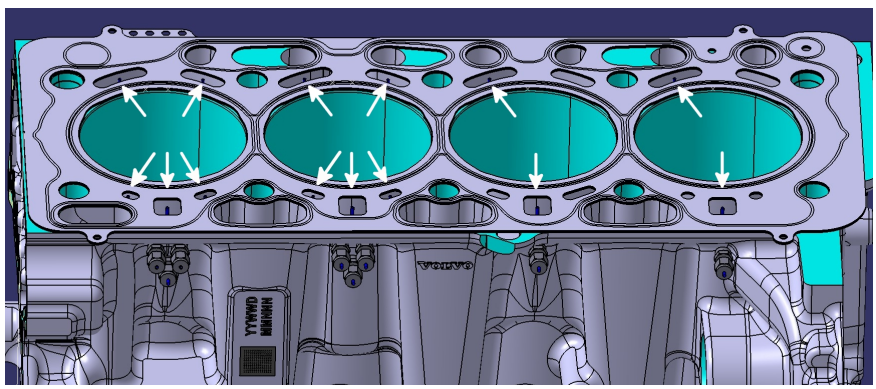

Figure 4.2: Thermocouple positions in cylinder head cooling channels, exhaust side view.

One K-type thermocouple was fitted in the feed line to the piston cooling oil rail, and two were fitted in funnel-shaped structures below the pistons to measure the oil return flow temperatures from cylinder 2 and 3. One of these is shown in the right part of Figure 4.3 where the structure and the pipe guiding oil from the piston outlet to the

funnel can be seen from below. All cylinders were fitted with Kistler pressure sensors to measure in-cylinder pressure used for the heat release analysis. Exhaust oxygen concentration was measured using an Etas lambda meter. Flow meters were installed to measure the mass flows of cooling water, air, and oil to the piston cooling. Fuel flow was measured using a Sartorius balance. Emission levels of unburned hydrocarbons (HC), nitrogen oxides (NO_x, carbon monoxide (CO) and carbon dioxide (CO_2) were measured using a Horiba system, which was also used for measuring EGR levels.

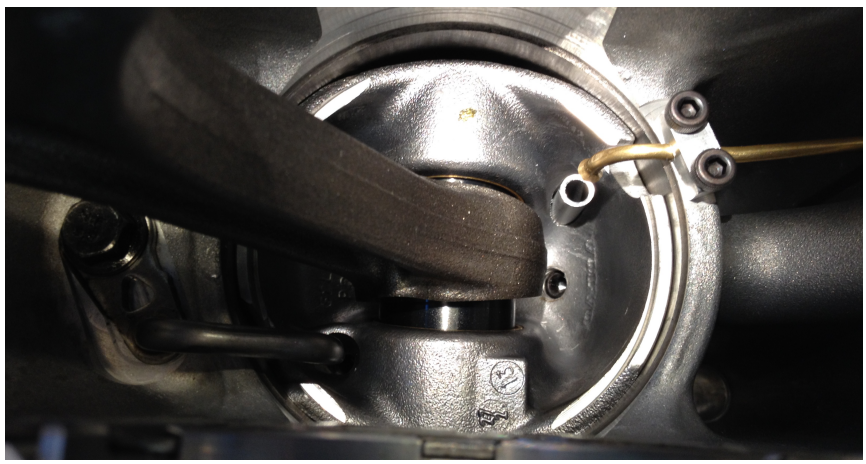

Figure 4.3: Position of thermocouple measuring piston oil return flow temperature.

K-type thermocouples were also placed in the inlet and exhaust ports to all cylinders, as well as in the cooling water before and after the engine.

4.5 Heat loss measurements and calculations

Heat is lost in all parts of the engine, and it is impossible to account for every single part. In this work focus was on heat losses to the cylinder head cooling water, piston oil cooling, and exhaust gas. Other losses such as combustion losses, friction, and heat losses to the engine block cooling were excluded to simplify the analysis. Figure 4.4 shows the heat losses accounted for, and typical values of the losses and indicated work found during the experiments.

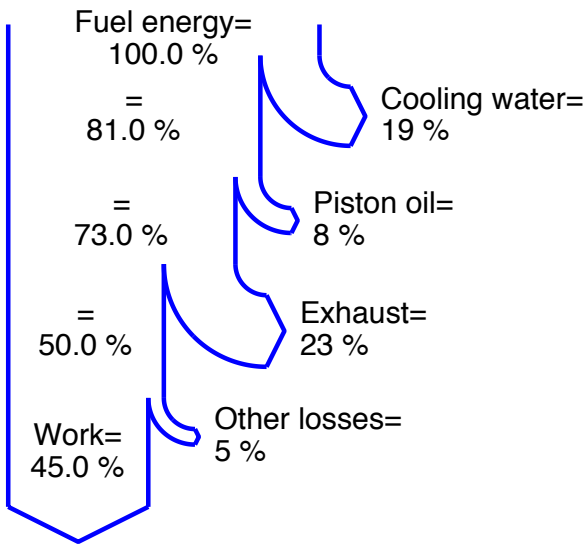

Figure 4.4: Chart showing approximate values of the heat losses and indicated work considered in this work.

Chapter 5

Experimental methodology

The presented work was performed as experiments using the equipment described in Chapter 4. Data were acquired and post processed to get the information required to draw conclusions regarding the heat losses. The post processing included heat release analysis and setting up the energy balance over the engine. Both procedures will be described in this chapter.

5.1 Experimental procedure

Heat transfer to the cooling media was measured at various engine conditions. Three measurement campaigns were performed, all regarding evaluation of heat losses: The first was run with the baseline piston, the second followed the same procedure as the first but with a stepped-bowl, and during the third spray parameters were varied.

All sets of measurements followed the same procedure. One speed-load test was performed, and during additional tests the following four parameters were swept: rail pressure, swirl, EGR and λ. The test specifications for the parameter sweeps are presented in Table 5.1. With the baseline geometry the swirl sweep was conducted at two different rail pressures to investigate the existence of spray-swirl interactions. All of the experimental work was performed at 1500 rpm and approximately 10.5 bar $IMEP_g$, except in the speed-load test where three different cases were tested. The speed-load cases are described by Table 5.2. The fuel flow was kept constant during all parameter sweeps, but varied between the different cases in the speed-load test.

The third set of measurements was focused on spray parameters. Besides the baseline 8-hole injectors, two full sets of injectors with 6 and 10 holes, respectively, were tested. The holes were designed to keep the flow rate equal to the baseline injectors.

Table 5.1: Test conditions during sweeps

Rail pressure [bar]	500, 1000, 1250, 1500, 2000
Swirl valve % open	0, 10, 20, 30, 40, 50, 60, 70, 80, 90, 100
EGR [%]	0, 12, 25
p_{in}, all except λ sweep [bar]	1.6

Table 5.2: Speed and load combinations

Case	Speed [rpm]	$IMEP_g$ [bar]	P_{in} [bar]	EGR [%]
1	2000	10.5	1.8	17 %
2	1500	10.5	1.6	15 %
3	1500	5.0	1.1	38 %

During all experiments four fuel injections were used, two pilot injections, main injection and a post injection. One reason for using multiple injections is that it is expected to help improving the air utilisation. The first injection targets the upper part of the bowl, and a second injection the lower part. This way the second injection is less likely to mix with O_2-depleted charge, which will reduce soot and CO emissions. Better air utilisation is also supposed to improve the EGR tolerance of the system [4].

One additional set of measurements was performed, varying injection timings, number of pilot injections, omitting the post injection and varying the pilot to main injection fuel ratio. During all these tests the fuel flow, speed and load were kept constant. The results of this campaign did not differ enough to show enough new and interesting trends and were thus not considered for publication as a separate paper. They will, however, be presented as a separate section in Chapter 6.

5.2 Heat release analysis

While running the engine at the different settings and configurations, pressure traces were recorded in all cylinders. Comparing the traces from the different cylinders, cylinder 3 was selected for the heat release calculations because it was the one closest to the average for this engine. For every data point, 3×300 engine cycles were recorded. However, to ensure a statistically reliable result, the data points were randomised. That means all three sets of engine cycles for the same data point were not recorded consecutively, but mixed with other data points. The rate of heat release (RoHR) and the accumulated heat release were calculated separately for every pressure trace, including Woschni's heat transfer model described in Chapter 2.3.

Calculating the rate of heat release (RoHR) gives a quantitative measure of how heat is released during the engine cycle. Starting with the in-cylinder pressure, the first law of thermodynamics, Equation (5.1) can be used to determine the RoHR at different points during the process. $\frac{dQ}{dt}$ is the rate of energy transferred to the system, $\frac{dU}{dt}$ is the rate of internal energy change, and $\frac{dW}{dt}$ is the rate of work transferred from the system.

$$\frac{dQ}{dt} = \frac{dU}{dt} + \frac{dW}{dt} \tag{5.1}$$

The internal energy U can be expressed as Equation (5.2), where m is the in-cylinder mass, C_v is the specific heat at constant volume, and T is the temperature.

$$U = mC_vT \tag{5.2}$$

Assuming that the mass is constant, the derivative of U can be expressed as Equation (5.3).

$$\frac{dU}{dt} = mC_v\frac{dT}{dt} \tag{5.3}$$

The ideal gas law is described by Equation (5.4), where p is the in-cylinder pressure, V is the cylinder volume and R is the specific gas constant.

$$pV = mRT \tag{5.4}$$

R and m are assumed constant, so taking the derivative of Equation (5.4) together with expressing T in terms of p and V results in Equation (5.5):

$$\frac{dp}{p} + \frac{dV}{V} = \frac{dT}{T} \tag{5.5}$$

Now Equation (5.4) and Equation (5.5) can be used to rewrite Equation (5.3) as Equation (5.6):

$$\frac{dU}{dt} = \frac{C_v}{R}\left(V\frac{dp}{dt} + p\frac{dV}{dt}\right) \tag{5.6}$$

Now all that is missing is an expression for the work from the system. Assuming again that the mass m is constant, this can be expressed as Equation (5.7)

$$\frac{dW}{dt} = p\frac{dV}{dt} \tag{5.7}$$

The gas constant R can be expressed as Equation (5.8), where C_p is the specific heat ratio at constant pressure.

$$R = C_p - C_v \tag{5.8}$$

The ratio of specific heats, γ, is defined by Equation (5.9)

$$\gamma = \frac{C_p}{C_v} \tag{5.9}$$

Substituting Equation (5.6) – (5.9) into Equation (5.1) results in the final Equation (5.10):

$$\frac{dQ}{dt} = \frac{\gamma}{\gamma - 1} p \frac{dV}{dt} + \frac{1}{\gamma - 1} V \frac{dp}{dt} \tag{5.10}$$

For engine applications it is more useful to study the RoHR as a function of crank angle degrees (CAD), θ. Often, and especially in this case, it is also needed to take heat losses to the combustion chamber walls into account. In this work these have been estimated using the Woschni heat transfer model described by Equation (2.23) [58]. Rewriting Equation (5.10) with $d\theta$ instead of dt and adding the heat transfer term results in the final equation for calculating the RoHR, Equation (5.11):

$$\frac{dQ}{d\theta} = \frac{\gamma}{\gamma - 1} p \frac{dV}{d\theta} + \frac{1}{\gamma - 1} V \frac{dp}{d\theta} + \frac{dQ_{ht}}{d\theta} \tag{5.11}$$

To further improve the model a term for the losses to crevices could be added. However, this effect is usually small and is thus neglected in this work.

The accumulated heat release can be calculated by integrating the rate of heat release, and from that the crank angle degree for 10 % burned (CA10), 50 % burned (CA50), and 90 % burned (CA90) can be calculated. The position of CA50 is called the combustion phasing, and the combustion duration is defined as CA90 - CA10.

5.3 Energy balance calculations

Temperatures were measured in the cooling water, engine oil, inlet and exhaust manifold. Special focus was on the cylinder head cooling, piston cooling and exhaust gas. As described in Chapter 4, thermocouples were placed in the cooling channels on each side of the cylinder head to measure the temperature difference. Temperature differences were also measured between the piston cooling gallery outlet and the oil rail feed line as well as between the exhaust and inlet manifold. These temperature differences were

used to calculate energy losses using Equation (5.12), where $\dot{m}_{medium}$ is the mass flow of the medium, $C_{p,low}$ and $C_{p,high}$ are the specific heats of the medium at the low and high temperature, respectively. ΔT_{medium} is the measured temperature difference in the medium between the low and high temperature measurement.

$$\Delta E_{medium} = \dot{m}_{medium} \frac{(C_{p,low} + C_{p,high})}{2} \Delta T_{medium} \tag{5.12}$$

The respective values could then be calculated as percentage of the original fuel energy. These were then added together in an energy balance diagram so the different cases could be compared.

5.4 ANOVA

ANOVA, Analysis of Variance, is a statistical method to determine if there is an actual difference between three or more samples [3]. For some of the points in the tests it was not obvious from a visual evaluation that there was a significant difference. In those cases, a one-way ANOVA analysis was performed to establish a difference. The methods compares the sample mean values to the grand mean value and takes into account the experimental error, which is the variation within each sample. The variation within the samples is separated from the variation between the samples, and comparing the two reveals if there is a difference between the sample means. Then a significance test, an F-test, is performed to test if the variances of the two means are equal. If the sample F-value is more extreme than the value for a specific confidence level, *e.g.* 95%, a difference between the samples has been established.

Chapter 6

Results and discussion

In this chapter the results of the experimental work will be presented and discussed. The results are presented in individual sections for each experimental campaign. Section 6.1 deals with the outcome of tests with different injection strategies. These results were not published, and are therefore discussed in more detail. Section 6.2 presents the results in Paper I, concerning heat loss characteristics of the baseline geometry and how heat loss is affected by different parameters. Section 6.3 shows the work from Paper II, comparing the heat loss characteristics of the stepped-bowl geometry to the baseline, and finally section 6.4 demonstrates how the different nozzle configurations affected heat loss. This forms the basis for Paper III.

6.1 Injection strategies

The tests with different injection strategies were performed at 10 bar $IMEP_n$ and an engine speed of 1500 rpm. The fuel flow was kept constant during all tests. The first test involved two pilot injections. The amount of fuel in the pilots was the same for all points, but their respective timings were changed. The second test was performed with one pilot injection injecting the same amount as the two pilots in the first test combined. The injection timing was again varied. The third test was with two pilot injections but no post injection. The amount of fuel in the post injection was instead added to the main injection. Lastly, a test was performed with one pilot injection, changing the pilot-to-main injection duration ratio. When the pilot injection duration was decreased the main injection duration was increased to maintain a constant fuel flow, and vice versa.

6.1.1 Injection timing, two pilot injections

The pilot injection timings of the test with two pilot injections are given in Table 6.1. They were moved in steps of 5 CAD, keeping them separated by minimum 6 CAD.

Table 6.1: Injection timings, two pilot injections

Pilot 1 [CAD BTDC]	Pilot 2 [CAD BTDC]
7	1
12	1
12	6
17	1
17	6
17	11

When injecting fuel earlier, the combustion phasing can also be expected to occur earlier. Both because there is fuel in the cylinder earlier, and because the fuel and air might be slightly more premixed which gives rise to faster combustion. However, only the pilot injections were moved forward and they only represent a small fraction of the total fuel injected. As can be seen in Figure 6.1, the combustion phasing (CA50) does take place a little earlier with earlier pilot injections. This trend seems to follow the second pilot injection rather than the first, even though the first seems to have some impact too. A small difference can be seen between the cases with the first pilot set at 7 and 12 CAD BTDC, but then when the first pilot injection is set as early as 17 CAD BTDC and the second is at 1 CAD BTDC, there is not much difference compared to the case with injections at 7 and 1 CAD BTDC. The difference is not significant until both pilots are put 10 CAD earlier than the 7, 1 case. Then CA50 jumps from just over 16 CAD ATDC to 15.5 CAD ATDC. However, the differences are generally quite small, which implies that the pilot injection timings are less important for the combustion process than the main injection. After all, they only contain approximately 10 % of the total fuel mass, but could still be expected to have some effect.

The combustion durations for the different injection timings are displayed in Figure 6.2. For most cases the combustion duration is quite similar. The only case that stands out is the one with the earliest injection timings for both pilots. A longer combustion duration could be expected with earlier pilot injection timing, because fuel is injected both earlier and during a longer total time. Thus, there is enough fuel to enable ignition to occur earlier in the engine cycle while the rest of the injections will burn at a similar rate for all cases since they are not altered. When only the first pilot injection is put earlier, there may not be enough fuel to make a burnable mixture. Thus, neither combustion phasing nor duration is affected significantly.

Combustion phasing and duration are both calculated from the heat release, which is described in Chapter 5.2. The lefthand side of Figure 6.3 shows the rate of heat release (RoHR) when altering the injection timing of the first pilot injection, and the righthand side shows the RoHR when the second pilot injection timing is changed. If the first peak in the main peak is being studied, it can be seen that when the second injection

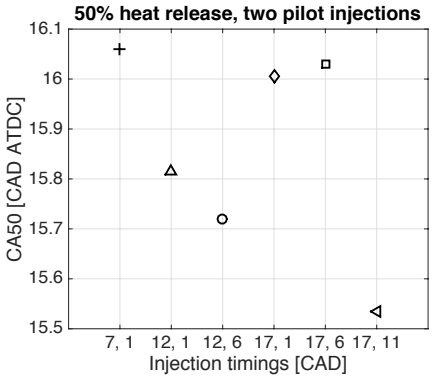

Figure 6.1: Combustion phasing at different pilot injection timings, two pilot injections.

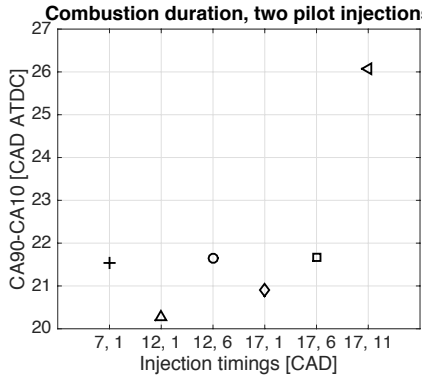

Figure 6.2: Combustion duration at different pilot injection timings, two pilot injections.

is put later this peak increases in height. when instead putting the first injection later, this peak reduces in height. Both behaviours could be explained by the level of premixing. If both pilots are injected early, they are ignited almost simultaneously and have almost finished burning before the main injection. If on the other hand both are injected late, they burn while the main injection starts, ignite it and finish as the main injection burns, giving rise to smoother combustion. There may also be a lower degree of premixing, which increases combustion duration. Setting both some distance apart or just a little earlier lets more of the fuel mix with air and thus increases the height of the combustion peak connected to the pilot injections. The main combustion event peaks a few CAD later when the premixed part of the main injection is over, and then while the mixing controlled combustion takes place there is a smaller peak when the post injection is ignited.

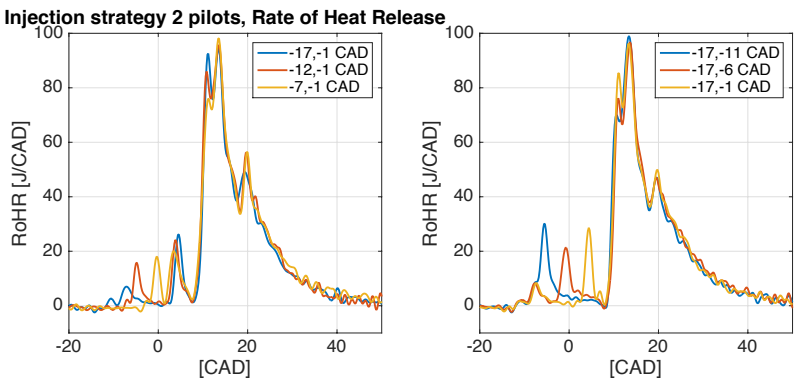

Figure 6.3: Rate of heat release at different pilot injection timings, two pilot injections. The left part shows varying the first injection timing and the right part shows varying the timing of the second injection.

The losses to the cylinder head cooling, piston oil cooling and exhaust gas are presented in Figure 6.4. Heat loss to the cylinder head stays relatively constant, but a slight trend can be seen towards less losses with earlier injection timings. This again seems to be mainly connected to the second pilot injection. With the pilot injections still reacting while injecting the main part of the fuel, it may result in a faster start of the main combustion. This also leads to high temperatures, which enhances cylinder head heat transfer. There is a somewhat similar trend for the exhaust losses, even though they rather seem to be a function of the mean value of the two injection timings. The piston oil losses follow the trend of the exhaust losses quite well. Small differences between the cases can be distinguished, but considering how small they are no real conclusions could be based on these results. It could be argued that early pilot injections are ignited earlier, and should thus leave less fuel to burn late in the cycle which could explain why there seem to be less exhaust losses at those conditions. However, looking at CA50 in Figure 6.1 and the RoHR in Figure 6.3 this argument is not supported.

The engine energy balance is shown in Figure 6.5. The total height of the bar for the case with late injection timings for both pilot injections is higher than the ones representing the other cases. This mainly seems to be the result of a larger amount of work extracted. The stack representing the case with a very early first injection and a late second injection (17, 1) also shows a comparably higher work output. The reason could be that more of the heat release occurs closer to top dead centre (TDC), which is beneficial for work extraction. Generally speaking, earlier pilot injections result in slightly lower heat losses while at the same time to some extent compromising the work output. But again, the differences between the cases are so small that no definitive conclusions could be drawn. This means that the pilot injection timings could be used to fulfil other goals, in terms of noise and emissions, without having any significant impact on the heat losses.

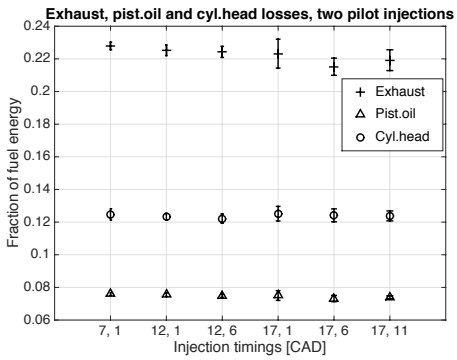

Figure 6.4: Fraction of fuel energy lost to cylinder head coolant, piston oil cooling and exhaust at different pilot injection timings, two pilot injections.

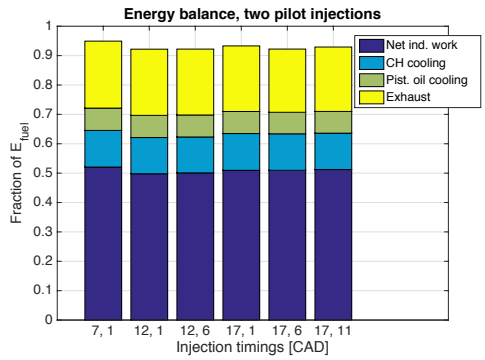

Figure 6.5: Engine energy balance at different pilot injection timings, two pilot injections.

6.1.2 Injection timing for one pilot

During the test with one pilot injection, the pilot injection timings were 12, 7 and 2 CAD BTDC. The injection duration of the single pilot was prolonged to get the same amount of fuel as with the two pilots in the previous test. The resulting combustion phasing are displayed in Figure 6.6. There is a fairly clear dependence on the pilot injection timing, even though the differences are again rather small. Moving the pilot injection forward 10 CAD only made approximately 1 CAD difference on the combustion phasing. Even though the pilot now contains more fuel, it is still only approximately 10 % of the total amount so the main part of the combustion is more important for the combustion phasing.

Even though the effect on the combustion phasing was fairly small, the combustion duration was affected significantly by the varying pilot injection timings, see Figure 6.7. This is not a very surprising result considering the rather large amount of fuel injected in the pilot. The fuel-air mixture gets rich enough to ignite with the first injection, while the main and post injections occur at the same time for all cases resulting in similar main combustion events. The first part of the combustion, pilot to main injection, is thus prolonged while the rest is unchanged.

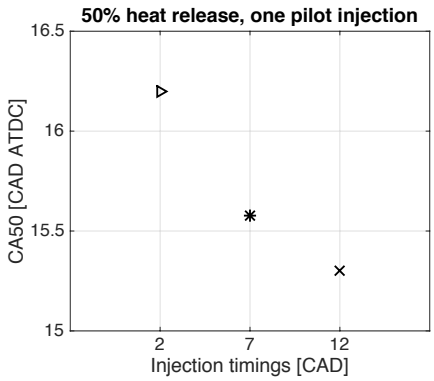

Figure 6.6: Combustion phasing at different pilot injection timing, one pilot injection.

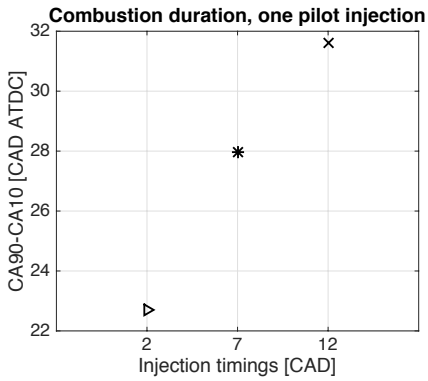

Figure 6.7: Combustion duration varying the pilot injection timing, one pilot injection.

The mentioned combustion characteristics can be clearly seen in Figure 6.8 where representative RoHR curves for the different injection timings are displayed. The peaks corresponding to the respective pilot injections are high, and in the case with the latest pilot injection the pilot is clearly still burning when the main injection is ignited. It also shows that the later, mixing controlled part of the combustion event including the post injection is similar for all cases. This verifies the theory that it is the first part of the combustion that is prolonged rather than the later part.

The losses to the different parts of the engine are presented in Figure 6.9. The same trend can be distinguished for both exhaust, piston oil and cooling water losses. The losses are consistently slightly higher for the earliest and the latest pilot injection tim-

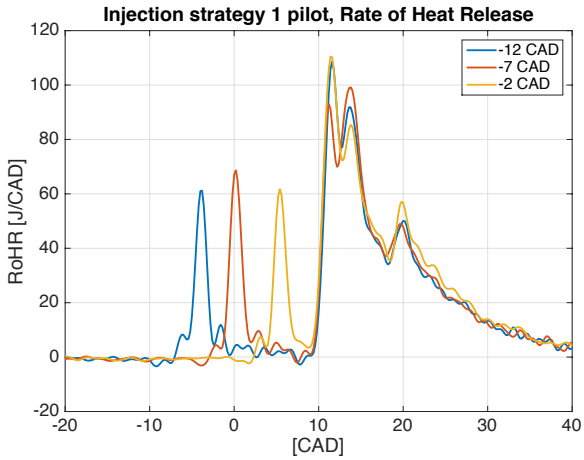

Figure 6.8: Rate of heat release varying the pilot injection timing, one pilot injection.

ing compared to the middle one. Again the differences are very small, but there are similarities between the earliest and latest timing also regarding the RoHR shown in Figure 6.8. Both of them are distinguished by a higher peak at the start of the main combustion. This normally results in higher in-cylinder temperature and higher heat losses, especially to the cylinder head and exhaust.

The energy balance chart presented in Figure 6.10 shows that the indicated work is reduced with earlier pilot injection. This could be related to the longer combustion duration.

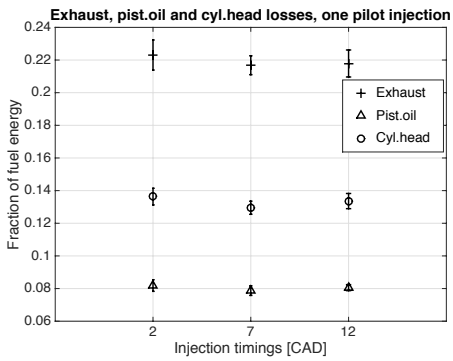

Figure 6.9: Fraction of fuel energy lost to cooling water, piston oil cooling and exhaust varying the pilot injection timing, one pilot injection.

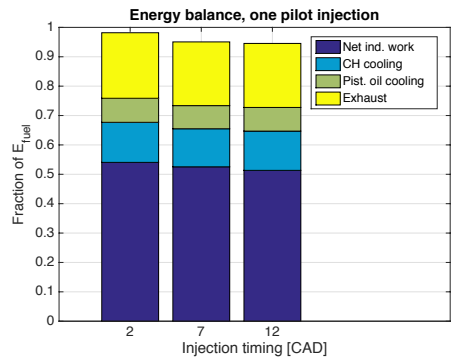

Figure 6.10: Engine energy balance varying the pilot injection timings, one pilot injection.

6.1.3 The effect of no post injection

The only thing separating this test from the baseline case was the lack of a post injection. To preserve the same fuel flow rate as in the previous cases the amount of fuel in the post injection was added to the main injection. Figure 6.11 shows the combustion phasing of the baseline case and the case without post injection. The difference is only approximately 0.5 CAD, with the slightly earlier combustion phasing without post injection. The post injection only contains a small amount of fuel compared to the main injection, so adding this to the main injection should not make a big difference. However, the time from the start of the pilot injection to the end of the last injection is shorter so a slightly earlier CA50 might be expected. On the other hand, the beginning of the combustion event is the same in both cases so it might as well have been that the combustion phasing were exactly the same. The error bars for the two cases overlap to some extent, meaning this result could be a random variation between the samples, especially considering that the mean values only differ about 0.4 CAD.

Figure 6.14 shows the mean combustion durations of the two cases. It is a bit surprising to see that the combustion duration increases by approximately 1 CAD without the post injection. It is a small difference and the error bars overlap somewhat, but it seems to be a real difference. If there is a statistically significant difference or not could be determined with an ANOVA test.

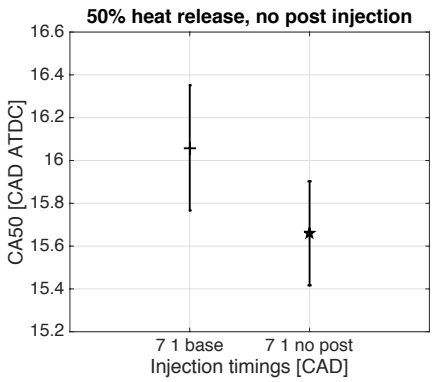

Figure 6.11: Combustion phasing, baseline case and without post injection.

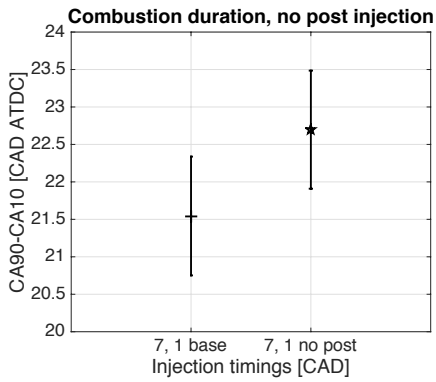

Figure 6.12: Combustion duration, baseline case and without post injection.

It is not obvious what causes this difference, but looking at Figure 6.13 there could be a slightly higher total degree of premixed combustion with the post injection. The post injection occurs while the main injection is burning, and is thus ignited immediately and burns fast. Without the post injection there is more fuel in the main injection. The premixed part looks similar in both cases while the mixing controlled combustion seems to go on slightly longer without the post injection. This is indicated by the RoHR curve for the case without post injection appearing slightly above the post injection case

during the later stage of the combustion. With more premixed combustion the mixture burns faster and, thus, the combustion duration should decrease.

The different parts of the heat losses for both cases are presented in Figure **??**. Exhaust losses are slightly lower without the post injection, which could be related to lower in-cylinder temperatures during the later, mixing controlled combustion. On the other hand this contradicts the previous hypothesis of a longer combustion duration, which should have the opposite effect. Losses to the cylinder head are somewhat increased without the post injection, which could indicate that more of the combustion takes place in the upper part of the combustion chamber. However, there is no evidence of a larger portion of the heat release taking place close to the cylinder head according to the heat release analysis. The piston oil losses also seem to increase slightly without the post injection. This is consistent with the higher cylinder head losses, because more fuel is injected in the bowl and close to the rim. If the combusting spray impinges on this area longer the piston gets hotter and, thus, more heat is transferred to the cooling oil.

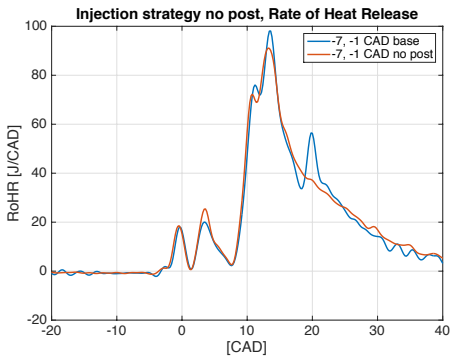

Figure 6.13: Rate of heat release, baseline case and no post injection.

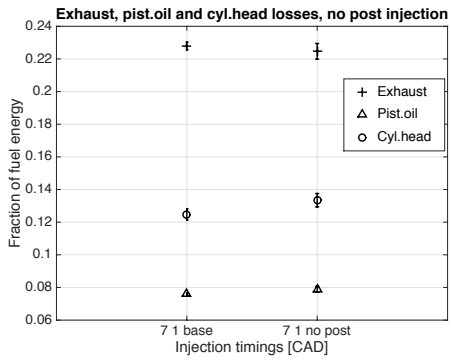

Figure 6.14: Fraction of fuel energy lost to cylinder head coolant, piston oil cooling and exhaust at different pilot injection timing, baseline case and no post injection.

The energy balances for the two cases were almost identical, with only a slight decrease in indicated work without the post injection. The lost work was substituted by an increase in cylinder head heat transfer loss.

Overall, skipping the post injection does not seem to have any major effect on heat losses. Losses to the cylinder head cooling do increase a bit, which slightly affects the net indicated work in a negative way.

6.1.4 Varying fuel fraction in pilot and main injection

Similar to the previous tests, the fuel flow was kept constant. One pilot injection was utilised, but now the injection durations of the pilot and main injections were varied so fuel was reallocated from the main to the pilot injection. The pilot and main injection durations tested are given in Table 6.2.

Table 6.2: Injection duration, pilot-to-main ratio

Pilot [μs]	Main [μs]
210	610
250	590
270	570
280	550
290	530

Figure 6.15 shows how the combustion phasing varies when increasing the fuel fraction in the pilot injection while keeping the total fuel flow constant. As more and more of the fuel is added to the pilot injection, the combustion phasing also gradually occurs earlier. This is quite easily explained considering that there is a gap between the pilot and main injections. Even though the amount of fuel in the pilot is not enough to reach 50 % burned, it will get closer to that point as more fuel is redistributed to the pilot injection.

The combustion durations for the different cases are presented in Figure 6.16. The first two points have similar combustion durations, as well as the last three, but between these two sets there is a sudden jump in duration. This could be a result of the increasing amount of fuel in the pilot injection, so in the first two cases CA10 does not occur until after the start of the main combustion, whereas in the last three cases it occurs already during the larger pilot injection. The combustion duration is a function of CA10 and CA90, as described in Chapter 5. Thus, if CA10 is reached during the pilot rather than the main combustion, the combustion duration will increase significantly.

The resulting RoHR for the different cases are presented in Figure 6.17. The peak corresponding to the pilot injection is increasing in height as expected with longer injection duration. The main combustion looks relatively unaffected by the reducing amount of fuel, the variations seem more random than related to decreased energy content. The only one standing out is the case with the shortest pilot and longest main injection, which has a higher main peak. A trend could have been expected with lower main peaks with shorter injection durations, but the variation within the samples is too large to reveal any such trend.

The losses to the considered parts of the engine are shown in Figure 6.18. The differences are so small it is difficult to find any obvious trends. There could be a slight trend of less exhaust losses with more fuel reallocated to the pilot injection, but the error bars cover so much of the span it cannot be concluded that there is a significant difference.

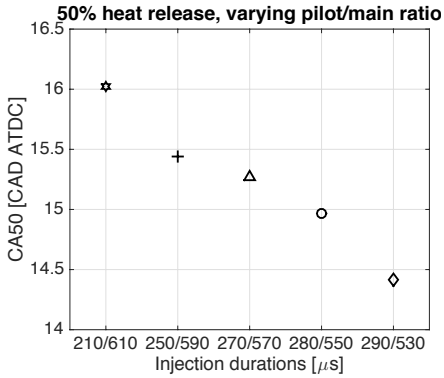

Figure 6.15: Combustion phasing, varying pilot/main ratio.

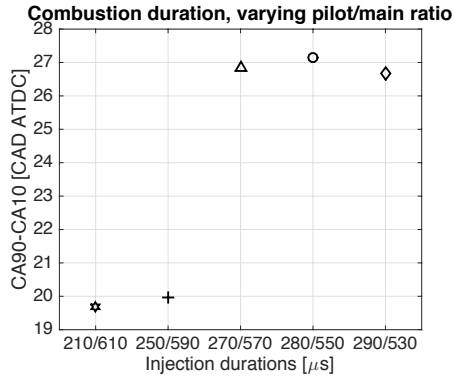

Figure 6.16: Combustion duration, varying pilot/main ratio.

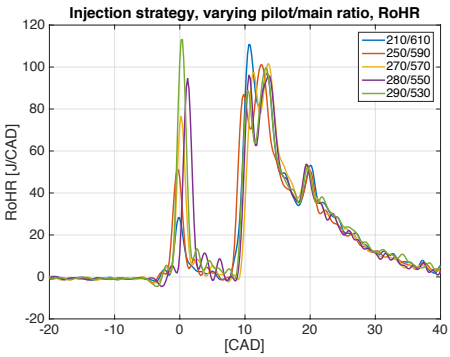

Figure 6.17: Rate of heat release at different pilot/main injection ratios.

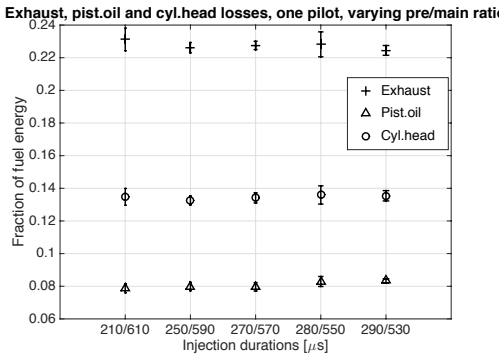

Figure 6.18: Fraction of fuel energy lost to exhaust, cylinder head cooling, and piston oil cooling at different pilot/main injection ratios.

The energy balance confirms the conclusion that the differences are too small to be of any real importance.

In conclusion, as far as heat losses are concerned neither the pilot injection timings, the existence of a post injection or the amount of fuel in the pilot injection is very important. Thus, the injection strategy can be optimised for other purposes than heat transfer, *e.g.* noise or emission reduction.

6.2 Heat transfer study of the baseline configuration

The literature study revealed that many different parameters can have an effect on the heat transfer distribution in the engine. However, many of the studies were performed with new combustion concepts, and not CDC mode. Many of them also focused on CFD studies rather than experimental work. Studies of light duty engine configurations have been made, but there seems to have been a larger interest in HD applications. This especially applies to combustion chamber geometries and swirl studies. Very few examples were found in the literature concerning spray-swirl interactions, so that was one major point of interest. In conclusion, there was a lack of experimental studies concerning the effect combustion system parameters have on the distribution of heat losses to the cooling media in LD diesel engines using CDC mode, and how to redirect them to the exhaust where the heat can be recovered. These factors constituted the main motivation behind the studies presented in Papers I, II and III. Using the original engine configuration a speed- and load test as well as several parameter sweeps were performed to see their respective effects on heat transfer. The purpose of the study in Paper I was to find out how various combustion system parameters affects heat losses in a LD engine operated in CDC mode. Another benefit of this study was to serve as a baseline case to be compared with the modified engine configurations tested later. All engine configurations were tested according to the same scheme, with one speed- and load test and four parameter sweeps including rail pressure, swirl, EGR and λ.

6.2.1 Speed and load effects

Three different combinations of two engine speeds and two load cases were performed. The three combinations were described in Table 5.2 in Chapter 5. All cases were performed at 1250 bar rail pressure.

The losses to exhaust, cylinder head cooling and piston oil cooling are presented in Figure 6.19. The speed-load test showed that exhaust losses are largest for the high speed, high load case, while the low speed, low load case experience significantly less exhaust losses compared to the high load cases. This indicates that load has a greater impact on exhaust losses than speed. Higher speed increases the combustion duration, resulting in hotter exhaust gases and, thus, increased heat losses to the exhaust gas. Heat losses to the piston cooling and to some extent the cylinder head increases with lower speed and load. At high speed and load the lower piston cooling loss could be due to combustion being less confined to the piston bowl and more spread out towards the cylinder head compared to the lower speed cases.

6.2.2 Parameter sweeps

Four parameter sweeps were performed: rail pressure, swirl, EGR and λ. All sweeps were performed at conditions corresponding to Case 2 in the speed-load test. During

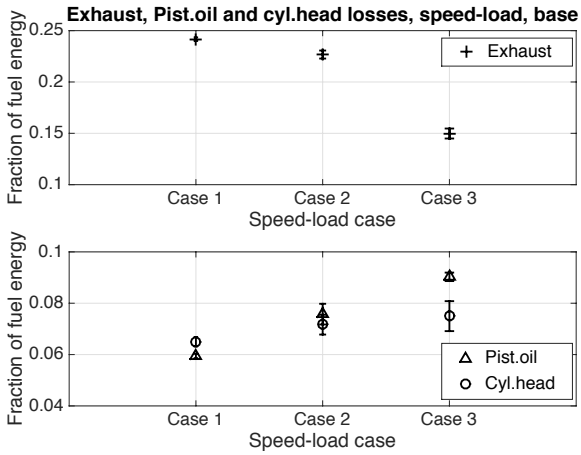

Figure 6.19: Engine heat losses for the different speed-load cases.

the rail pressure sweep the injection durations were adjusted to keep a constant fuel flow.

Rail pressure sweep Rail pressure affects injection duration, spray penetration and impingement but could also have an effect on turbulence. Heat transfer to the different parts of the cooling system and exhaust gas showed that the part of the fuel energy lost to the exhaust gas decreased slightly with higher rail pressure, even though errors were relatively large compared to the difference between the mean values. Higher rail pressure requires shorter injection duration to maintain constant fuel flow, which results in shorter combustion duration and higher RoHR. The peak cylinder temperature was also higher. These factors contribute to higher in-cylinder temperature and thus, increased wall heat transfer. The shorter combustion duration at higher rail pressures means that less heat is lost to the exhaust gas. A longer combustion duration results in lower peak cylinder pressure and temperature.

Similar to the cylinder head losses, piston cooling losses increase slightly with rail pressure. Higher rail pressure gives more wall impingement, which increases piston wall temperature and thus cooling losses. Higher rail pressure may also increase the turbulence level, which according to previous research could increase convective heat transfer.

There were significant differences between the characteristic RoHR for the different rail pressures, see Figure 6.20. In the 500 bar case the pressure trace was much smoother and the main peak lower and broader than in the 2000 bar case, which demonstrates a very tall and narrow main peak. This indicates that the 2000 bar case had a larger portion of premixed combustion than the 500 bar case, which is almost entirely mixing controlled due to the long injection duration.

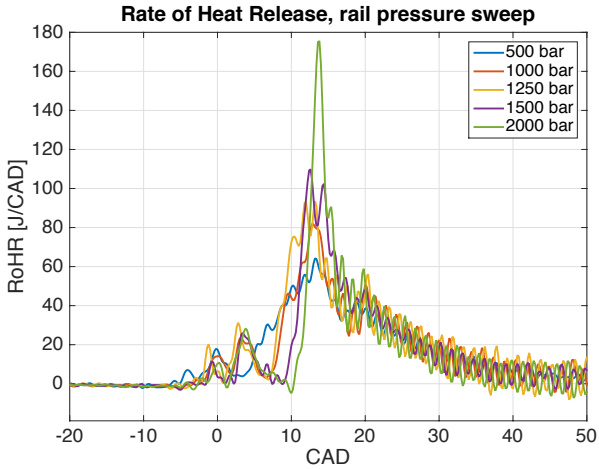

Figure 6.20: Rate of heat release at different rail pressures.

Swirl sweep The swirl sweeps were performed at two rail pressures: 500 and 1250 bar, both with similar results. No discernible effect was found on heat transfer neither to walls nor to cooling media or exhaust gases. These results were also supported by the lack of effect due to swirl on combustion phasing and combustion duration. A few previous studies resulted in similar findings. Fridriksson *et al.* [18] concluded that the CDC bowls in the study showed more heat transfer at high swirl levels than at lower levels, but more open bowl types experienced unchanged or even increased heat transfer at reduced swirl levels. It was also suggested that this behaviour could be explained by the combustion chamber velocity field. For some geometries higher swirl levels seemed to push the high velocity field away from the wall and further into the bowl, while periphery velocity stayed relatively constant. In these cases reduced swirl would have no effect because convective heat transfer would not be affected [18].

EGR sweep Heat loss to the exhaust gas decreased significantly when EGR levels increased. Heat loss to the cylinder head cooling water increased slightly with higher EGR levels, which seems contradictory because in-cylinder temperatures are expected to drop with EGR.

Higher EGR levels prolonged combustion duration, and also caused a rise in inlet temperature. These factors could contribute to the decreasing piston oil heat losses at higher EGR levels. Exhaust losses and piston oil cooling all decrease significantly when the EGR level increases. This is consistent with the theory that in-cylinder temperatures decrease at higher EGR levels. Delayed CA50 and longer combustion duration are said to increase exhaust gas temperatures. However, EGR serves as an inert gas which absorbs heat and should thus reduce heat transfer to the exhaust and cooling media, which is also confirmed by the behaviour of the losses.

The most significant difference in the RoHR for the different EGR levels was the height of the premixed peak, which was taller and slightly earlier at lower EGR levels. It also revealed a slower RoHR for higher EGR levels. Higher EGR levels also decreased the air flow to the engine, reducing the amount of available oxygen which impaired air entrainment into the spray and could, together with reduced temperatures, lead to slower combustion.

Lambda sweep Heat losses to the cylinder head cooling water decreased at higher λ values, while losses to piston cooling oil increased slightly. This can be explained by the earlier combustion phasing found at the higher λ values. Combustion duration was found to increase slightly with higher λ, so the mixing controlled part of the combustion seems to grow somewhat. A leaner charge should keep the in-cylinder temperature down due to the excess air acting as a heat sink, decreasing wall heat transfer. On the other hand the higher pressure should increase the heat transfer coefficient h_c, as described by Equation (2.23). Exhaust losses were found to increase with λ. This could also be an effect of the prolonged combustion duration.

The RoHR showed larger peaks for the lowest and highest λ values. The explanation for the high peak at the lowest λ seems to be that the pilot injections start to burn very late, *e.g.* the first pilot does not ignite at all. As a result, when combustion finally starts it is very aggressive because the pilots have not had the chance to smooth out the ignition. On the other side of the sweep the pilot injections start to burn earlier and have almost finished before the main injection ignites, thus resulting in a taller peak. Gas velocity and turbulence may also play a role, because of throttling to reach lower λ values. Less air is then forced into the cylinder and thus lower gas velocities could be obtained. At higher pressures higher gas velocities could be expected, which then may break up the in-cylinder flow into high turbulence which speeds up combustion.

Summary and conclusions The main conclusions from Paper I were that load had a larger effect on heat losses than speed. Low EGR levels, low rail pressure and high λ increase exhaust temperatures while swirl did not have any effect on this at all.

6.3 Comparison of bowl geometries

It has been stated several times in the literature that the bowl geometry can be of major importance for heat loss characteristics. According to the CFD studies by Fridriksson *et al.* [18] the stepped-bowl geometry could have favourable heat loss characteristics compared to the baseline bowl. It also seemed interesting in terms of response to swirl. This presented another opportunity to study spray-swirl interactions. The study presented in Paper II was performed to see if the CFD findings also applied to a real engine.

Identical parameter sweeps were performed with the conventional baseline bowl and the stepped-bowl, the same as in Paper I. The results were then compared with regard to heat losses to cooling media and exhaust gas. The experimental work consisted of three parts: The previously discussed tests with the baseline geometry, an STP pre-study for the stepped-bowl, and finally the speed-load test and parameter sweeps.

6.3.1 Spray target position

During the baseline bowl tests the nominal nozzle protrusion was used. After switching to the stepped-bowl, an STP test was performed to examine the best nozzle protrusion for this geometry. Due to the importance of STP for emission formation, that was were the main emphasis was. The hypothesis for this pre-study was that the nozzle protrusion should be increased compared to the nominal position because of the geometrical characteristics of the stepped-bowl. An optimised STP would direct fuel both upwards and into the bowl, enabling better use of the oxygen [15, 49]. Four positions were tested at the same speed-load cases as in the speed and load test.

Soot measurements for the stepped-bowl are shown in Figure 6.21. With the stepped-bowl soot emissions decreased significantly with larger nozzle protrusion for all test points. It also confirmed that the stepped-bowl enhances air utilisation and decreases soot emissions. CO emissions also decreased with larger nozzle protrusion in the high load cases, while the low load case had a minimum at nominal nozzle protrusion. CO emissions were still lower than with the baseline bowl at all conditions.

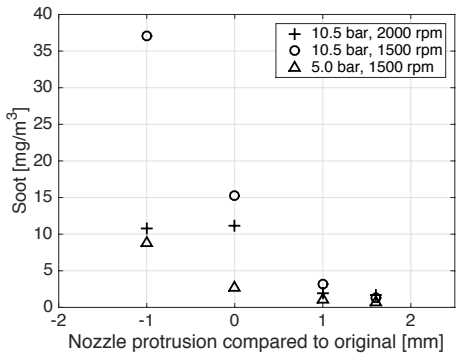

Figure 6.21: Soot emissions for the three speed-load cases with different nozzle protrusions into the stepped-bowl geometry.

6.3.2 Speed and load test

Both piston configurations resulted in much higher exhaust losses in the high load cases and more cooling losses in the two lower speed cases. Especially the piston cooling

loss increased at lower speed and load. For the stepped-bowl the exhaust losses were increased compared to the baseline case, mainly at high speed and load. This bowl also resulted in higher piston cooling losses. The cylinder head cooling losses were similar for the two geometries.

The combustion durations are shown in Figure 6.22. At higher load, regardless of speed, the stepped-bowl gives significantly shorter combustion duration than the baseline bowl. At lower load the combustion duration was similar for both bowls. The engine energy balances in Figure 6.23 showed that for the higher load cases the indicated work was slightly higher with the stepped-bowl, and so were the exhaust losses as previously mentioned. In the low load case the stepped-bowl showed lower indicated work.

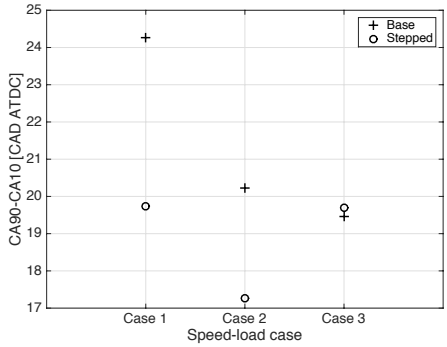

Figure 6.22: Speed-load test combustion duration, both geometries.

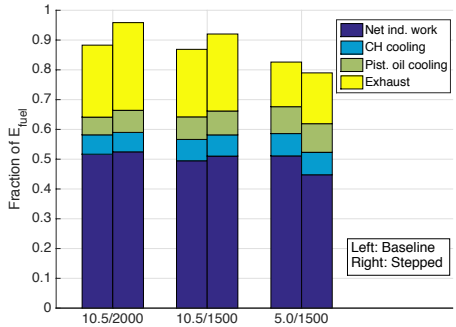

Figure 6.23: Speed-load test energy balance, both geometries. Baseline left and stepped-bowl right in each case.

6.3.3 Parameters

Changing the combustion chamber geometry results in changed in-cylinder flow pattern, which affects both combustion and spray behaviour. To get a better understanding of the characteristics of the stepped-bowl, the four parameter sweeps previously performed with the baseline geometry were performed again with the stepped-bowl.

Rail pressure sweep The two bowl designs showed similar trends for all losses. Exhaust losses decreased as rail pressure increased, while cooling losses increased. This is a result of the shorter injection duration that reduced combustion duration. The stepped-bowl geometry again gave the highest exhaust losses. It also slightly reduced the cylinder head cooling losses, while increasing losses to the piston cooling.

Shorter combustion duration was again achieved with the stepped-bowl. The difference between the geometries even increased with higher rail pressures. The shorter combustion duration, also meaning faster RoHR and higher temperature, could be responsible

for the behaviour of the losses. When more of the combustion occurs in the bowl the piston will get hotter and, thus, cooling oil temperature will increase. The cylinder head cooling losses then decrease, indicating less wall heat transfer to the rest of the combustion chamber, and more heat left in the exhaust.

Swirl sweep During the swirl sweep no discernible effect was found on heat transfer to the exhaust for either geometry. Cylinder head cooling losses increased slightly with higher swirl for both geometries, and so did the piston cooling losses. The swirling motion is predominantly found inside the bowl, so naturally the bowl heat losses should be affected the most. Comparing the two geometries, exhaust losses were slightly higher with the baseline piston. This could be an effect of longer combustion duration. Piston oil losses were similar for both geometries while cylinder head losses were higher with the stepped-bowl. Maybe improved heat transfer characteristics in the stepped-bowl at low swirling conditions could be outweighed by higher gas velocity in the squish region, which could then explain part of the higher cylinder head losses.

CA50 stayed relatively similar for all swirl levels, but there was a slight trend towards earlier CA50 with the stepped-bowl with increased swirl, and the opposite with the baseline geometry. Combustion durations were shorter with the stepped-bowl over the full swirl range. For the stepped-bowl combustion duration was only slightly shorter at the highest swirl levels, suggesting that the combustion was affected very little. In the baseline case, combustion duration was much more affected with shorter combustion at higher swirl levels. Higher swirl rates should speed up the mixing controlled combustion phase and decrease combustion duration.

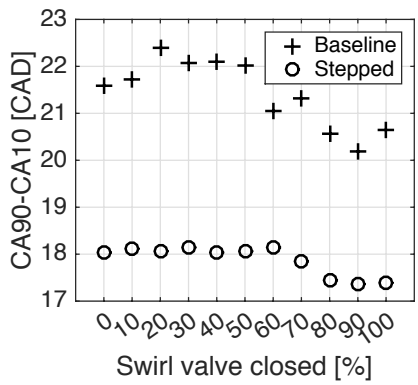

Figure 6.24: Swirl sweep combustion duration for both geometries.

EGR sweep Higher EGR rates decreased in-cylinder temperatures, and, thus, most heat losses. Only the cylinder head cooling losses stayed relatively constant. A difference here was that the stepped-bowl gave less heat losses to the piston cooling, except at the

highest EGR level. Cylinder head cooling losses were also reduced with the stepped-bowl, while exhaust losses were increased. This was the only time the stepped-bowl gave rise to lower in-cylinder temperatures than the baseline bowl. This could explain why the cooling losses were decreased, contrary to the results of the other sweeps.

The rate of heat release showed that for all cases the peak was slightly higher with the stepped-bowl, but the later part of the combustion was also shorter than with the baseline bowl. In the 0% EGR case the shapes of the RoHR were similar, whereas in the other cases the rising edge of the peak was steeper with the stepped-bowl. Again, the stepped-bowl gave faster combustion than the baseline.

Lambda sweep The λ sweep had a large effect on the RoHR with the stepped-bowl. The main peak grew very tall and narrow compared to the baseline geometry. This could be explained by the heat release of the second pilot injection occurring later and closer to the main injection with the stepped-bowl, indicating that they merge into a main combustion peak. This gives rise to very intense and fast combustion, especially at lower λ values. The later part of the mixing controlled combustion was somewhat slower at lower λ values for both geometries. The stepped-bowl gave higher exhaust losses, and heat losses to cooling water were also increased. Higher RoHR normally also increases the in-cylinder temperature, which could explain the consistently higher heat losses to cooling media. Otherwise the trends are quite similar for both geometries.

Throughout this study, the stepped-bowl featured shorter combustion duration and higher exhaust losses than the baseline geometry. In most cases the piston cooling losses were also slightly increased while cylinder head cooling losses were reduced with the stepped-bowl. Except for these differences, the general trends were similar for both geometries.

Summary and conclusions Lessons learned from Paper II were that the stepped-bowl geometry significantly increased exhaust losses, and was less sensitive to swirl in terms of effect on combustion. The stepped-bowl was also found to require a larger nozzle protrusion than the baseline geometry to reduce soot formation.

6.4 Comparison of nozzle configurations

The aim of the work presented in Paper III was to experimentally compare the effect on heat transfer characteristics using three sets of injectors featuring different number of holes. The separation of the sprays as well as the hole size could affect mixing, wall contact and other parameters that influence heat transfer. The same speed-load and parameter sweeps were performed as in the studies in Paper I and II.

6.4.1 Speed and load test

The heat losses to exhaust, cylinder head cooling and piston cooling for the three different speed and load combinations followed the same trends for all injectors. Losses to exhaust and piston cooling were lower with the 8-hole injectors. Cylinder head losses were similar for all injectors, but differed more for the higher load and speed case. The 8-hole injectors showed higher cylinder head loss than the others, and the 6-hole injectors gave the least loss in the high load cases. The 10-hole injectors gave the least cylinder head loss for the low speed and load case.

For all cases the RoHR was lower with the 10-hole injectors, while the other two are relatively similar. Combustion was slower with the 10-hole injectors, except at low load where the peak was significantly narrower. The later part of the combustion was similar to the 8-hole injector case. The 6-hole injectors reduced combustion duration with a taller and narrower RoHR. The later combustion phase was significantly slower with the 10-hole injectors.

The heat release behaviour was reflected in the combustion phasing and duration. The flow characteristics of the injectors were supposed to be similar, but the 6- and 10-hole injectors required longer injection durations to maintain correct fuel flow. This made keeping the combustion phasing constant somewhat difficult, especially at low speed and load. Phasing was constantly later with the 6-hole injectors and mostly earlier with the 8-hole injectors.

The combustion durations reflect the injection durations in the high load cases. The 8-hole injectors had shorter injection duration, but at low load the 6-hole injectors had shorter combustion duration. This was unexpected because of long injection duration and late phasing compared to the other injectors.

The engine energy balance showed similar net indicated work for all injectors at high load. The 8-hole injectors generally presented less total heat loss than the others. At low load the work differed between the injectors, with lowest for the 6-hole injectors and highest for the 10-hole injectors.

6.4.2 Parameter sweeps

In order to be able to compare results, the same parameter sweeps were performed for the injectors as previously with the piston geometries.

Rail Pressure Sweep Injection durations were adjusted for every set of injectors to achieve the same fuel flow. The 6-hole injectors required the longest injections and the 8-hole injectors the shortest. The 8-hole injectors gave the least exhaust losses, probably due to their shorter combustion duration. Short combustion duration often increases piston cooling losses, which were highest with the 6-hole injectors. This could also be an effect of different penetration length. The larger holes of the 6-hole injectors

could give a longer penetration so a larger bowl area gets in contact with the burning spray, giving rise to higher piston cooling losses.

The RoHR showed that the 6-hole injectors gave the tallest peak and shortest late part of combustion. This also shows in the combustion duration. The 10-hole injectors had slower combustion than the others. At lower rail pressures the 6-hole injectors were fastest burning, but from 1250 bar rail pressure and up the 6- and 8-hole injectors give similar results.

The 6-hole injectors gave rise to the highest NO_x emissions, as shown in Figure 6.25. This was probably connected to the faster combustion. The 8- and 10-hole injectors gave similar results for all rail pressures.

There were significant differences in soot emissions between the 6- and 10-hole injectors. At low rail pressures the 10-hole injectors had significantly higher soot emissions than the 6-hole injectors.

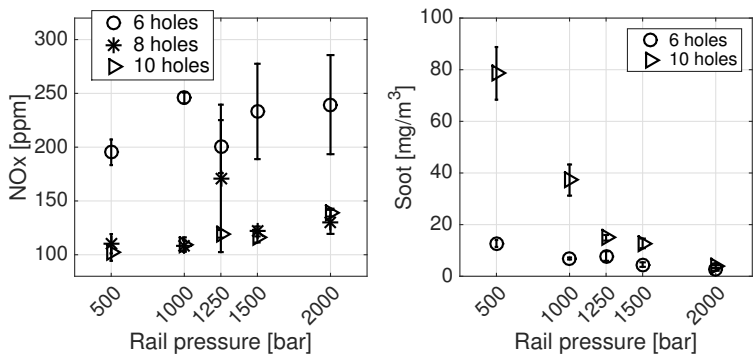

Figure 6.25: Engine out NO_x (left) and soot (right) at different rail pressures.

Swirl sweep Exhaust losses rarely seemed to be affected at all by the swirl level, which is consistent with the findings in Paper I and II. As shown in Figure 6.26 the 6-hole injectors gave rise to less exhaust loss than the other two, which are both on similar levels. Heat loss to the piston oil cooling was similar for the 6- and 10-hole injectors, but higher for the 8-hole injectors. The cylinder head loss follows the same trend, even if the differences are small.

The RoHR and combustion phasing were almost unaffected by swirl level. All injectors showed decreasing combustion duration at higher swirl levels. The 8-hole injectors had the fastest combustion, then 6-holes and 10-holes.

The energy balances did not show any discernible differences between the injectors. The main differences were the distribution of heat losses and the combustion duration, where the 6-hole injectors generally were fastest and the 10-hole injectors slowest.

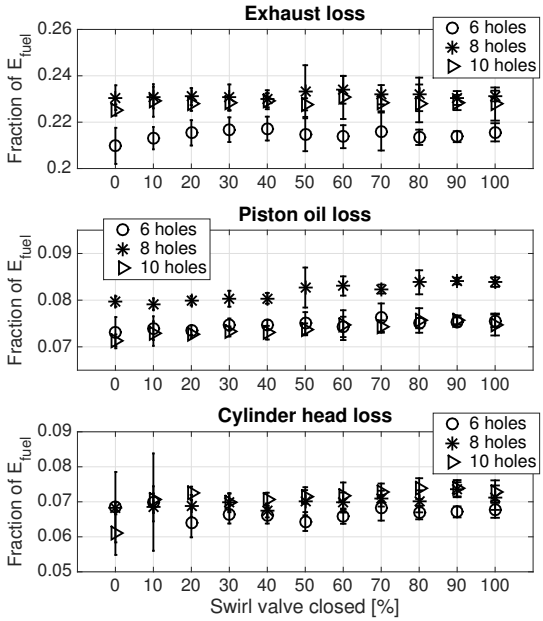

Figure 6.26: Fraction of fuel energy lost to cylinder head coolant, piston oil cooling and exhaust at different swirl levels.

EGR sweep The slight differences in EGR levels between the tree injector geometries were considered small enough to not have any significant effect on the result. The 8-hole injectors consistently gave the least exhaust losses, while the other two gave similar loss levels. Piston cooling losses were highest with the 6-hole injectors, which also had the least cylinder head losses. Highest cylinder head losses were given by the 8-hole injectors, but the 10-hole injectors increased those losses most at higher EGR levels.

The 6-hole injectors gave the fastest combustion and the 10-hole injectors the slowest. With the 8-hole injectors phasing was delayed more with EGR than with the other injectors, which resulted in even slower combustion duration.

The RoHR showed faster mixing controlled combustion phase for the 6-hole injectors, more at higher EGR levels. The main peak was similar for all injectors, the main difference was in the later part. This could explain why the cylinder head losses increase with EGR level for the 10-hole injectors. The energy balance revealed that despite slow combustion, the 10-hole injectors gave the highest indicated work at all EGR levels. This differs from the other parameter sweeps.

Lambda sweep During the λ sweep the exhaust losses increased at higher λ values for all injectors. The 10-hole injectors showed the highest exhaust losses and the 8-hole injectors the lowest. Piston cooling losses were highest with the 6-hole injectors,

but decreased at the highest λ value. With the 8-hole injectors piston cooling losses increased with λ, while they were unaffected with the 10-hole injectors. Cylinder head losses decreased with higher λ values for all injectors, but were generally lowest with the 8-hole injectors.

The RoHR demonstrated shorter combustion for the 6-hole injectors, which also had earlier start of combustion. The 10-hole injectors consistently had a lower main peak. Higher λ values resulted in earlier combustion phasing, but mostly for the 8-hole injectors. Combustion duration was shorter with 6-hole injectors and longer with 10-hole injectors.

The energy balance showed that net indicated work increased with λ. The extracted work was similar for all injectors, but mostly slightly lower with the 10-hole injectors. NO_x and soot emissions are presented in Figure 6.27. NO_x levels were highest with the 6-hole injectors and lowest with the 8-hole injectors. At lower λ soot levels were much higher with the 10-hole injectors than with 6-hole injectors, but at higher λ levels both injectors were comparable.

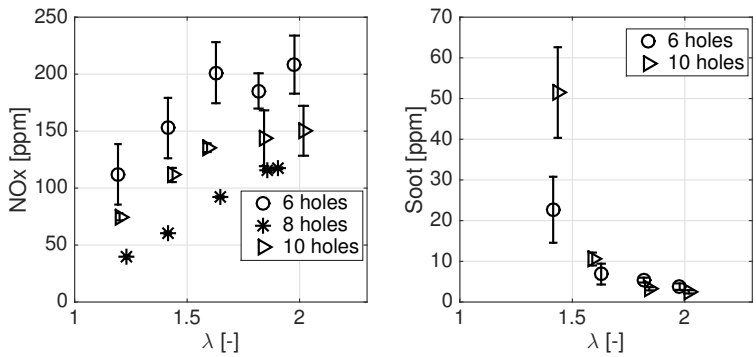

Figure 6.27: Engine out NO_x (left) and soot (right) at different λ values.

Summary and conclusions The results from Paper III showed that number of injector holes had some effect on heat transfer. A larger number of smaller holes increased combustion duration and exhaust losses, with a slight penalty of less work.

Chapter 7

Conclusions

Engine heat transfer has been studied in many ways for a long time. Despite this, a lack of understanding of heat losses in modern light duty diesel engines operated in conventional diesel combustion mode was identified. With increasing demands on engine efficiency, a significant interest in waste heat recovery systems has emerged. Thereby incentives for directing heat losses towards the exhaust rather than the cooling system have arisen.

Compression ignition engines are known for their soot-NO_x trade off. Avoiding soot easily increases NO_x emissions and vice versa. If the combustion process is designed to avoid soot, there is a need for a NO_x after treatment system, which requires rather high light-off temperatures. Until the correct temperature is reached, it does not work properly. Higher exhaust temperatures reduce the time before sufficient NO_x reduction is achieved.

The literature study also revealed that many different parameters can have an effect on the heat transfer distribution in the engine. However, very few examples were found in the literature concerning spray-swirl interactions. The in-cylinder flow-field greatly affects combustion and spray behaviour, and should thus be of utmost importance for heat transfer.

7.1 Achieving high exhaust temperature in a CDC engine

If high exhaust temperature is the goal, there are several ways to adjust the combustion system parameters to achieve this. The number one suggestion would be to use a wide and shallow bowl geometry, such as the stepped-bowl. Two piston geometries were tested, and the stepped-bowl consistently gave higher exhaust temperatures than the

re-entrant bowl. It was also less affected by swirl level. The stepped-bowl featured low soot levels with correct STP, but also high NO_x emissions.

The EGR level also had a significant effect on in-cylinder temperature and, thus, also exhaust temperature. Low EGR levels resulted in high temperatures, but this also increased NO_x emissions.

Speed and load both increased exhaust temperature, but high load had a much more significant effect than high speed. This could be a bonus effect when downsizing engines, as more heat will be available in the exhaust to be used in waste heat recovery systems.

Rail pressure was another parameter that affected exhaust heat. Low rail pressures increased combustion duration, giving higher exhaust temperatures and less piston cooling losses. However, slow combustion resulted in higher emissions of soot.

A high air/fuel ratio, λ, increased exhaust temperatures but also the indicated work. This is another effect that is beneficial in terms of downsizing. However, the high temperature increased NO_x emissions, even though the levels plateaued at the higher λ levels.

Nozzle configuration can have an effect on exhaust heat. The tests showed that it seemed to depend on fuel flow rate through the injector almost as much as hole number. A larger number of holes often increased exhaust temperature. Unfortunately it was often at the expense of slightly lower work.

Injection strategies can be varied in many ways. The results showed that with both one and two pilot injections, late injection timing for the pilots and as much fuel as possible in the main injection increased exhaust heat. However, the differences were small so it might be better to adjust the injection strategy to fulfil other demands such as noise and emissions.

Swirl was not found to have any effect at all on exhaust temperature. It did affect cooling losses, but not to any significant extent in this engine.

7.2 Suggestions for a WHR engine

One of the general trends today is downsizing. A smaller engine is operated at a higher load and more excess air, which improves efficiency. After Euro 6 there is also a trend of reducing EGR levels and letting engine out NO_x increase, because a NO_x after treatment system will anyway be necessary. These trends will, according to the studies presented in this thesis, increase exhaust temperatures. Another trend is towards higher rail pressures. The main purpose with high rail pressure is to reduce soot formation, but as evident by the presented results this will also reduce the fraction of heat lost to exhaust gases.

An engine designed for using a WHR system is suggested to be downsized to run at high load an high levels of excess air. Besides increasing exhaust heat loss this also improves

efficiency. The combustion chamber should be of a wide and shallow type, such as the stepped-bowl tested in this work. The combustion system should be designed to oxidise soot without the need for high rail pressures, which reduce exhaust heat loss. This would also improve mechanical efficiency.

Bibliography

[1] M.J. Abedin, H.H. Masjuki, M.A. Kalam, A. Sanjid, S.M.A. Rahman, and B.M. Masum. Energy balance of internal combustion engines using alternative fuels. *Renewable and Sustainable Energy Reviews*, 26:20–33, 2013.

[2] K. Anandavelu, N. Alagumurthi, and C.G. Saravannan. Performance, combustion, and emission characteristics of a low heat loss diesel engine operated on eucalyptus oil and diesel fuel blends. *Energy Sources, Part A: Recovery, Utilization and Environmental Effects*, 36(15):1697–1709, 2014.

[3] Ö. Andersson. *Experiment!* John Wiley & Sons, Ltd, 2012.

[4] Ö. Andersson and P. C. Miles. *Diesel and Diesel LTC Combustion.* John Wiley & Sons, Ltd, 2014.

[5] W.J.D. Annand. Heat transfer in the cylinders of reciprocating internal combustion engines. In *Proceeding of the Institution of Mechanical Engineers*, volume 177, pages 983–90, 1963.

[6] A. Aziz Hairuddin, A.P. Wandel, and T. Yusaf. Effect of different heat transfer models on a diesel homogeneous charge compression ignition engine. *International Journal of Automotive and Mechanical Engineering*, 8(1):1292–1304, 2013.

[7] Y. Bakhshan and A.H. Shadaei. Quasi-dimensional modeling of a cng fueled hcci engine combustion using detailed chemical kinetic. *Journal of Applied Fluid Mechanics*, 6(2):239–247, 2013.

[8] M. Bargende, G. Hohenberg, and G. Woschni. An equation for calculating transient heat-transfer in spark ignition engines. In *Proceedings of Eurotherm*, volume 15, pages 163–178, 1991.

[9] L. Cao, A. Bhave, H. Su, S. Mosbach, M. Kraft, A. Dris, and R.M. McDavid. Influence of injection timing and piston bowl geometry on PCCI combustion and emissions. *SAE Technical Papers*, pages 1019–1033, 2009.

[10] S.H. Chan and K.A. Khor. Effect of thermal barrier coated piston crown on engine characteristics. *Journal of Materials Engineering and Performance*, 9(1):103–109, 2000.

[11] D. Crabb, M. Fleiss, J.E. Larsson, and J. Somhorst. New modular engine platform from Volvo. *MTZ*, 74:4–11, 2013.

[12] C.L. Cummins. *Internal fire*. Carnot Press, 1976.

[13] S. Das and C. E. Roberts. Factors affecting heat transfer in a diesel engine: Low heat rejection engine revisited. 04 2013. doi: 10.4271/2013-01-0875.

[14] A.B. Dempsey, N. Ryan Walker, and R. Reitz. Effect of piston bowl geometry on dual fuel reactivity controlled compression ignition (RCCI) in a light-duty engine operated with gasoline/diesel and methanol/diesel. *SAE International Journal of Engines*, 6(1):78–100, 2013.

[15] J.G. Dolak, Y. Shi, and R. Reitz. A computational investigation of stepped-bowl piston geometry for a light duty engine operating at low load. *SAE Technical Papers*, 2010.

[16] C. Eiglmeier, H. Lettmann, G. Stiesch, and G.P. Merker. A detailed phenomenological model for wall heat transfer prediction in diesel engines. *SAE Technical Papers*, 2001.

[17] M. Fathi, R.K. Saray, and M.D. Checkel. The influence of exhaust gas recirculation (egr) on combustion and emissions of n-heptane/natural gas fueled homogeneous charge compression ignition (HCCI) engines. *Applied Energy*, 88(12):4719–4724, 2011.

[18] H.S. Fridriksson, M. Tuner, Ö. Andersson, B. Sunden, H. Persson, and M. Ljungqvist. Effect of piston bowl shape and swirl ratio on engine heat transfer in a light-duty diesel engine. *SAE Technical Papers*, 1, 2014.

[19] E. Gingrich, J. Ghandhi, and R. Reitz. Experimental investigation of piston heat transfer in a light duty engine under conventional diesel, homogeneous charge compression ignition, and reactivity controlled compression ignition combustion regimes. *SAE International Journal of Engines*, 7(1):375–386, 2014.

[20] T. Hashizume, S. Ishiyama, T. Ogawa, T. Tomoda, M. Kono, and K. Inagaki. Low cooling heat loss and high efficiency diesel combustion using restricted in-cylinder flow. pages 43–49, 2012.

[21] M. Heinle, M. Bargende, and H.J. Berner. Some useful additions to calculate the wall heat losses in real cycle simulations. *SAE Technical Papers*, 2012.

[22] T. Hejwowski and A. Weronski. The effect of thermal barrier coatings on diesel engine performance. *Vacuum*, 65(3-4):427–432, 2002.

[23] J. B. Heywood. *Internal Combustion Engine Fundamentals*. McGraw-Hill, Inc., 1988.

[24] G. F. Hohenberg. Advanced approaches for heat transfer calculations, 02 1979. SAE paper 790825.

[25] International Energy Agency IEA. 2015 key world energy statistics, 2015.

[26] B. Johansson, Ö. Andersson, P. Tunestål, and M. Tunér. *Combustion Engines*. Media-Tryck Lund, 2014.

[27] A.P. Kleemann and A.D. Gosman. Heat transfer sensitivity study for an advanced diesel engine. *SAE Technical Papers*, 2003.

[28] S. Kokjohn, R. Hanson, D. Splitter, J. Kaddatz, and R. Reitz. Fuel reactivity controlled compression ignition (RCCI) combustion in light- and heavy-duty engines. *SAE International Journal of Engines*, 4(1):360–374, 2011.

[29] M. Kono, M. Basaki, M. Ito, T. Hashizume, S. Ishiyama, and K. Inagaki. Cooling loss reduction of highly dispersed spray combustion with restricted in-cylinder swirl and squish flow in diesel engine. *SAE Technical Papers*, 2012.

[30] F. Köpple, D. Seboldt, P. Jochmann, A. Hettinger, A. Kufferath, and M. Bargende. Experimental investigation of fuel impingement and spray-cooling on the piston of a gdi engine via instantaneous surface temperature measurements. *SAE International Journal of Engines*, 7(3), 2014.

[31] S. Kumar, M. Kumar Chauhan, and Varun. Numerical modeling of compression ignition engine: A review. *Renewable and Sustainable Energy Reviews*, 19:517–530, 2013.

[32] G. Mavropoulos and D. Hountalas. Exhaust phases in a DI diesel engine based on instantaneous cyclic heat transfer experimental data. *SAE Technical Papers*, 2, 2013.

[33] G.C. Mavropoulos, C.D. Rakopoulos, and D.T. Hountalas. Experimental assessment of instantaneous heat transfer in the combustion chamber and exhaust manifold walls of air-cooled direct injection diesel engine. *SAE Technical Papers*, 2008.

[34] G.C. Mavropoulos, C.D. Rakopoulos, and D.T. Hountalas. Experimental investigation of instantaneous cyclic heat transfer in the combustion chamber and exhaust manifold of a DI diesel engine under transient operating conditions. *SAE Technical Papers*, 2009.

[35] A.J. Modi and D.C. Gosai. Experimental study on thermal barrier coated diesel engine performance with blends of diesel and palm biodiesel. *SAE International Journal of Fuels and Lubricants*, 3(2):246–259, 2010.

[36] Y.S.H. Najjar. Protection of the environment by using innovative greening technologies in land transport. *Renewable and Sustainable Energy Reviews*, 26:480–491, 2013.

[37] Complete Dictionary of Scientific Biography. Nusselt, Ernst Kraft Wilhelm, 2008. http://www.encyclopedia.com/doc/1G2-2830903203.html. Retrieved 2014-11-11.

[38] H. Osada, N. Uchida, K. Shimada, and Y. Aoyagi. Reexamination of multiple fuel injections for improving the thermal efficiency of a heavy-duty diesel engine. *SAE Technical Papers*, 2, 2013.

[39] F. Payri, X. Margot, A. Gil, and J. Martin. Computational study of heat transfer to the walls of a DI diesel engine. *SAE Technical Papers*, 2005.

[40] F. Perini, A. Dempsey, R. Reitz, D. Sahoo, and et al. A computational investigation of the effects of swirl ratio and injection pressure on mixture preparation and wall heat transfer in a light-duty diesel engine. *SAE Technical Papers*, 2013.

[41] B.R. Prasath, P. Tamilporai, and M.F. Shabir. Theoretical modeling and experimental study of combustion and performance characteristics of biodiesel in turbocharged low heat rejection D.I diesel engine. *World Academy of Science, Engineering and Technology*, 37:435–445, 2010.

[42] W. Qiong, Z. Xin, J. Pinwen, and L. Jianhua. Comparison of a radiation model with experiment in a diesel engine. *SAE Technical Papers*, 1998.

[43] M.A. Said, D.R. Buttsworth, and T.F. Yusaf. A review of radiation heat transfer measurement for diesel engines using the two-colour method. pages 202–207, 2009.

[44] M.F. Shabir, P. Tamilporai, and B. Rajendra Prasath. Analysis of combustion, performance and emission characteristics of turbocharged LHR extended expansion DI diesel engine. *World Academy of Science, Engineering and Technology*, 61:60–71, 2010.

[45] A. Sharief, T.K. Chandrashekar, A.J. Antony, and B.S. Samaga. Study on heat transfer correlation in IC engines. *SAE Technical Papers*, 2008.

[46] I. Sher, D. Levinzon-Sher, and E. Sher. Miniaturization limitations of HCCI internal combustion engines. *Applied Thermal Engineering*, 29(2-3):400–411, 2009.

[47] S. Skeen, J. Manin, L. Pickett, K. Dalen, and A. Ivarsson. Quantitative spatially resolved measurements of total radiation in high-pressure spray flames. *SAE Technical Papers*, 1, 2014.

[48] D. Splitter, M. Wissink, S. Kokjohn, and R. Reitz. Effect of compression ratio and piston geometry on RCCI load limits and efficiency. *SAE Technical Papers*, 2012.

[49] J. Styron, B. Baldwin, B. Fulton, D. Ives, and S. Ramanathan. Ford 2011 6.7l power stroke®diesel engine combustion system development. *SAE Technical Papers*, 2011.

[50] J. Sun, J.A. Bittle, and T.J. Jacobs. Influencing parameters of brake fuel conversion efficiency with diesel / gasoline operation in a medium-duty diesel engine. *SAE Technical Papers*, 2, 2013.

[51] B. Sundén. *Värmeöverföring*. Studentlitteratur, 2006.

[52] I. Taymaz. The effect of thermal barrier coatings on diesel engine performance. *Surface and Coatings Technology*, 201(9-11 SPEC. ISS.):5249–5252, 2007.

[53] J. Tiainen, I. Kallio, A. Leino, and R. Turunen. Heat transfer study of a high power density diesel engine. *SAE Technical Papers*, 2004. cited By 0.

[54] A. Uzun, I. Çevik, and M. Akçil. Effects of thermal barrier coating on a turbocharged diesel engine performance. *Surface and Coatings Technology*, 116-119:505–507, 1999.

[55] C.J. Weingartz, C.L. Anderson, and S.A. Miers. Determination of heat transfer augmentation due to fuel spray impingement in a high-speed diesel engine. *SAE Technical Papers*, 2009.

[56] A. Wimmer, R. Pivec, and T. Sams. Heat transfer to the combustion chamber and port walls of IC engines - measurement and prediction. *SAE Technical Papers*, 2000.

[57] G. Woschni. A universally applicable equation for the instantaneous heat transfer coefficient in the internal combustion engine. 02 1967. SAE paper 670931.

[58] G. Woschni. Determination of local heat transfer coefficients at the piston of a high speed diesel engine by evaluation of measured temperature distribution. 02 1979. SAE paper 790834.

[59] Y. Wu, B. Chen, and F. Hsieh. Heat transfer model for small-scale air-cooled spark-ignition four-stroke engines. *International Journal of Heat and Mass Transfer*, 49(21 - 22):3895 – 3905, 2006.

Nomenclature

Abbreviations

ANOVA	Analysis of Variance
ATDC	After top dead centre
BDC	Bottom dead centre
BMEP	Brake mean effective pressure
BSFC	Brake specific fuel consumption
$BSNO_x$	Brake specific NO_x
BTDC	Before top dead centre
CA10	Crank angle for 10 % of total heat release
CA50	Crank angle for 50 % of total heat release
CA90	Crank angle for 90 % of total heat release
CAD	Crank angle degree
CDC	Conventional diesel combustion
CDCC	Conventional diesel combustion chamber
CFD	Computational fluid dynamics
CI	Compression ignition
CLMEP	Combustion loss mean effective pressure
CO	Carbon monoxide
CO_2	Carbon dioxide
DI	Direct injection
DoE	Design of experiment
EGR	Exhaust gas recirculation
EVO	Exhaust valve opening
EXMEP	Exhaust mean effective pressure
FMEP	Friction mean effective pressure
FuelMEP	Fuel mean effective pressure
HC	Hydrocarbon
HCCI	Homogeneous charge compression ignition
HD	Heavy duty
HTMEP	Heat transfer mean effective pressure
ICE	Internal combustion engine
IMEP	Indicated mean effective pressure
IVC	Inlet valve closing
LD	Light duty
LHR	Low heat rejection
LTC	Low temperature combustion
MEP	Mean effective pressure
NO_x	Nitrogen oxides, NO and NO_2 combined
PCCI	Premixed charge compression ignition
PMEP	Pump mean effective pressure

PPC	Partially premixed combustion
QMEP	Heat mean effective pressure
rpm	Revolutions per minute
RoHR	Rate of heat release
SI	Spark ignition
SOC	Start of combustion
SOI	Start of injection
STP	Spray target position
TDC	Top dead centre
WHR	Waste heat recovery

Symbols

A	Area
B	Bore
C_p	Specific heat at constant pressure
C_v	Specific heat at constant volume
ϵ	Dissipation per time and mass unit
η	Efficiency
γ	Specific heat ratio (C_p/C_v)
h_c	Heat transfer coefficient
k	Thermal conductivity
λ	Relative air/fuel ratio
l_I	Integral scale
l_K	Kolmogorov scale
l_M	Micro scale
L	Characteristic length
m	Mass
μ	Dynamic viscosity
ν	Kinematic viscosity
N	Engine speed or number of measurements
n_T	Stroke factor
Nu	Nusselt number
ϕ	Relative fuel/air ratio
p	Pressure
P	Power
q or Q	Heat
$\dot{Q}$	Heat flow
Q_{LHV}	Lower heating value
R	Specific gas constant
Re	Reynolds number
ρ	Density
R_x	Autocorrelation coefficient
σ	Stefan-Boltzmann constant
$\bar{S}_p$	Mean piston speed
θ	Crank angle
t or τ	Time
T or t	Temperature
T_C	Temperature cold fluid
T_H	Temperature hot fluid
U	Internal energy
$\bar{U}$	Mean velocity
v	Velocity
V	Volume
V_D	Displaced volume

w	Local average in-cylinder gas velocity
W	Work

Scientific publications

Author contributions

Paper i: Effects of Spray-Swirl Interactions on Heat Losses in a Light Duty Diesel Engine

The objective was to investigate the influence of speed, load, rail pressure, swirl, EGR and λ on heat losses to cooling media and exhaust gases in a light duty diesel engine operated in conventional diesel combustion mode. Load had a greater influence than speed. High rail pressure decreased combustion duration and heat loss to the exhaust. Swirl had no distinguishable effect on heat losses. EGR gave longer combustion duration and less exhaust heat loss. Increased λ reduced combustion duration but increased temperature.

The author performed the experiments, analysed the data and wrote the paper.

Paper ii: Experimental Comparison of Heat Losses in Stepped-Bowl and Re-Entrant Combustion Chambers in a Light Duty Diesel Engine

Two piston bowl geometries were compared during conventional diesel combustion in a light-duty diesel engine: A conventional re-entrant bowl and a wider, shallower stepped-bowl. The stepped-bowl reduced combustion duration and increased exhaust losses.

The author performed the experiments, analysed the data and wrote the paper.

Paper iii: Experimental Comparison of Heat Losses in a Light Duty Diesel Engine with Various Injector Geometries

Three sets of injectors with 6, 8, and 10 holes, respectively, were tested in a light duty diesel engine operated in conventional diesel combustion mode. In general, a larger

number of holes gave longer combustion duration and higher exhaust losses. With the 10-hole injectors, combustion was significantly affected by swirl and thus soot levels were greatly reduced.

The author performed the experiments, analysed the data and wrote the paper.

Paper i

Proceedings of the ASME 2015 International Mechanical Engineering Congress and Exposition
IMECE2015
November 13-19, 2015, Houston, Texas

IMECE2015-53606

EFFECTS OF SPRAY-SWIRL INTERACTIONS ON HEAT LOSSES IN A LIGHT DUTY DIESEL ENGINE

Jessica Dahlström*
Division of Combustion Engines
Department of Energy Sciences
Lund University
Lund, Sweden
Email: jessica.dahlstrom@energy.lth.se

Öivind Andersson
Martin Tunér
Division of Combustion Engines
Department of Energy Sciences
Lund University
Lund, Sweden
oivind.andersson@energy.lth.se
martin.tuner@energy.lth.se

Håkan Persson
Diesel Concepts & Attributes
VOLVO CAR CORPORATION
SE-405 31 Göteborg, Sweden
hakan.hp.persson@volvocars.com

ABSTRACT

Heat loss is one of the greatest energy losses in engines. More than half of the heat is lost to cooling media and exhaust losses, and they thus dominate the internal combustion engine energy balance. Complex processes affect heat loss to the cylinder walls, including gas motion, spray-wall interaction and turbulence levels. The aim of this work was to study and improve the heat transfer characteristics of conventional diesel combustion. Speed, load, injection pressure, swirl level, EGR rate and air/fuel ratio (λ) were varied in a multi-cylinder engine. Temperature measurements in the engine cooling media were used to set up the engine energy balance and find out how much heat was lost to cooling media in different parts of the engine. Based on these calculations and heat release analysis, conclusions could be drawn regarding how heat losses in different parts of the engine were affected by changes in these parameters. Load was found to be more influential than speed, swirl did not have any effect on heat transfer, and EGR and λ both increased cooling water losses while piston losses were reduced.

NOMENCLATURE

ANOVA Analysis of Variance
CA50 Crank angle at 50 % heat release
CAD ATDC Crank Angle Degrees After Top Dead Centre
CDC Conventional Diesel Combustion
CO_2 Carbon dioxide
EGR Exhaust Gas Recirculation
ICE Internal Combustion Engine
HCCI Homogeneous Charge Compression Ignition
HD Heavy Duty
$IMEP_g$ Gross Indicated Mean Effective Pressure
LD Light Duty
PPC Partially Premixed Combustion
RoHR Rate of Heat Release
λ Relative air/fuel ratio

INTRODUCTION

The global energy consumption is increasing, and despite increased efforts to convert to renewable energy sources, fossil fuel consumption is still on the rise. This also results in increasing emissions of greenhouse gases, such as carbon dioxide (CO_2), which contribute to global warming. Further development of ICEs is central in addressing this problem, and has resulted in large improvements of efficiency and emissions. Further efficiency improvement requires a deeper look into engine heat losses.

Some of the efforts to reduce heat losses concern low heat rejection engines, where all or parts of the combustion chamber walls are coated with a ceramic coating to prevent heat trans-

*Address all correspondence to this author.

fer. However, studies of the effects on engine performance are contradictory. Losses to cooling water are reduced because most of the heat stays inside the combustion chamber, resulting in increased exhaust temperatures [1–4]. Volumetric efficiency often decrease [2–4], even though fuel economy and thermodynamic efficiency are reported to improve [3–6]. There is still a long way to go before this becomes a viable concept.

Reports show that there are significant efficiency differences between different engine sizes. A comparison between heavy duty (HD) and light duty (LD) engines shows that LD engines consistently demonstrate lower efficiencies than HD engines. One explanation could be that they have higher surface to volume ratios [7], but the increased heat losses in LD engines could also be caused by high swirl ratios and less favourable combustion chamber design [8]. However, there are few examples in the literature addressing the role heat transfer may play in this.

Speed and load both have significant effects on heat transfer. Higher engine speed results in less time for heat exchange [9], but at the same time turbulence increases and thus also convective heat transfer [10]. However, several studies confirm that load seems to be more influential than speed [11–14].

High temperature and pressure, long combustion duration and flame-wall interaction was found to cause high heat transfer losses according to Sun *et al.* [14]. Mavropoulos *et al.* [11] found that the heat transfer coefficient varies significantly between different locations in the combustion chamber depending on whether the wall is in contact with the flame front or not. This conclusion is also supported by Kleemann *et al.* [15]. Another way of reducing heat flux is later combustion timing [16] which has also been proven to reduce peak radiation [17], although this could have negative effects on heat losses in some parts of the engine.

Several studies concern the heat transfer characteristics of different bowl geometries. A stepped-bowl piston with low surface-to-volume ratio was found to reduce wall heat transfer [18]. Another research group optimised a chamfered, re-entrant bowl with low swirl and an 8-hole nozzle [19]. This system provided a more uniform equivalence ratio field than the wide re-entrant bowl it was compared to, except along the cylinder liner where a lean region was found to prevent heat loss to the coolant. Fridriksson *et al.* found that the conventional re-entrant diesel geometry in their study had lower thermodynamic efficiency and higher heat losses than more shallow and open geometries, such as the stepped bowl and a tapered, lipless piston [20]. At high load the shallow, open piston bowls displayed more heat transfer in the bowl, while the conventional types showed more bowl-lip heat transfer. This was found to coincide with the location of the hot gases. A low surface-to-volume ratio, often assumed to reduce heat transfer, was only found to directly influence heat transfer before the start of spray-driven combustion. After that, other combustion parameters and turbulence were more influential [20]. The study by Fridriksson *et al.* included the geometry used in the present setup.

The injector nozzle-hole orientation and number of holes have a documented effect on wall heat transfer. These parameters require optimisation with a specific combustion chamber geometry. Reduced injection duration can be achieved with larger hole sizes which increases the rate of heat release (RoHR). This generally improves efficiency, but the effect can be offset by increased heat transfer losses [21].

The most thoroughly investigated gas flow pattern affecting heat transfer is swirl. In general, low swirl levels seem to produce low heat loss [20]. However, different geometries show dissimilar responses to swirl ratio changes, which may be due to different velocity fields. Convective heat flux is related to rotational gas motion, which was mainly found to increase close to the outer walls where spray the momentum is largest at the end of injection. Low swirl was found to reduce heat loss for CDC geometries, while the more open piston geometries experienced increased heat losses as near-wall fluid velocity increased when swirl level decreased [20]. Another CFD study found that high swirl ratios significantly increased wall heat transfer and delayed the ignition timing [22]. An experimental CDC study showed that the mean piston surface temperature increased with higher swirl, suggesting an increased steady state heat transfer component [16]. Eiglmeier *et al.* [23] found that heat flux peaks increased with turbocharging, which was explained by intensified turbulence. The convective heat transfer was also found to increase [23].

EGR has a documented effect on heat transfer. Theoretically, the heat transfer coefficient is proportional to pressure and inversely proportional to temperature. This was also confirmed experimentally by Fathi *et al.* [24]. However, the heat transfer coefficient does not vary significantly with EGR, since increased EGR rates reduce both charge temperature and pressure. Convective heat transfer reduces as a result of the reduced temperature difference between charge and wall [24]. Das *et al.* [21] also obtained significant heat loss reduction with increased EGR, which was explained by the increased charge mass requiring more heat to increase charge temperature.

A field that has not been widely studied is spray-swirl interaction effects on heat transfer, where little can be found in the literature. As mentioned above there is also a lack of understanding of heat transfer as a possible characteristic difference between LD and HD engines. Fig. 1 shows the modelled flow field in a CDC combustion chamber [25]. The high velocity field caused by the swirling motion can be seen as a red area close to the bowl wall. If higher injection pressure generates a motion towards the centre of the bowl of this high velocity field, high swirl levels may not promote heat transfer because high gas velocities will not be found close to the wall. The aim of the present work was to experimentally study heat transfer in a LD engine, by looking into spray-swirl interactions as well as effects of other

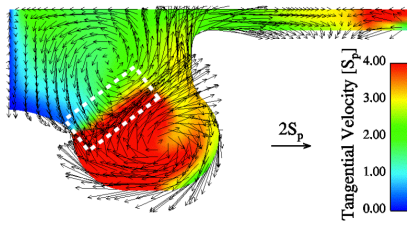

FIGURE 1. MODELLED VELOCITY PROFILE AT 12 CAD ATDC FOR A CDC COMBUSTION CHAMBER AT A CASE WITH HIGH SWIRL [25].

parameters such as λ and EGR. The hypothesis was that there is a balance between injection pressure and swirl rate.

EXPERIMENTAL SETUP

Experiments were performed in a 4-cylinder light-duty engine with Denso injectors. Engine specifications are presented in Table 1. In order to set up the engine energy balance, temperature and mass flow measurements were needed. All cylinders were instrumented with thermocouples for measuring temperature differences in the cooling system. The cylinder head was equipped with T-type thermocouples in all cooling channels for cylinder 3 and 4, the other cylinders only had one on the inlet and one on the exhaust side. Figure 2 shows the thermocouple positions viewed from the exhaust side. One K-type thermocouple was fitted in the feed line to the piston cooling oil rail, and two were fitted in funnel-shaped structures below the pistons to measure the oil return flow temperatures from cylinder 2 and 3. One of these is shown in Figure 3 where the structure and the pipe guiding oil from the piston outlet to the funnel can be seen from below. All cylinders were fitted with Kistler pressure sensors to measure in-cylinder pressure used for the heat release analysis. Exhaust oxygen concentration was measured using an Etas lambda meter. Flow meters were installed to measure the mass flows of cooling water, air, and oil to the piston cooling. Fuel flow was measured using a Sartorius balance.

EXPERIMENTAL METHODOLOGY

Heat transfer to the cooling media was measured at various engine conditions. One speed-load test was performed, and during additional tests the following four parameters were swept: rail pressure, swirl, EGR and λ. The swirl sweep was conducted at two different rail pressures to investigate the existence of spray-swirl interactions. All of the experimental work was

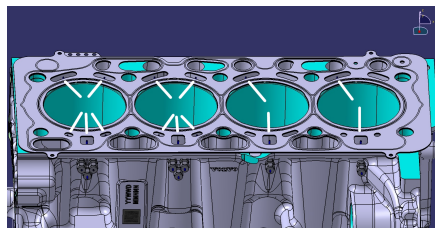

FIGURE 2. THERMOCOUPLE POSITIONS IN CYLINDER HEAD COOLING CHANNELS, EXHAUST SIDE VIEW.

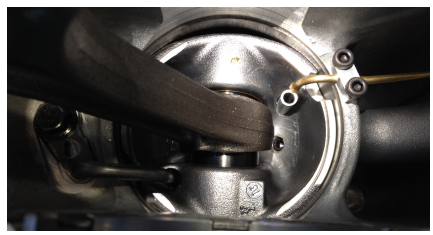

FIGURE 3. POSITION OF THERMOCOUPLE MEASURING PISTON OIL RETURN FLOW TEMPERATURE.

TABLE 1. ENGINE SPECIFICATIONS

Displaced volume [l]	0.492
Stroke [mm]	93.2
Bore [mm]	82
Connecting rod [mm]	147
Compression ratio [-]	15.8
No. of injector holes	8

performed at 1500 rpm and approximately 10.5 bar IMEPg, except in the speed-load test where case 1 was performed at 2000 rpm and case 3 at 5.5 bar $IMEP_g$. The fuel flow was kept constant during all parameter sweeps, but varied between the different cases in the speed-load test. The same injection strategy was used throughout this work, and consisted of two pilot injections,

main injection and one post-injection. All data points were repeated three times and the tests were randomised to exclude any background variables affecting the results.

The rate of heat release (RoHR), $dQ/d\theta$, was calculated from the pressure trace for all 3x300 engine cycles using Eqn. (1) [26]. The specific heat ratio is represented by γ, p is the cylinder pressure and V is the cylinder volume.

$$\frac{dQ}{d\theta} = \frac{\gamma}{\gamma-1}p\frac{dV}{d\theta} + \frac{1}{\gamma-1}V\frac{dp}{d\theta} + \frac{dQ_{ht}}{d\theta} \quad (1)$$

Q_{ht} represents the heat transfer losses and is calculated using the Woschni heat transfer model described by Eqn. (2) [27], where h_c is the heat transfer coefficient, C is a constant adapting the model to a specific engine, B is the engine bore, T denotes temperature and w is the local average in-cylinder gas velocity.

$$h_c = CB^{-0.2}p^{0.8}T^{-0.53}w^{0.8} \quad (2)$$

The measured temperature differences in the cooling media and exhaust gas were used to calculate energy losses using Eqn. (3), where $flow_{medium}$ is the mass flow of the medium, $C_{p,low}$ and $C_{p,high}$ are the specific heats of the medium at the low and high temperature, respectively. ΔT_{medium} is the measured temperature difference in the medium between the low and high temperature measurement.

$$\Delta E_{medium} = flow_{medium}\frac{(C_{p,low}+C_{p,high})}{2}\Delta T_{medium} \quad (3)$$

Speed and Load Effects

Three different combinations of two engine speeds and two load cases were run with three randomised repetitions of each combination, each repetition containing 300 consecutive cycles. The three combinations, case 1-3, are described in Table 2. All cases were performed at 1250 bar rail pressure.

Rail Pressure Sweep

The rail pressure sweep was based on speed and load case 2, to which CA50 and heat release were matched. Inlet pressure was kept constant at 1.6 bar, and the EGR level was approximately 25 %. The rail pressure was varied in five steps between 500 and 2000 bar, see Table 3.

Swirl Sweep

During the swirl sweep the inlet pressure and EGR level were kept constant at the same values as during the rail pressure sweep, and the rail pressure was set to 1250 bar. The swirl valve was set in 11 different positions between 0 and 100 % open, representing maximum to minimum swirl level, respectively.

The swirl sweep was repeated at 500 bar rail pressure to find out if a lower rail pressure would result in different spray-swirl interaction effects.

TABLE 2. SPEED AND LOAD COMBINATIONS

Case	Speed [rpm]	$IMEP_g$ [bar]	P_{in} [bar]	EGR [%]
1	2000	10.5	1.8	17 %
2	1500	10.5	1.6	15 %
3	1500	5.0	1.1	38 %

TABLE 3. TEST CONDITIONS DURING SWEEPS

Rail pressure [bar]	500, 1000, 1250, 1500, 2000
Swirl valve % open	0, 10, 20, 30, 40, 50, 60, 70, 80, 90, 100
EGR [%]	0, 11, 25
p_{in}, all except λ sweep [bar]	1.6

EGR Sweep

The EGR sweep was performed with constant inlet and rail pressure, the same levels as described for the swirl sweep. This ensured that the λ value did not change. The EGR levels were set to approximately 0, 11 and 25 %.

Lambda Sweep

During the λ sweep the rail pressure was set to 1250 bar and the EGR level was 25 %. The fuel flow was kept constant while inlet pressure was varied, resulting in λ values between 1.0 and 1.9. Higher values required inlet manifold pressures which could not be reached due to safety reasons. This test effectively showed the effect on heat transfer of varying the in-cylinder pressure.

RESULTS AND DISCUSSION

For all five test series in this work (the speed-load test and the four parameter sweeps), the collected pressure, flow and temperature data were used to calculate the heat release and set up the engine energy balance. Beyond net indicated work, the energy balances only include heat losses to the cooling water over

the cylinder head, piston cooling oil, and exhaust gas. All other heat transfer losses to the cooling media from other parts of the engine are omitted because this work focuses on heat transfer from the combustion chamber. Combustion and pumping losses are not included either, which together with the other omitted losses explains why the energy balance charts do not add up to 100 %.

Speed-Load Test

The heat losses to exhaust, cylinder head cooling and piston cooling for the three different speed and load combinations, case 1-3, are presented in Fig. 4. Exhaust losses are largest for case 1, which is characterised by both high speed and load. For case 2, with the same load but lower speed than case 1, exhaust losses are still quite high whereas for case 3 with low speed as well as low load exhaust losses drop significantly. This indicates that load has a greater impact on exhaust losses than speed, which is consistent with previous research. With higher speed the combustion duration (measured in CAD) increases, which results in hotter gases in the beginning of the exhaust stroke and, thus, increased heat losses to the exhaust gas. case 2 and 3 had almost exactly the same combustion duration, approximately 4 CAD shorter than case 1. Fig. 5 and Fig. 6 show the in-cylinder pressure trace and RoHR for case 1 and 3, respectively. Comparing the two cases the RoHR for case 1 is clearly extended over a longer crank angle interval than the corresponding one for case 3. The width of the main peak can also be seen to differ, which corresponds to the longer injection duration for case 1. The main peak is also taller for case 1 than for case 3 because of the larger amount of injected fuel.

Both heat losses to the cylinder head cooling and piston cooling oil show the opposite trend. For case 2 and 3 the cylinder head losses can not be distinguished from each other according to the error bars, even though their mean values differ. On the other hand, the losses to the piston cooling are well separated for the different cases. In case 1 the low piston cooling loss could be explained by combustion occuring to a greater extent outside the piston bowl and closer to the cylinder head compared to the lower speed cases. The difference between the lower speed cases may be of similar nature. Less fuel is being burned in the low load case, which results in shorter injection duration and all fuel may be burned in the piston bowl. This could also explain the insignificant difference between the cylinder head cooling losses for case 2 and 3. In conclusion, both speed and load have an influence on heat transfer, but load seems to be the most important factor.

The engine energy balance for the different cases is presented in Fig. 7, where the changes in heat losses to the exhaust gas and piston cooling can be clearly seen. Another visible trend is that with lower speed and load more of the losses seem to occur in other parts of the engine than the combustion chamber. It should be noted that the sum of the losses is not 100 %, which can be explained by only the major losses being included as explained above.

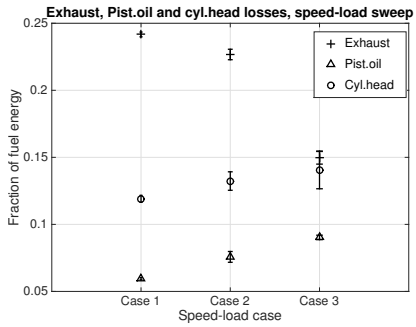

FIGURE 4. FRACTION OF FUEL ENERGY LOST TO CYLINDER HEAD COOLANT, PISTON OIL COOLING AND EXHAUST AT DIFFERENT SPEED AND LOAD CONDITIONS.

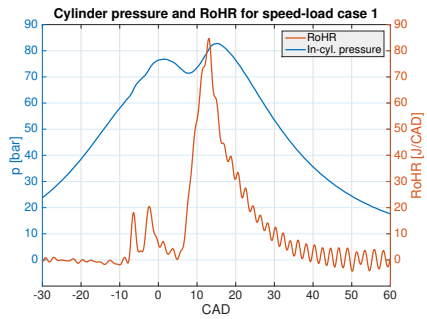

FIGURE 5. IN-CYLINDER PRESSURE AND RoHR, SPEED-LOAD CASE 1 WITH HIGH SPEED AND LOAD.

Rail Pressure Sweep

Heat transfer to the different parts of the cooling system and exhaust gas showed some dependence on rail pressure. Fig. 8

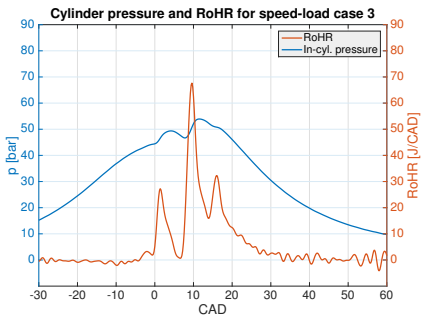

FIGURE 6. IN-CYLINDER PRESSURE AND RoHR, SPEED-LOAD CASE 3 WITH LOW SPEED AND LOAD.

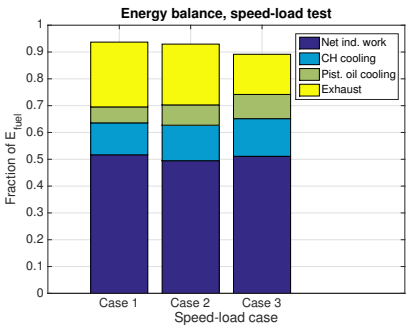

FIGURE 7. ENGINE ENERGY BALANCE AT DIFFERENT SPEED AND LOAD CONDITIONS.

shows the energy lost to the cylinder head cooling water, piston oil cooling and exhaust gas. The part of the fuel energy lost to the exhaust gas seems to decrease with higher rail pressure, even though error bars are relatively large compared to the difference between the mean values. Higher rail pressure requires shorter injection duration to maintain constant fuel flow, which results in shorter combustion duration and higher RoHR. The peak cylinder temperature also becomes higher. These factors contribute to higher in-cylinder temperature and thus, increased wall heat

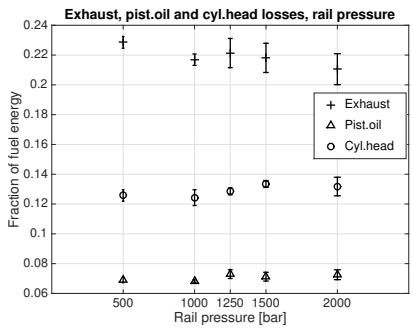

FIGURE 8. FRACTION OF FUEL ENERGY LOST TO CYLINDER HEAD COOLANT, PISTON OIL COOLING AND EXHAUST AT DIFFERENT RAIL PRESSURES.

transfer. The shorter combustion duration at higher rail pressures means that combustion has ended long before the exhaust stroke, and thus less heat is lost to the exhaust gas. A longer combustion duration results in a larger part of the heat being released after TDC, while the piston moves downward, leading to lower peak cylinder pressure and temperature. In-cylinder pressure and characteristic RoHR for the lowest and highest rail pressures are depicted in Fig. 9 and 10, respectively. There are significant differences between the two cases. In the 500 bar case the pressure trace is much smoother and the RoHR main peak is lower and broader than in the 2000 bar case, which demonstrates a very tall and narrow main peak. This also indicates that the 2000 bar case has a larger portion of premixed combustion before the mixing controlled phase than the 500 bar case, which is almost entirely mixing controlled due to the long injection duration.

Similar to the cylinder head losses, piston cooling losses increase slightly with rail pressure. With higher rail pressure more of the burning spray will impinge on the walls of the piston bowl, which increases piston wall temperature and thus cooling losses. Higher rail pressure may also increase the turbulence level, which according to previous research could increase convective heat transfer.

The engine energy balance was set up for the different cases, and is presented in Fig. 11. The differences between the cases are so small that it is difficult to distinguish how they change in the figure, and with all included fractions added the total energy balance does not differ significantly over the swept pressure range.

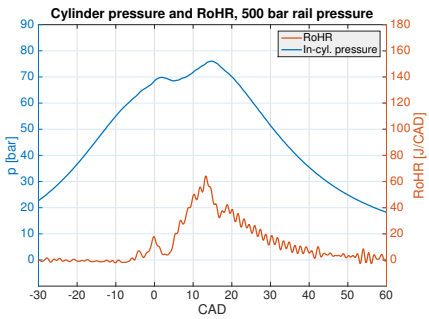

FIGURE 9. IN-CYLINDER PRESSURE AND RoHR, 500 BAR RAIL PRESSURE.

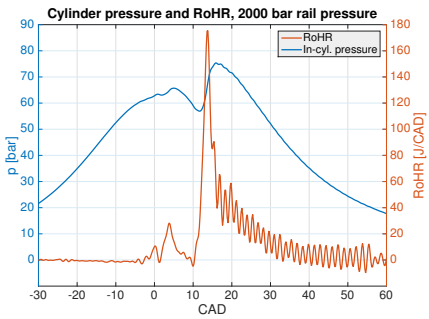

FIGURE 10. IN-CYLINDER PRESSURE AND RoHR, 2000 BAR RAIL PRESSURE.

Swirl Sweep

The swirl sweeps were performed at two rail pressures: 500 and 1250 bar. However, both rail pressures gave similar results. No discernible effect was found on heat transfer neither to walls nor to cooling media or exhaust gases, which can be seen in Fig. 12. These results were also supported by the lack of effect due to swirl on combustion timing and combustion duration. This contradicts previous research, which in most cases found heat losses to increase with swirl. There are, however, a few

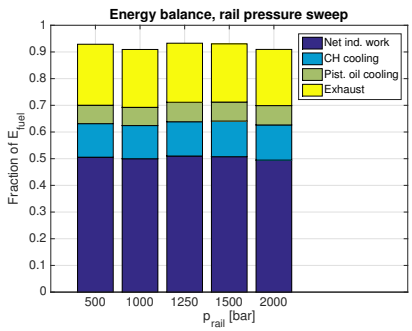

FIGURE 11. ENGINE ENERGY BALANCE AT DIFFERENT RAIL PRESSURES.

studies which resulted in similar findings. Fridriksson *et al.* [20] concluded that the heat transfer characteristics of different piston geometries do not respond the same way to changes in swirl level. The CDC bowls in the study showed more heat transfer at high swirl levels than at lower levels, but more open bowl types experienced unchanged or even increased heat transfer at reduced swirl levels. CFD studies suggested that this behaviour could be explained by the behaviour of the combustion chamber velocity field. For some geometries higher swirl levels seemed to push the high velocity field away from the wall and further into the bowl, while periphery velocity stayed relatively constant. Hence, in these cases reduced swirl would have no effect because convective heat transfer would not be affected. However, the results Fredriksson found for the geometry used in this setup did not show such an effect in the analysed part of the engine cycle [20].

The engine energy balance for the different swirl levels is presented in Fig. 13. The results for the different swirl conditions are remarkably similar, not even the height of the stacks varies significantly. This confirms the results in Fig. 12.

EGR Sweep

The resulting losses to exhaust gas, cylinder head cooling and piston cooling are displayed in Fig.14. The most obvious trend is for the heat loss to the exhaust gas, which decreases significantly when EGR levels increase. Heat loss to the cylinder head cooling water seems to increase slightly with higher EGR levels, which seems contradictory because in-cylinder temperatures are expected to drop with EGR. The differences are small, but a one-way ANOVA was performed for the cylinder

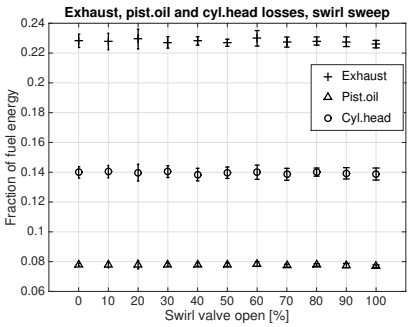

FIGURE 12. FRACTION OF FUEL ENERGY LOST TO CYLINDER HEAD COOLANT, PISTON OIL COOLING AND EXHAUST AT DIFFERENT SWIRL LEVELS.

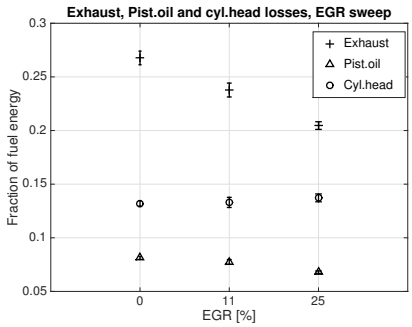

FIGURE 14. FRACTION OF FUEL ENERGY LOST TO CYLINDER HEAD COOLANT, PISTON OIL COOLING AND EXHAUST AT DIFFERENT EGR LEVELS.

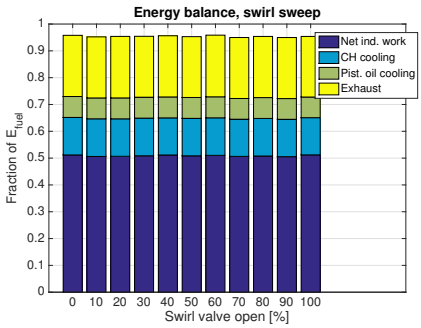

FIGURE 13. ENGINE ENERGY BALANCE AT DIFFERENT SWIRL LEVELS.

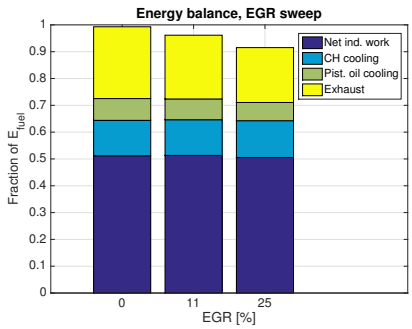

FIGURE 15. ENGINE ENERGY BALANCE AT DIFFERENT EGR LEVELS.

head cooling as well as the piston cooling results, which showed that there is a difference between the points in Fig. 14 at a 99.9 % significance level ($p < 0.001$).

Higher EGR levels prolonged combustion duration, and also caused a rise in inlet temperature. These factors could contribute to the decreasing piston oil heat losses at higher EGR levels. Exhaust losses, heat transfer to cylinder walls and piston oil cooling all decrease significantly when the EGR level increases. This is consistent with the theory that in-cylinder temperatures decrease at higher EGR levels. Delayed CA50 and longer combustion duration have been said to increase exhaust gas temperatures. However, EGR serves as an inert gas which absorbs heat and should thus reduce heat transfer to the walls and cooling media, which is also confirmed by Fig. 14.

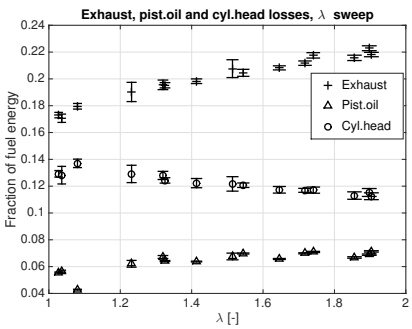

FIGURE 16. FRACTION OF FUEL ENERGY LOST TO CYLINDER HEAD COOLANT, PISTON OIL COOLING AND EXHAUST AT DIFFERENT λ LEVELS.

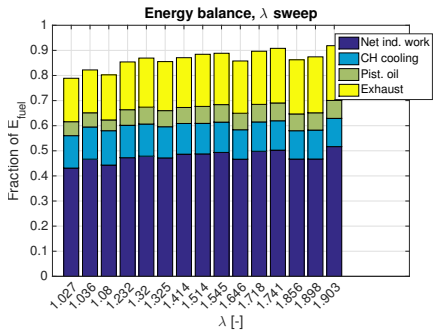

FIGURE 17. ENGINE ENERGY BALANCE AT DIFFERENT λ LEVELS.

Lambda Sweep

The λ sweep was performed by increasing the inlet pressure to achieve higher λ values, so in fact what is being studied is the effect of higher in-cylinder pressure and excess air. Fig. 16 shows that the heat losses to the cylinder head cooling water decrease at higher λ values. Heat losses to piston cooling oil tend to increase slightly with higher λ values. This can be explained by the earlier combustion timing found at the higher λ values, as discussed above for the EGR sweep. Combustion duration was found to increase slightly with higher λ, so the mixing controlled part of the combustion seems to grow somewhat. A leaner charge should keep the in-cylinder temperature down due to the excess air acting as a heat sink, which decreases wall heat transfer. On the other hand the higher pressure should increase the heat transfer coefficient h_c, as described by Eqn.(2). High pressure normally increases burn rate, which could contribute to the combustion duration stabilising at higher λ values instead of increasing monotonically. Exhaust losses were found to increase with λ, as displayed in Fig. 16. This could also be an effect of the prolonged combustion duration.

The engine energy balance at the different λ values is presented in Fig. 17. The trends seen in Fig. 16 are distinguishable here too, as well as the general trend of the sum of the included parts increasing with higher λ. There is also a slight increase in the extracted work. One of the reasons for lower efficiency at low λ values is lower combustion efficiency, but more importantly the thermodynamic efficiency decreases due to decreasing γ-value during the expansion.

SUMMARY AND CONCLUSIONS

A parameter study was performed in a multi-cylinder LD diesel engine. A speed-load test as well as rail pressure, swirl, EGR and λ sweeps were conducted. Two swirl sweeps were performed at different rail pressures.

1. The speed-load test showed that exhaust losses are largest for the high speed, high load case, while the low speed, low load case experience significantly less exhaust losses compared to the high load cases. This indicates that load has a greater impact on exhaust losses than speed. Higher speed increases the combustion duration, resulting in hotter exhaust gases and, thus, increased heat losses to the exhaust gas. Heat losses to the piston cooling and to some extent the cylinder head increases with lower speed and load. At high speed and load the low piston cooling loss could be due to combustion being less confined to the piston bowl and more spread out towards the cylinder head compared to the lower speed cases.
2. The rail pressure sweep showed that heat losses to cooling water and piston oil increase with higher rail pressure, while exhaust losses decrease. This could be explained by changed injection durations which affected combustion duration. Short combustion duration means more heat release before TDC resulting in high peak pressure and temperature. At long combustion duration more heat is released after TDC leading to lower peak pressure and temperature. Heat transfer to cylinder walls increase with rail pressure, possibly due to more spray-wall contact with higher rail pressure.

3. The swirl sweeps remarkably showed no effect from swirl on heat transfer. The same result was found for both high and low rail pressure. This could be due to the spray affecting the in-cylinder flow pattern, so the near-wall gas velocity may stay relatively unchanged and thus not alter the convective heat transfer characteristics.
4. Heat losses to cooling water tend to increase with more EGR, while heat losses to piston oil decreases at higher EGR levels. Both exhaust losses and heat transfer to cylinder walls decrease at higher EGR levels. EGR has a lowering effect on the average in-cylinder temperature, which delays combustion timing and prolongs combustion duration and thus explains the present trends.
5. At higher λ values heat losses to cooling water decrease, while heat losses to piston oil and exhaust tend to increase. The temperature reducing characteristics of a lean charge competes with the heat transfer increasing characteristics of high pressure, which may explain the trends for the cooling media. There were no obvious trends in the heat transfer to cylinder walls.

The present study will be followed by a similar study using a different combustion chamber design to see how the heat transfer characteristics change with another geometry. Future plans also include studying the effects on heat transfer when varying different injector parameters.

REFERENCES

[1] Abedin, M., Masjuki, H., Kalam, M., Sanjid, A., Rahman, S., and Masum, B., 2013. "Energy balance of internal combustion engines using alternative fuels". *Renewable and Sustainable Energy Reviews,* ***26***, pp. 20–33.

[2] Uzun, A., Çevik, I., and Akçil, M., 1999. "Effects of thermal barrier coating on a turbocharged diesel engine performance". *Surface and Coatings Technology,* ***116-119***, pp. 505–507.

[3] Hejwowski, T., and Weronski, A., 2002. "The effect of thermal barrier coatings on diesel engine performance". *Vacuum,* ***65***(3-4), pp. 427–432.

[4] Taymaz, I., 2007. "The effect of thermal barrier coatings on diesel engine performance". *Surface and Coatings Technology,* ***201***(9-11 SPEC. ISS.), pp. 5249–5252.

[5] Chan, S., and Khor, K., 2000. "Effect of thermal barrier coated piston crown on engine characteristics". *Journal of Materials Engineering and Performance,* ***9***(1), pp. 103–109.

[6] Modi, A., and Gosai, D., 2010. "Experimental study on thermal barrier coated diesel engine performance with blends of diesel and palm biodiesel". *SAE International Journal of Fuels and Lubricants,* ***3***(2), pp. 246–259.

[7] Sher, I., Levinzon-Sher, D., and Sher, E., 2009. "Miniaturization limitations of HCCI internal combustion engines". *Applied Thermal Engineering,* ***29***(2-3), pp. 400–411.

[8] Kokjohn, S., Hanson, R., Splitter, D., Kaddatz, J., and Reitz, R., 2011. "Fuel reactivity controlled compression ignition (RCCI) combustion in light- and heavy-duty engines". *SAE International Journal of Engines,* ***4***(1), pp. 360–374.

[9] Payri, F., Margot, X., Gil, A., and Martin, J., 2005. "Computational study of heat transfer to the walls of a DI diesel engine". *SAE Technical Papers*.

[10] Andersson, O., and Miles, P. C., 2014. *Diesel and Diesel LTC Combustion*. John Wiley & Sons, Ltd.

[11] Mavropoulos, G., Rakopoulos, C., and Hountalas, D., 2009. "Experimental investigation of instantaneous cyclic heat transfer in the combustion chamber and exhaust manifold of a DI diesel engine under transient operating conditions". *SAE Technical Papers*.

[12] Sharief, A., Chandrashekar, T., Antony, A., and Samaga, B., 2008. "Study on heat transfer correlation in IC engines". *SAE Technical Papers*.

[13] Najjar, Y., 2013. "Protection of the environment by using innovative greening technologies in land transport". *Renewable and Sustainable Energy Reviews,* ***26***, pp. 480–491.

[14] Sun, J., Bittle, J., and Jacobs, T., 2013. "Influencing parameters of brake fuel conversion efficiency with diesel / gasoline operation in a medium-duty diesel engine". *SAE Technical Papers,* ***2***.

[15] Kleemann, A., and Gosman, A., 2003. "Heat transfer sensitivity study for an advanced diesel engine". *SAE Technical Papers*.

[16] Gingrich, E., Ghandhi, J., and Reitz, R., 2014. "Experimental investigation of piston heat transfer in a light duty engine under conventional diesel, homogeneous charge compression ignition, and reactivity controlled compression ignition combustion regimes". *SAE International Journal of Engines,* ***7***(1), pp. 375–386.

[17] Said, M., Buttsworth, D., and Yusaf, T., 2009. "A review of radiation heat transfer measurement for diesel engines using the two-colour method". pp. 202–207.

[18] Dolak, J., Shi, Y., and Reitz, R., 2010. "A computational investigation of stepped-bowl piston geometry for a light duty engine operating at low load". *SAE Technical Papers*.

[19] Styron, J., Baldwin, B., Fulton, B., Ives, D., and Ramanathan, S., 2011. "Ford 2011 6.7l power stroke®diesel engine combustion system development". *SAE Technical Papers*.

[20] Fridriksson, H., Tuner, M., Andersson, O., Sunden, B., Persson, H., and Ljungqvist, M., 2014. "Effect of piston bowl shape and swirl ratio on engine heat transfer in a light-duty diesel engine". *SAE Technical Papers,* ***1***.

[21] Das, S., and Roberts, C. E., 2013. "Factors affecting heat transfer in a diesel engine: Low heat rejection engine revisited". doi: 10.4271/2013-01-0875.

[22] Perini, F., Dempsey, A., Reitz, R., Sahoo, D., and et al., 2013. "A computational investigation of the effects of swirl ratio and injection pressure on mixture preparation and wall heat transfer in a light-duty diesel engine". *SAE Technical Papers*.

[23] Eiglmeier, C., Lettmann, H., Stiesch, G., and Merker, G., 2001. "A detailed phenomenological model for wall heat transfer prediction in diesel engines". *SAE Technical Papers*.

[24] Fathi, M., Saray, R., and Checkel, M., 2011. "The influence of exhaust gas recirculation (egr) on combustion and emissions of n-heptane/natural gas fueled homogeneous charge compression ignition (HCCI) engines". *Applied Energy,* ***88***(12), pp. 4719–4724.

[25] Miles, P., RempelEwert, B., and Reitz, R., 2003. "Squish-swirl and injection-swirl interaction in direct-injection diesel engines". SAENA SECTION , Italy.

[26] Heywood, J. B., 1988. *Internal Combustion Engine Fundamentals*. McGraw-Hill, Inc.

[27] Woschni, G., 1979. "Determination of local heat transfer coefficients at the piston of a high speed diesel engine by evaluation of measured temperature distribution". SAE paper 790834.

Paper ii

SAE INTERNATIONAL

Experimental Comparison of Heat Losses in Stepped-Bowl and Re-Entrant Combustion Chambers in a Light Duty Diesel Engine

2016-01-0732
Published 04/05/2016

Jessica Dahlstrom, Oivind Andersson, and Martin Tuner
Lund University

Håkan Persson
Volvo Car Corporation

CITATION: Dahlstrom, J., Andersson, O., Tuner, M., and Persson, H., "Experimental Comparison of Heat Losses in Stepped-Bowl and Re-Entrant Combustion Chambers in a Light Duty Diesel Engine," SAE Technical Paper 2016-01-0732, 2016, doi:10.4271/2016-01-0732.

Abstract

Heat loss is one of the greatest energy losses in engines. More than half of the heat is lost to cooling media and exhaust losses, and they thus dominate the internal combustion engine energy balance. Complex processes affect heat loss to the cylinder walls, including gas motion, spray-wall interaction and turbulence levels. The aim of this work was to experimentally compare the heat transfer characteristics of a stepped-bowl piston geometry to a conventional re-entrant diesel bowl studied previously and here used as the baseline geometry. The stepped-bowl geometry features a low surface-to-volume ratio compared to the baseline bowl, which is considered beneficial for low heat losses. Speed, load, injection pressure, swirl level, EGR rate and air/fuel ratio (λ) were varied in a multi-cylinder light duty engine operated in conventional diesel combustion (CDC) mode. Temperature measurements in the engine cooling media were used to set up the engine energy balance and find out how much heat was lost to cooling media in different parts of the engine. Based on these calculations and heat release analysis, conclusions could be drawn regarding how heat losses in different parts of the engine were affected by changes in these parameters. Results were compared to previously published CFD simulations and it was concluded how the heat transfer characteristics differ between the two piston designs.

Introduction

The global energy consumption is increasing, and despite increased efforts to convert to renewable energy sources, fossil fuel consumption is still on the rise. This also results in increasing emissions of greenhouse gases, such as carbon dioxide (CO_2), which contribute to global warming. Further development of internal combustion engines (ICEs) is central in addressing this problem, and has resulted in large improvements of efficiency and emissions. Further efficiency improvement requires a deeper look into engine heat losses.

Some of the efforts to reduce heat losses concern low heat rejection engines, where all or parts of the combustion chamber walls are coated with a ceramic coating to prevent heat transfer. However, studies of the effects on engine performance are contradictory with reports of both increased and decreased fuel consumption and total heat transfer [3]. Losses to cooling water are reduced because most of the heat stays inside the combustion chamber, resulting in increased exhaust temperatures [1,2,3,4]. Volumetric efficiency often decreases [2,3,4], even though fuel economy and thermodynamic efficiency are reported to improve [3,4,5,6]. So far, the benefits have not been shown to outweigh the drawbacks and render this a viable concept.

Reports show significant efficiency differences between different engine sizes. A comparison between heavy duty (HD) and light duty (LD) engines shows that LD engines consistently demonstrate lower efficiencies than HD engines. One explanation could be that they have higher surface-to-volume ratios [7], but the increased heat losses could also be caused by high swirl ratios and less favourable combustion chamber designs [8]. However, there are few examples in the literature addressing the role heat transfer may play in this.

Speed and load both have significant effects on heat transfer. Higher engine speed results in less time for heat exchange [9], but at the same time turbulence increases and thus also convective heat transfer [10]. However, several studies confirm that load seems to be more influential than speed [11,12,13,14].

High temperature and pressure, long combustion duration and flame-wall interaction has been found to cause high heat transfer losses [14]. Another research team found that the heat transfer coefficient varies significantly between different locations in the combustion chamber depending on whether the wall is in contact with the flame front or not [11]. This conclusion is also supported by other researchers [15]. Another way of reducing heat flux is later

combustion timing [16] which has also been proven to reduce peak radiation [17], although this could have negative effects on heat losses in some parts of the engine.

Several studies concern the heat transfer characteristics of different bowl geometries. A stepped-bowl piston with low surface-to-volume ratio was found to reduce wall heat transfer [18]. Another research group optimised a chamfered, re-entrant bowl with low swirl and an 8-hole nozzle [19]. This system provided a more uniform equivalence ratio field than the wide re-entrant bowl it was compared to, except along the cylinder liner where a lean region was found to prevent heat loss to the coolant. Fridriksson et al. found that the conventional reentrant diesel geometry in their study had lower thermodynamic efficiency and higher heat losses than more shallow and open geometries, such as stepped-bowl and a tapered, lipless piston [20]. At high load the shallow, open piston bowls displayed more heat transfer in the bowl, while the conventional types showed more bowl-lip heat transfer. This was found to coincide with the location of the hot gases. A low surface-to-volume ratio, often assumed to reduce heat transfer, was only found to directly influence heat transfer before the start of spray-driven combustion. After that, other combustion parameters and turbulence were more influential [20]. The study by Fridriksson et al. included the geometry used in a previous study by the authors of this paper, which forms the baseline to which the present stepped-bowl results are compared [21].

The injector nozzle-hole orientation and number of holes have a documented effect on wall heat transfer [22]. These parameters require optimisation with a specific combustion chamber geometry. Reduced injection duration can be achieved with larger hole size, which increases the rate of heat release (RoHR). This generally improves efficiency, but the effect can be offset by increased heat transfer losses [22] and soot.

The most thoroughly investigated gas flow pattern affecting heat transfer is swirl. In general, low swirl levels seem to produce low heat loss [20]. However, different geometries show dissimilar responses to swirl ratio changes, which may be due to different velocity fields. Convective heat flux is related to rotational gas motion, which was mainly found to increase close to the outer walls. Low swirl was found to reduce heat loss for conventional diesel combustion chamber (CDCC) geometries, while the more open piston geometries experienced increased heat losses as near-wall fluid velocity increased when swirl level decreased [20]. Another CFD study found that high swirl ratios significantly increased wall heat transfer and delayed the ignition timing [23]. An experimental CDC study showed that the mean piston surface temperature increased with higher swirl, suggesting an increased steady state heat transfer component [16]. Eiglmeier et al. [24] found that heat flux peaks increased with turbocharging, which was explained by intensified turbulence. The convective heat transfer was also found to increase [24].

EGR has a documented effect on heat transfer. Theoretically, the heat transfer coefficient is proportional to pressure and inversely proportional to temperature. This was also confirmed experimentally by Fathi et al. [25]. However, the heat transfer coefficient does not vary significantly with EGR, since increased EGR rates reduce both charge temperature and pressure. Convective heat transfer reduces as a result of the reduced temperature difference between charge and wall [25]. Das et al. [22] also obtained significant heat loss reduction with increased EGR, which was explained by the increased charge mass requiring more heat to increase charge temperature.

Although spray-swirl interactions could significantly affect the heat losses they have not been widely studied. As shown in Figure 1, before fuel injection a swirl-supported combustion system places the gas with the highest tangential velocity at the outer bowl wall, maximizing the convective heat losses in this region. After fuel injection, however, the spray has entrained gas with low tangential velocity at the central bowl region and transported it to the wall. This transport sets up a vertical vortex at the wall, which displaces the high velocity gas towards the center (bottom part of Figure 1). The vortex thereby decreases the convective heat transfer to the wall during combustion. The radial location of the gas with highest tangential velocity is determined by a balance between its centrifugal force and the inward force exerted by the spray-induced vortex. The centrifugal force is determined by the swirl ratio, whereas the inward force is determined by the injection pressure. The aim of the present work was to experimentally study heat transfer in a LD engine with two different bowl geometries, by looking into spray-swirl interactions as well as effects of other parameters such as λ and EGR. One hypothesis was that the balance between injection pressure and swirl ratio would affect the heat transfer. Another hypothesis was that this balance would be altered when the bowl geometry changes. The previous CFD study by Fridriksson et al. [20] showed a potential for reduced heat losses with the stepped-bowl compared to the baseline geometry used in this study as well as in previous work [21].

Experimental Setup

Experiments were performed in a 4-cylinder light-duty engine with Denso injectors. Engine specifications are presented in Table 1. Two piston bowl geometries were tested, the baseline CDCC geometry and a stepped-bowl geometry. The combustion chamber surface-tovolume ratio has been assumed an important parameter affecting heat transfer. The surface-to-volume ratio of the stepped-bowl was only 87% of the baseline value [20], and was therefore an interesting alternative to test regarding heat transfer charachteristics. Figure 2 depicts the baseline geometry and the contours of the wider, shallower stepped-bowl. The stepped-bowl was scaled to match the compression ration of the baseline piston bowl. To set up the engine energy balance, temperature and mass flow measurements were needed. All cylinders were instrumented with thermocouples for measuring temperature differences in the cooling system.

Measurements of the cooling water temperature difference over the cylinder head were performed to calculate heat losses to the cylinder head. The cooling water flows up from the engine block to the cylinder head through channels on the inlet side, and returns to the engine block through channels on the exhaust side. The cylinder head was equipped with T-type thermocouples in all cooling channels for cylinder 3 and 4, while the other cylinders only had one on the inlet and one on the exhaust side (marked with white arrows in Figure 3). Except for the thermocouples in the middle channels on the exhaust side of cylinder 3 and 4, the thermocouples on the exhaust side were connected in pairs to the corresponding ones on the inlet side to measure the cooling water temperature difference over the cylinder

head with as little measurement error as possible. The thermocouples in the middle channels were used to measure the absolute temperature in the cooling water leaving the cylinder head.

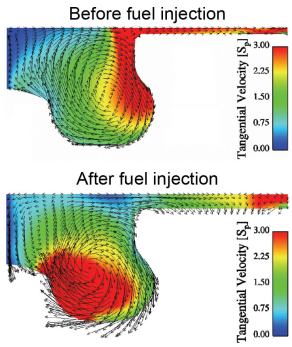

Figure 1. The fuel injection event limits the convective heat transfer to the outer bowl wall by displacing gas with high tangential velocity towards the centre (adapted from [26]).

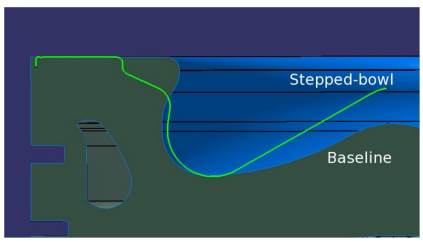

Figure 2. Baseline piston and contour of the stepped-bowl geometry.

Table 1. Engine specifications

Displaced volume [l]	0.492
Stroke [mm]	93.2
Bore [mm]	82
Connecting rod [mm]	147
Compression ratio	15.8:1
Number of valves	4
No. of injector holes	8

One K-type thermocouple was fitted in the feed line to the piston cooling oil rail, and two were fitted in funnel-shaped structures below the pistons to measure the oil return flow temperatures from cylinder 2 and 3. These two were assumed representative for all cylinders. One of these is shown in Figure 4, where the structure and the pipe guiding oil from the piston outlet to the funnel can be seen from below.

All cylinders were fitted with Kistler pressure sensors to measure incylinder pressure used for the heat release analysis. Exhaust oxygen concentration was measured using an Etas lambda meter.

The mass flow of cooling water over the cylinder head was measured using a GL Flow turbine flow meter, mass flow of air fed to the engine was measured using a Bronkhorst In-Flow meter, and oil mass flow to the piston cooling was measured with a Macnaught oval meter. Fuel flow was measured using a Sartorius balance.

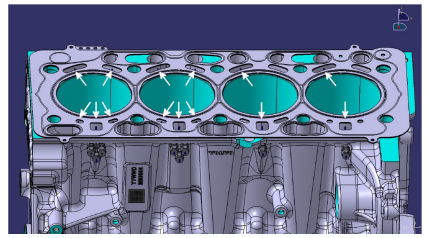

Figure 3. Thermocouple positions in cylinder head cooling channels, exhaust side view.

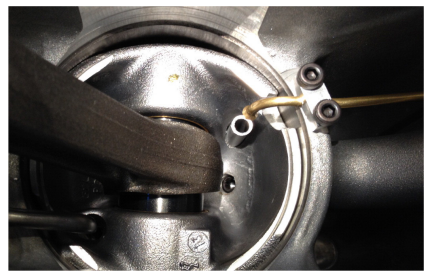

Figure 4. Position of thermocouple measuring piston oil return flow temperature (right).

Experimental Methodology

Heat transfer to the cooling media was measured at various engine conditions. One speed-load test was performed, and during additional tests the following four parameters were swept: rail pressure, swirl, EGR and λ. The swirl sweep was conducted at two different rail pressures to investigate the existence of spray-swirl interactions. All of the experimental work was performed at 1500 rpm and approximately 10.5 bar IMEPg, except in the speed-load test where case 1 was performed at 2000 rpm and case 3 at 5.5 bar IMEPg. The fuel flow was kept constant during all parameter sweeps, but varied between the different cases in the speed-load test. The same injection strategy was used throughout this work, and consisted of two pilot injections, main injection and one post-injection. All data points were repeated three times and the tests were randomised to exclude any background variables affecting the results.

The rate of heat release (RoHR), $dQ/d\theta$, was calculated from the pressure trace for all 3×300 engine cycles using Eqn. (1) [27]. The specific heat ratio is represented by γ, p is the cylinder pressure and V is the cylinder volume.

$$\frac{dQ}{d\theta} = \frac{\gamma}{\gamma-1} p \frac{dV}{d\theta} + \frac{1}{\gamma-1} V \frac{dp}{d\theta} + \frac{dQ_{ht}}{d\theta} \quad (1)$$

Q_{ht} represents the heat transfer losses and was calculated using the Woschni heat transfer model described by Eqn. (2) [28], where h_c is the heat transfer coefficient, C is a constant adapting the model to a specific engine, B is the engine bore, T denotes temperature and w is the local average in-cylinder gas velocity.

$$h_c = CB^{-2} p^{0.8} T^{-0.53} w^{0.8} \quad (2)$$

The measured temperature differences in the cooling media and exhaust gas were used to calculate energy losses, ΔQ_{medium}, using Eqn. (3), where $\dot{m}_{medium}$ is the mass flow of the respective medium (air, cylinder head cooling water, and oil), $C_{p,low}$ and $C_{p,high}$ are the specific heats of the medium at the low and high temperature, respectively. ΔT_{medium} is the measured temperature difference in the medium between the low and high temperature measurement.

$$\Delta Q_{medium} = \dot{m}_{medium} \frac{C_{p,low} + C_{p,high}}{2} \Delta T_{medium} \quad (3)$$

When calculating heat loss to the exhaust gas the values of C_p were approximated with the values for air. The error was regarded as small enough for the results to still be valid.

Spray Target Position

The first part of the experimental work was the tests with the baseline geometry. During these tests the nominal nozzle protrusion was used. After switching pistons to the stepped-bowl geometry, a spray target position (STP) test was performed to examine the best possible nozzle protrusion for this geometry. The STP is crucial for emission formation, in particular soot emissions. With a conventional reentrant bowl, such as the baseline bowl in this study, the STP is usually chosen slightly below the bowl lip. The corresponding part of the stepped-bowl is located further down into the bowl, so the hypothesis for this pre-study for the second part of the experimental work was that the nozzle protrusion should be increased. This was performed by machining the bottom of the injector wells approximately 1 mm and using injector washers of different thickness. Too high STP would direct the fuel upwards instead of into the bowl, thus impairing mixing and increasing soot formation. An optimized STP would direct part of the fuel upwards, and most of it into the bowl. This enables combustion to take place in both the top and bottom part of the bowl, making better use of the oxygen [18,19].

Four positions were tested: the baseline position, 1 mm above the baseline (denoted -1 mm), 1 mm below (denoted 1 mm), and finally 1.6 mm below (denoted 1.6 mm). It was not possible to increase the nozzle protrusion further due to limitations of the minimum washer thickness. Experiments were performed at the same speed-load cases as described in Table 2. Unfortunately the soot meter was not installed at the time the baseline tests were performed, so soot measurements are only shown for the stepped-bowl.

Speed-Load test

Three different combinations of two engine speeds and two load cases were performed with three randomised repetitions of each combination, each repetition containing 300 consecutive cycles. The three combinations, case 1-3, are described in Table 2. All cases were performed at 1250 bar rail pressure.

Table 2. Speed and load combinations

Case	Speed [rpm]	IMEPg [bar]	p_{in} [bar]	EGR[%]
1	2000	10.5	1.8	17
2	1500	10.5	1.6	15
3	1500	5.0	1.1	38

Rail Pressure Sweep

Rail pressure has a significant impact on heat transfer, which was confirmed by the previously published study [21]. Higher pressure reduces injection duration, and thereby also combustion duration. The rail pressure sweep was based on speed and load case 2, to which CA50 and heat release were matched. Inlet pressure was kept constant at 1.6 bar, and the EGR level was approximately 25 %. Table 3 shows the five rail pressures between 500 and 2000 bar which were included in the sweep, as well as the settings for the variables in the other sweeps. All sweeps were performed with all variables kept as constant as possible except for the one that was swept.

Table 3. Test conditions during sweeps

Rail pressure [bar]	500, 1000, 1250, 1500, 2000
Swirl valve [% open]	0, 10, 20, 30, 40, 50, 60, 70, 80, 90, 100
EGR [%]	0, 12, 25
p_{in}, all except λ sweep [bar]	1.6

Swirl Sweep

Several studies have found increased wall heat losses at higher swirl levels. However, this has also been found to depend on the combustion chamber geometry, which is of interest in this study.

During the swirl sweep the inlet pressure and EGR level were kept constant at the same values as during the rail pressure sweep, and the rail pressure was set to 1250 bar. As stated in Table 3, the swirl valves were set in 11 different positions between 0 and 100 % open, representing maximum to minimum swirl level, respectively.

In a previous experiment [21] the swirl sweep was repeated at 500 bar rail pressure to find out if a lower rail pressure would result in different spray-swirl interaction effects. The conclusion was that the results were similar to the 1250 bar case.

EGR Sweep

The EGR sweep was performed with constant inlet and rail pressure, the same levels as described for the swirl sweep. The EGR levels were set to approximately 0, 12 and 25 %. Especially the middle EGR level differed slightly between the sweep performed with the baseline geometry and the stepped-piston, with a somewhat lower

level for the baseline geometry. EGR serves as inert gas, which absorbs energy when heated and, thus, reduces in-cylinder temperatures. This is expected to also reduce heat losses.

Lambda Sweep

During the λ sweep the rail pressure was set to 1250 bar and the EGR level was 25 %. The fuel flow was kept constant while inlet pressure was varied, resulting in λ values between 1.0 and 1.9. Higher values required higher inlet manifold pressures, which could not be reached due to safety reasons. This was an issue especially during the sweep performed with the stepped-bowl, which is why this sweep contains less measurement points. The test effectively showed the effect on heat transfer of varying the in-cylinder pressure. High pressure normally increases temperature. On the other hand, the excess air serves as an inert gas, absorbing energy when heated and thus reducing the in-cylinder temperature. This should also have some effect on heat losses.

Results and Discussion

The STP test was considered a pre-study to the test series with the stepped-bowl, and should be viewed separately from the rest of the tests. The outcome of the STP test was then used for all stepped-bowl tests.

For the five test series in this work (the speed-load test and the four parameter sweeps), the collected pressure, flow and temperature data were used to calculate the heat release and set up the engine energy balance. Beyond net indicated work, the energy balances only include heat losses to the cooling water over the cylinder head, piston cooling oil, and exhaust gas. All other heat transfer losses to the cooling media from other parts of the engine, such as the block, are omitted because this work focuses on heat transfer from the combustion chamber. The cylinder head cooling loss makes up approximately 50% of the total cooling water loss, which should be kept in mind when evaluating the presented energy balance charts. Combustion and pumping losses are not included either, which together with the other omitted losses explains why the energy balance charts do not add up to 100 %.

Spray Target Position Test

Dolak et al. [18] concluded that the stepped-bowl performed better than a conventional re-entrant bowl in terms of soot and CO emissions in a LD engine, as a result of better air utilisation. The STP test described here aimed at finding out if this was the case also for this downscaled piston bowl, and which nozzle protrusion was most beneficial in this respect. As described above, soot measurements could not be performed with the baseline piston, so Figure 5 only shows results for the stepped-bowl. For the baseline piston the nominal nozzle protrusion was used. It is very clear that the soot emissions decrease with larger nozzle protrusion for all tested speed-load combinations. Thus, this confirms the hypothesis. However, the resulting CO emissions do not follow the same trend for all test cases. As is evident in Figure 6, CO emissions do decrease monotonically with nozzle protrusion for the higher load cases 1 and 2, whereas the low load case 3 behaves differently.

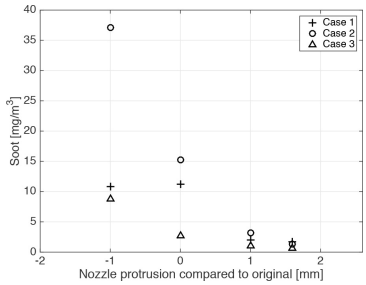

Figure 5. Soot emissions for the three speed-load cases with different nozzle protrusions into the stepped-bowl geometry.

Case 3 produces the most CO emissions with both the baseline piston and the stepped-bowl, even though they are lower with the stepped-bowl. For case 3, the CO emissions seem to have a minimum close to the original nozzle position. However, considering the results for all speed-load combinations, it was decided to use the largest nozzle protrusion for the following parameter sweeps with the stepped-bowl.

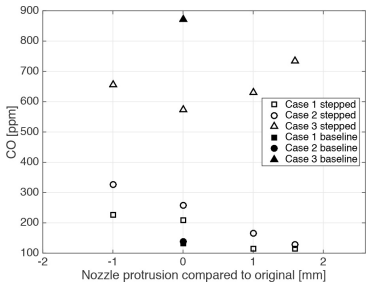

Figure 6. CO emissions for the three speed-load cases during the STP test with the stepped-bowl, and with the baseline geometry.

Speed-Load Test

The heat losses to exhaust, cylinder head cooling and piston cooling for the three different speed and load combinations, case 1-3, are presented in Figure 7 for both the baseline and stepped-bowl. Error bars represent one standard deviation calculated from the three replicates combined, 900 measurements in total. Both configurations result in similar trends, with much higher exhaust losses in the high load cases and more cooling losses in the two lower speed cases. Especially the piston cooling oil loss increases at lower speed and load.

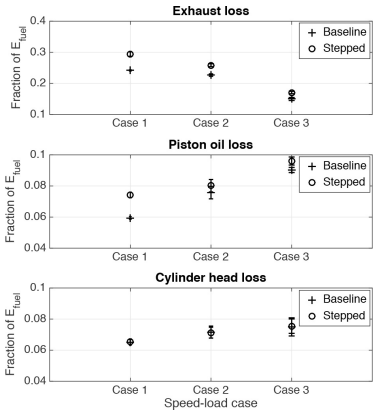

Figure 7. Losses to exhaust gas, cylinder head cooling, and piston oil cooling for the speed-load test with both geometries.

For the stepped-bowl the exhaust losses are increased compared to the baseline case, mainly at high speed and load. This bowl also resulted in higher piston cooling losses, which is consistent with the findings of Fridriksson et al. [20]. The cylinder head cooling losses are similar for the two geometries.

As evident in Figure 8, the combustion phasing was almost identical with both piston geometries. Hence, differences are not due to different phasing.

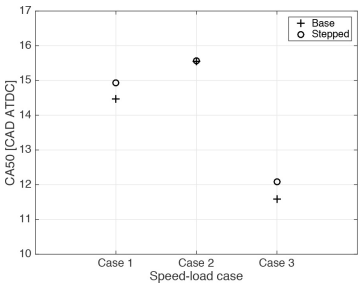

Figure 8. Crank angle degree at 50 % heat release for the speed-load tests with both geometries.

Dolak et al. [18] suggested that the stepped-bowl improved charge preparation with multiple injections by allowing fuel to target both the upper and lower portions of the bowl. This allows for better use of the oxygen in the cylinder, which could result in faster combustion. A higher degree of premixing also reduces combustion duration by decreasing the mixing controlled part of the combustion event. Figure 9 shows that there is a significant difference in combustion duration between the two geometries, except in the low load case. The stepped-bowl gives rise to faster combustion compared to the baseline geometry. This is different from the results of Fridriksson et al., who found longer combustion durations for this bowl. Shorter combustion duration is related to a higher rate of heat release (RoHR), because the same amount of energy is released in a shorter time interval.

Shorter combustion duration also leads to higher in-cylinder temperatures, which could increase cooling losses. Figure 7 shows that cooling losses were only slightly increased, which could in turn explain the larger fraction of fuel energy ending up in the exhaust gas. Fridriksson et al. also concludes that convective heat losses were significantly reduced with the stepped-bowl. Faster combustion also means that more of the fuel is burned inside the bowl instead of in the upper part of the combustion chamber. This may be the reason why piston cooling losses are increased with the stepped-bowl, while losses to the cylinder head are relatively similar to the baseline bowl. The rate of heat release shown in Figure 10 demonstrates that the stepped-bowl to the left indeed has a taller and steeper premixed peak than the baseline case to the right at all test conditions.

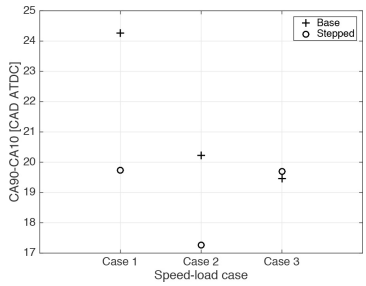

Figure 9. Combustion duration for the speed-load tests with both geometries.

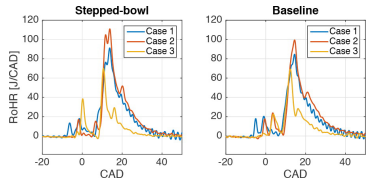

Figure 10. Rate of heat release for all tested speed and load cases. Stepped-bowl to the left and baseline to the right.

The energy balances for the baseline geometry and the stepped-bowl are presented in Figure 11. The left stack in each case represents the baseline bowl, and the right stack shows the stepped-bowl. The higher exhaust losses for the stepped-bowl can be clearly distinguished, and also that the losses in general follow the same pattern as with the baseline geometry. The higher exhaust losses at higher load also show that load has a greater impact on these losses than speed, because Case 1 and 2 were performed at the same load, and Case 2 and 3 at the same speed.

Rail Pressure Sweep

The previous study with the baseline geometry showed that rail pressure has an effect on heat transfer to the different parts of the cooling system. The two bowl designs show similar trends, as presented in Figure 12. Exhaust losses decrease as rail pressure increases while cooling losses increase. This is a result of the shorter injection duration and, thus, shorter combustion duration. The stepped-bowl geometry again resulted in higher exhaust losses than the baseline geometry. It also slightly reduced the cylinder head cooling losses, while increasing losses to the piston cooling.

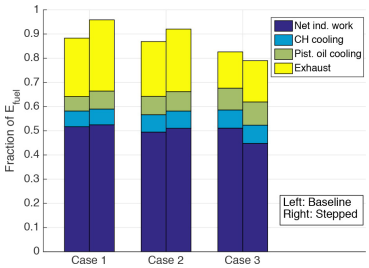

Figure 11. Energy balance for the speed-load test with both bowl geometries, baseline to the left and stepped-bowl to the right in each case.

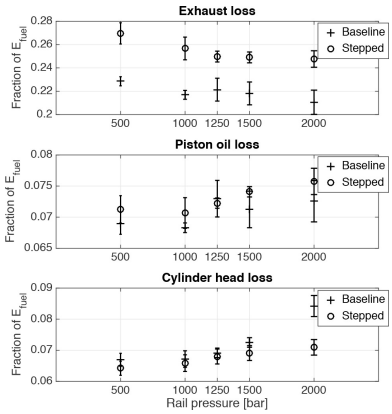

Figure 12. Losses to exhaust gas, cylinder head cooling and piston oil cooling for the rail pressure sweep with both geometries.

The combustion phasing, CA50, is shown in Figure 13 for both geometries. These are quite similar. The combustion durations for the different rail pressures and bowl designs are presented in Figure 14. Shorter combustion duration is again achieved with the stepped-bowl. The difference between the geometries even increases with higher rail pressures, from approximately 3 CAD at 500 bar to 6 CAD at 2000 bar. The shorter combustion duration, also meaning faster heat release and higher temperature, could be responsible for the behaviour of the losses in Figure 12. When more of the combustion occurs in the bowl the piston will get hotter and, thus, the cooling oil temperature will also increase. The cylinder head cooling losses then decrease, indicating less wall heat transfer to the rest of the combustion chamber, and more heat being left in the exhaust.

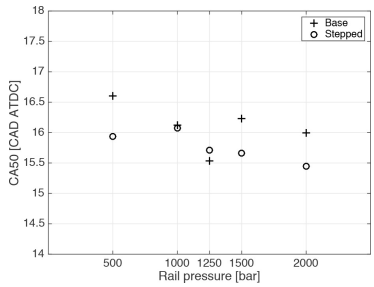

Figure 13. Crank angle degree at 50 % heat release for the rail pressure sweep with both geometries.

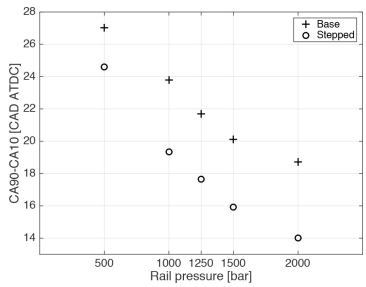

Figure 14. Combustion duration for the rail pressure sweep with both geometries.

The energy balances for the baseline geometry and the stepped-bowl are shown in Figure 15. The net indicated work is similar for both configurations. The main difference lies in the heat losses as discussed above, e.g. the increased heat loss to the exhaust with the stepped-bowl.

Swirl Sweep

Studying Figure 16 showing the heat losses for the different swirl valve positions, no discernible effect was found on heat transfer to the exhaust for either geometry. Cylinder head cooling losses seem to increase ever so slightly with higher swirl for both geometries, while the same trend for the piston oil cooling is much more obvious. This result is in agreement with previous research, which concluded that heat losses increase with higher swirl levels. The swirling motion is predominantly found inside the bowl, so it follows naturally that the bowl heat losses should be affected the most. Comparing the two geometries, exhaust losses were slightly higher with the baseline piston. This could be an effect of longer combustion duration. Piston oil losses were similar for both geometries while cylinder head losses were higher with the stepped-bowl. The simulations performed by

Fridriksson et al. [20] showed lower gas velocities near the wall with less swirl for the geometry here referred to as the baseline. According to the simulations the near-wall gas velocity in the stepped-bowl was not decreased by reduced swirl levels. In the squish area the gas velocity was even increased. Maybe the improved heat transfer characteristics in the stepped-bowl at low swirling conditions could be outweighed by the higher gas velocity in the squish region, which could then explain part of the higher cylinder head losses.

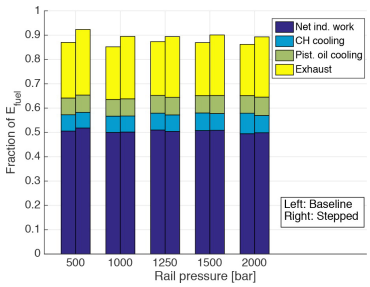

Figure 15. Energy balance for the rail pressure sweeps with both geometries.

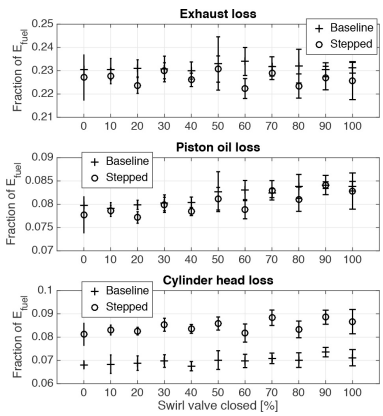

Figure 16. Losses to exhaust gas, cylinder head cooling, and piston oil cooling for the swirl sweep with both geometries.

Figure 17shows that 50 % heat release occurred slightly later with the baseline geometry than with the stepped-bowl. The figure also shows that CA50 stays relatively similar for different swirl cases, even though there is a slight trend towards earlier CA50 with the stepped-bowl with increased swirl, and the opposite with the baseline geometry.

Figure 18 displays the combustion durations, which were shorter with the stepped-bowl over the full swirl range. For the stepped-bowl the combustion duration was only slightly shortened at the highest swirl levels. This suggests that the combustion event was affected very little, by the swirl valve position. In the baseline case, combustion duration was much more affected with shorter combustion at higher swirl levels. In theory, higher swirl rates should speed up the mixing controlled combustion phase and, thus, decrease combustion duration. However, only the test with the baseline piston showed this effect. Maybe the stepped-bowl improves mixing, as mentioned above, to the extent that swirl is no longer an important factor. Regarding heat losses, swirl seems to give similar results for both configurations.

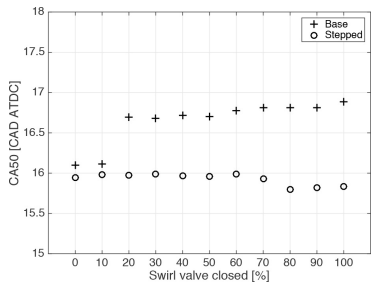

Figure 17. Crank angle degree at 50 % heat release for the swirl sweep with both geometries.

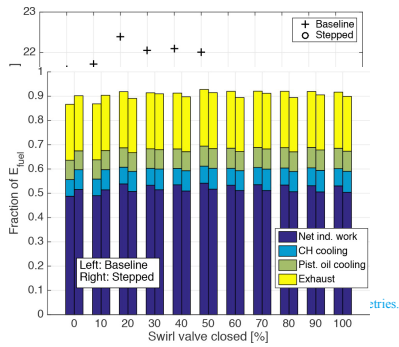

Figure 19. Energy balances for the swirl sweeps with both bowls.

The energy balances presented in Figure 19 for the baseline and the stepped-bowl geometries do not provide much further information. Both geometries show similar energy balances, except for the larger cylinder head losses in case of the stepped-bowl. The net indicated work could be seen to increase somewhat with higher swirl with the baseline piston, while it stays at the same level or decreases slightly with the stepped-bowl. The extracted work could be negatively affected when the swirl valves are closed to increase the swirl level, thereby increasing pumping losses.

EGR Sweep

The EGR sweeps with the two piston geometries were performed in the exact same way. However, the middle point differed slightly with approximately 11 % EGR in the baseline case and 12 % in the

stepped-bowl case. This difference was considered so small that it would not have any significant effect on the result. The heat losses for the two EGR sweeps are presented in Figure 20. The results for the EGR sweeps are mostly consistent with the other parameter tests. As expected, higher EGR rates decreases in-cylinder temperatures, and, thus, most heat losses. It is only the cylinder head cooling that stays relatively constant. A difference here is that less heat losses to the piston cooling were found with the stepped-bowl, except at the highest EGR level. The cylinder head cooling losses were also reduced with the stepped-bowl, while exhaust losses were increased. This parameter sweep was the only one where the stepped-bowl gave rise to lower in-cylinder temperatures than the baseline bowl. This could explain why all studied cooling losses were decreased, contrary to the results of the other sweeps.

Figure 21 shows that CA50 was kept more constant with the stepped-bowl than with the baseline piston, which could have some effect on the results. Later combustion phasing could increase exhaust losses due to later combustion resulting in higher exhaust temperatures.

The combustion durations presented in Figure 22 are increased with higher EGR rates, especially with the baseline bowl. This could partly be a result of the later combustion phasing. The stepped-bowl reduced the combustion duration. The larger difference at higher EGR levels could either indicate a higher EGR tolerance for the stepped-bowl or, as mentioned above, be an effect of the later combustion phasing with the baseline piston.

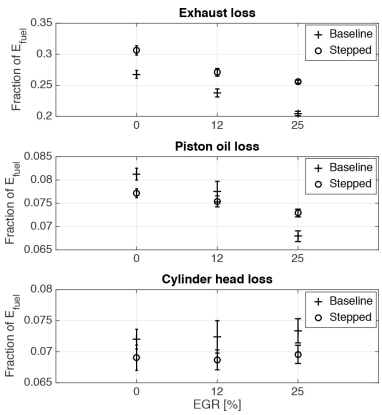

Figure 20. Losses to exhaust gas, cylinder head cooling, and piston oil cooling for the EGR sweep with both geometries.

Similar trends can be distinguished in Figure 23 showing the energy balances for both geometries, which is also another way to present the losses in Figure 20. The exhaust losses seem to be reduced more with the baseline piston, despite later phasing and longer combustion duration. On the other hand this is a reasonable result considering the higher cooling losses with this piston.

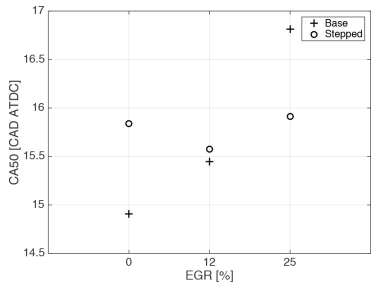

Figure 21. Crank angle degree at 50 % heat release for the EGR sweep with both geometries.

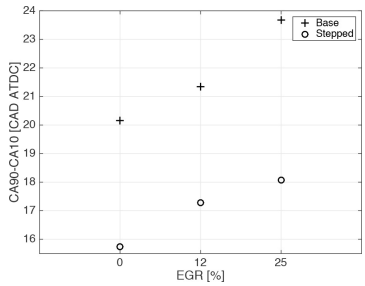

Figure 22. Combustion duration for the EGR sweep with both geometries.

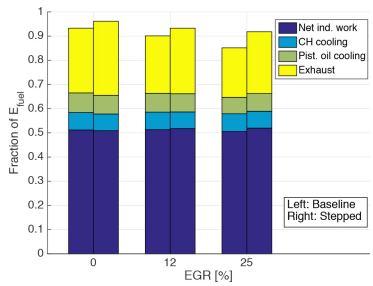

Figure 23. Energy balance for the EGR sweep with baseline geometry.

Lambda Sweep

Increasing the inlet pressure had a large effect on the RoHR with the stepped-bowl. As can be seen in Figure 24-25 showing the baseline and stepped-bowl RoHR, respectively, the main peak grew much higher and narrower compared to the baseline geometry. The premixed peaks differ more with the λ value with the stepped-bowl. This could be a result of the already better mixing combined with increased burn rate with higher pressure. However, the heat release of the second pilot injection occurs later and closer to the main heat release with the stepped-bowl, indicating that they merge into the

main combustion peak. This gives rise to a very intense and fast premixed combustion, especially at lower λ values. On the other hand, the mixing controlled combustion seems to be somewhat slower at lower λ values than at higher ones. Heat losses during the λ sweep for the baseline geometry and stepped-bowl.are shown in Figure 26 Higher exhaust losses were again found with the stepped-bowl, but this time heat losses to cooling water were also increased. Higher RoHR normally also increases the in-cylinder temperature, which could explain the consistently higher heat losses to cooling media. Otherwise the trends are quite similar for both geometries.

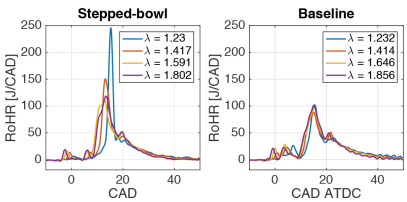

Figure 24. Rate of heat release for the λ sweep with the stepped-bowl (left) and baseline geometry (right).

According to Figure 27 higher lambda values seem to put the combustion phasing earlier with both geometries. The effect is more prominent with the baseline geometry, but the trend can be seen also with the stepped-bowl. One reason for this could be the increased pressure, which has a well-known effect on auto ignition. Hence, higher pressure earlier in the cycle results in shorter ignition delay. Earlier start of combustion at higher λ values is also demonstrated by the RoHR displayed in Figure 24 and 25.

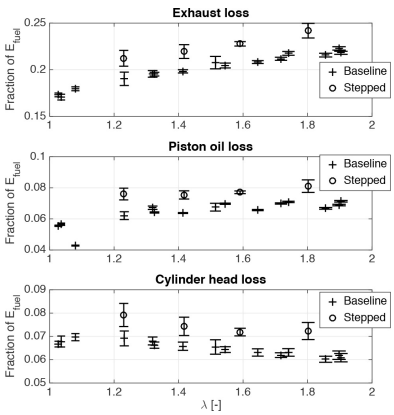

Figure 25. Losses to exhaust gas, cylinder head cooling, and piston oil cooling for the λ sweeps with both geometries.

The combustion durations are presented in Figure 28, which for the stepped-bowl follow the results presented above. It is reduced significantly both compared to the baseline bowl and with higher λ values. This is most likely a result of the steep and narrow RoHR, and maybe also better mixing during the mixing controlled phase.

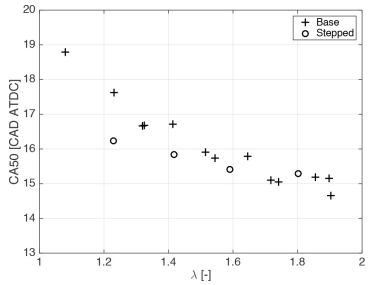

Figure 26. Crank angle degree at 50 % heat release for the λ sweeps with both geometries.

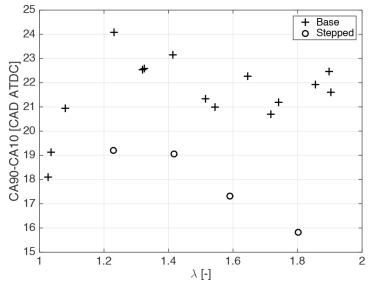

Figure 27. Combustion duration for the λ sweep with both geometries.

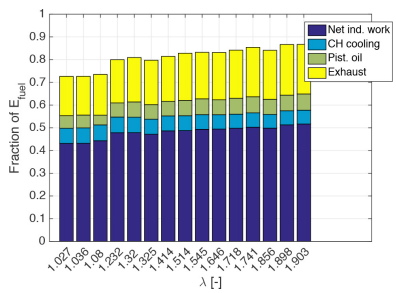

Figure 28. Energy balance for the λ sweep with baseline geometry.

Figure 29 and 30 present the energy balances for the baseline and the stepped-bowl geometries, respectively. In both cases the exhaust losses can be seen to increase with higher λ values. With the baseline piston the indicated work also increases with higher λ values. Shorter combustion duration and earlier combustion phasing results in more energy being released closer to TDC, which is beneficial for work extraction.

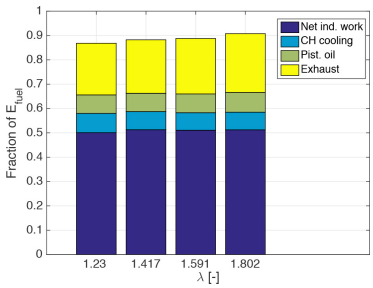

Figure 29. Energy balance for the λ sweep with stepped-bowl.

Summary/Conclusions

A comparison was made between a conventional diesel combustion chamber geometry and a new stepped-bowl geometry with regard to heat losses to cooling media and exhaust gas. The experimental work consisted of three parts: The previously published tests with the baseline geometry, a pre-study concerning spray target position for the stepped-bowl, and finally the same speed-load test and parameter sweeps first performed with the baseline geometry. The swept parameters were rail pressure, swirl, EGR and λ.

Throughout the experiments, the stepped-bowl featured shorter combustion duration and higher exhaust losses than the baseline geometry. In most cases the piston cooling losses were also slightly increased while cylinder head cooling losses were reduced with the stepped-bowl. Except for these differences, the general trends were similar for both geometries. If the sum of the losses is unchanged, increased exhaust losses could be beneficial compared to other losses. Exhaust heat could be utilised in turbochargers or other waste heat recovery systems.

1. The speed-load test showed higher exhaust losses for the high speed, high load cases than for the case with low speed and load. This indicated that load has a greater impact on exhaust losses than speed. Cylinder head and piston cooling losses show the opposite trend. Higher exhaust losses were found with the stepped-bowl than with the baseline geometry. Oil and cylinder head cooling losses were similar for both bowls. The stepped-bowl also gave shorter combustion durations.
2. The rail pressure sweep resulted in more heat losses to cooling water and piston oil with higher rail pressure, while exhaust losses decreased. The injection duration changes with rail pressure. This affects combustion duration, which in turn has an effect on exhaust losses. With the stepped-bowl combustion duration was reduced and exhaust losses increased, while cylinder head and piston cooling losses were slightly reduced.
3. The swirl sweep showed no discernible effect on heat transfer to the exhaust for either geometry. Cylinder head cooling losses increased slightly with higher swirl for both geometries, while piston oil cooling losses were more obviously increased. The stepped-bowl presented higher cylinder head cooling loss, slightly lower exhaust losses, and similar piston cooling losses compared to the baseline geometry. The combustion duration was more significantly shortened by higher swirl with the baseline piston than with the stepped-bowl. The energy balances were similar for both geometries.
4. Higher EGR levels resulted in increased cylinder head cooling losses and decreased piston cooling and exhaust losses with both geometries. The stepped-bowl reduced heat losses to piston and cylinder head cooling somewhat compared to the baseline geometry. Exhaust losses were increased with the stepped-bowl, but the difference between 0 and 25 % EGR was slightly smaller. Combustion duration was reduced with the stepped-bowl. The energy balance shows the same trends for both geometries.
5. At higher λ values heat losses to cooling water decrease, while heat losses to piston oil and exhaust tend to increase. The RoHR was significantly higher and narrower with the stepped-bowl, which seems to be a result of mixing between the second pilot and main injection. Both exhaust, cylinder head and piston cooling losses were higher with the stepped-bowl. Combustion duration was also decreased.

Now that the impact of these two bowl geometries has been investigated, focus will be shifted towards spray parameters.

References

1. Abedin, M., Masjuki, H., Kalam, M., Sanjid, A. et.al, 2013. “Energy balance of internal combustion engines using alternative fuels”. Renewable and Sustainable Energy Reviews, 26, pp. 20-33.
2. Uzun, A. C, evik, I., and Akc jl, M., 1999. “Effects of thermal barrier coating on a turbocharged diesel engine performance”. *Surface and Coatings Technology*, 116-119, pp. 505-507.
3. Hejwowski, T., and Weronski, A., 2002. “The effect of thermal barrier coatings on diesel engine performance”. *Vacuum*, 65(3-4), pp. 427-432.
4. Taymaz, I., 2007. “The effect of thermal barrier coatings on diesel engine performance”. *Surface and Coatings Technology*, 201(9-11 SPEC. ISS.), pp. 5249-5252.
5. Chan, S., and Khor, K., 2000. “Effect of thermal barrier coated piston crown on engine characteristics”. *Journal of Materials Engineering and Performance*, 9(1), pp. 103-109.
6. Modi, A. and Gosai, D., "Experimental Study on Thermal Barrier Coated Diesel Engine Performance with Blends of Diesel and Palm Biodiesel," *SAE Int. J. Fuels Lubr.* 3(2):246-259, 2010, doi:10.4271/2010-01-1519.
7. Sher, I., Levinzon-Sher, D., and Sher, E., 2009. “Miniaturization limitations of HCCI internal combustion engines”. *Applied Thermal Engineering*, 29(2-3), pp. 400-411.
8. Kokjohn, S., Hanson, R., Splitter, D., Kaddatz, J. et al., "Fuel Reactivity Controlled Compression Ignition (RCCI) Combustion in Light- and Heavy-Duty Engines," *SAE Int. J. Engines* 4(1):360-374, 2011, doi:10.4271/2011-01-0357.
9. Payri, F., Margot, X., Gil, A., and Martin, J., "Computational Study of Heat Transfer to the Walls of a DI Diesel Engine," SAE Technical Paper 2005-01-0210, 2005, doi:10.4271/2005-01-0210.
10. Andersson, O., and Miles, P. C., 2014. *Diesel and Diesel LTC Combustion*. John Wiley & Sons, Ltd.
11. Mavropoulos, G., Rakopoulos, C., and Hountalas, D., "Experimental Investigation of Instantaneous Cyclic Heat Transfer in the Combustion Chamber and Exhaust Manifold of a DI Diesel Engine under Transient Operating Conditions," SAE Technical Paper 2009-01-1122, 2009, doi:10.4271/2009-01-1122.

12. Sharief, A., Chandrashekar, T., Antony, A., and Samaga, B., "Study on Heat Transfer Correlation in IC Engines," SAE Technical Paper 2008-01-1816, 2008, doi:10.4271/2008-01-1816.
13. Najjar, Y., 2013. "Protection of the environment by using innovative greening technologies in land transport". *Renewable and Sustainable Energy Reviews*, 26, pp. 480-491.
14. Sun, J., Bittle, J., and Jacobs, T., "Influencing Parameters of Brake Fuel Conversion Efficiency with Diesel / Gasoline Operation in a Medium-Duty Diesel Engine," SAE Technical Paper 2013-01-0273, 2013, doi:10.4271/2013-01-0273.
15. Kleemann, A. and Gosman, A., "Heat Transfer Sensitivity Study for an Advanced Diesel Engine," SAE Technical Paper 2003-01-0561, 2003, doi:10.4271/2003-01-0561.
16. Gingrich, E., Ghandhi, J., and Reitz, R., "Experimental Investigation of Piston Heat Transfer in a Light Duty Engine Under Conventional Diesel, Homogeneous Charge Compression Ignition, and Reactivity Controlled Compression Ignition Combustion Regimes," *SAE Int. J. Engines* 7(1):375-386, 2014, doi:10.4271/2014-01-1182.
17. Said, M., Buttsworth, D., and Yusaf, T., 2009. "A review of radiation heat transfer measurement for diesel engines using the two-colour method". ICEE 2009. 3rd International Conference on Energy and Environment. pp. 202-207. doi: 10.1109/ICEENVIRON.2009.5398645
18. Dolak, J., Shi, Y., and Reitz, R., "A Computational Investigation of Stepped-Bowl Piston Geometry for a Light Duty Engine Operating at Low Load," SAE Technical Paper 2010-01-1263, 2010, doi:10.4271/2010-01-1263.
19. Styron, J., Baldwin, B., Fulton, B., Ives, D. et al., "Ford 2011 6.7L Power Stroke® Diesel Engine Combustion System Development," SAE Technical Paper 2011-01-0415, 2011, doi:10.4271/2011-01-0415.
20. Fridriksson, H., Tuner, M., Andersson, O., Sunden, B. et al., "Effect of Piston Bowl Shape and Swirl Ratio on Engine Heat Transfer in a Light-Duty Diesel Engine," SAE Technical Paper 2014-01-1141, 2014, doi:10.4271/2014-01-1141.
21. Dahlstrom, J., Andersson, O., Persson, H. and Tunér, M., 2015. "Effects of Spray-Swirl Interactions on Heat Losses in a Light Duty Diesel Engine". IMECE2015-53606.
22. Das, S. and Roberts, C., "Factors Affecting Heat Transfer in a Diesel Engine: Low Heat Rejection Engine Revisited," SAE Technical Paper 2013-01-0875, 2013, doi:10.4271/2013-01-0875.
23. Perini, F., Dempsey, A., Reitz, R., Sahoo, D. et al., "A Computational Investigation of the Effects of Swirl Ratio and Injection Pressure on Mixture Preparation and Wall Heat Transfer in a Light-Duty Diesel Engine," SAE Technical Paper 2013-01-1105, 2013, doi:10.4271/2013-01-1105.
24. Eiglmeier, C., Lettmann, H., Stiesch, G., and Merker, G., "A Detailed Phenomenological Model for Wall Heat Transfer Prediction in Diesel Engines," SAE Technical Paper 2001-01-3265, 2001, doi:10.4271/2001-01-3265.
25. Fathi, M., Saray, R., and Checkel, M., 2011. "The influence of exhaust gas recirculation (EGR) on combustion and emissions of n-heptane/natural gas fueled homogeneous charge compression ignition (HCCI) engines". Applied Energy, 88(12), pp. 4719-4724.
26. Miles, P.C., Rempelewert, B.H. and Reitz, R.D. (2003) Squish-swirl and injection-swirl interaction in direct-injection diesel engines. ICE 2003: 6th International Conference on Engines for Automobiles, Sept. 14-19, Capri, Naples, Italy.
27. Heywood, J. B., 1988. "Internal Combustion Engine Fundamentals". McGraw-Hill, Inc.
28. Woschni, G. and Fieger, J., "DETERMINATION OF LOCAL HEAT TRANSFER COEFFICIENTS AT THE PISTON OF A HIGH SPEED DIESEL ENGINE BY EVALUATION OF MEASURED TEMPERATURE DISTRIBUTION," SAE Technical Paper 790834, 1979, doi:10.4271/790834.

Contact Information

Jessica Dahlström
+46 46 2223999
Jessica.Dahlstrom@energy.lth.se

Acknowledgement

The authors would like to thank the Swedish Energy Agency for funding this project.

Definitions/Abbreviations

ANOVA - Analysis of Variance
CA50 - Crank angle at 50 % heat release
CAD ATDC - Crank Angle Degrees After Top Dead Centre
CDC - Conventional Diesel Combustion
CDCC - Conventional Diesel Combustion Chamber
CO2 - Carbon dioxide
EGR - Exhaust Gas Recirculation
ICE - Internal Combustion Engine
HCCI - Homogeneous Charge Compression Ignition
HD - Heavy Duty
IMEPg - Gross Indicated Mean Effective Pressure
LD - Light Duty
PPC - Partially Premixed Combustion
RoHR - Rate of Heat Release
STP - Spray Target Position
λ - Relative air-fuel ratio

The Engineering Meetings Board has approved this paper for publication. It has successfully completed SAE's peer review process under the supervision of the session organizer. The process requires a minimum of three (3) reviews by industry experts.

ISSN 0148-7191

http://papers.sae.org/2016-01-0732

Paper iii

Experimental Comparison of Heat Losses in a Light-Duty Diesel Engine with Various Injector Geometries

Lund University[a,*], Jessica Dahlström, Öivind Andersson, Martin Tunér

Lund University

Håkan Persson

VOLVO CAR CORPORATION

[a] *Ole Römers väg 1, Lund, Sweden*
[b] *SE-405 31 Göteborg, Sweden*

Abstract

Heat loss is one of the greatest energy losses in engines. More than half of the heat is lost to cooling media and exhaust losses, and they thus dominate the internal combustion engine energy balance. Complex processes affect heat loss to the cylinder walls, including gas motion, spray-wall interaction and turbulence levels. The aim of this work was to experimentally compare the heat transfer characteristics of a multi-cylinder, light duty (LD) diesel engine using three sets of injectors featuring different number of holes. The separation of the sprays as well as the hole size could affect mixing, wall contact and other parameters that could influence heat transfer. Speed, load, injection pressure, swirl level, EGR rate and air/fuel ratio (λ) were varied in the engine operated in conventional diesel combustion (CDC) mode. Temperature measurements in the engine cooling media were used to set up the engine energy balance and find out how much heat was lost to exhaust and cooling media in different parts of the engine. Based on these calculations and heat release analysis, conclusions could be drawn regarding how heat losses in different parts of the engine were affected by changes in these parameters and how the heat transfer characteristics differ between the three injector designs.

Keywords: `heat transfer`, diesel, internal combustion engine, injector, swirl

1. Introduction

The global energy consumption is increasing, and despite increased efforts to convert to renewable energy sources, fossil fuel consumption is still on the rise. This also results in increasing emissions of greenhouse gases, such as carbon dioxide (CO_2), which contribute to global warming. Further development of internal combustion engines (ICEs) is central in addressing this problem, and has resulted in large improvements of efficiency and emissions. Further efficiency improvement requires a deeper look into engine heat losses.

Some of the efforts to reduce heat losses concern low heat rejection engines, where all or parts of the combustion chamber walls are coated with a ceramic coating to prevent heat transfer. However, studies of the effects on engine performance are contradictory with reports of both increased and decreased fuel consumption and total heat transfer [1]. Losses to cooling water are reduced because most of the heat stays inside the combustion chamber, resulting in increased exhaust temperatures [2, 3, 1, 4]. Volumetric efficiency often decreases [3, 1, 4], even though fuel economy and thermodynamic efficiency are reported to improve [1, 4, 5, 6]. So far, the benefits have not been shown to outweigh the drawbacks and render this a viable concept.

Reports show significant efficiency differences between different engine sizes. A comparison between heavy duty (HD) and light duty (LD) engines shows that LD engines consistently demonstrate lower efficiencies than HD engines. One explanation could be that they have higher surface-to-volume ratios [7], but the increased heat losses could also be caused by high swirl

[*] Jessica Dahlström
Email address: `jessica.dahlstrom@energy.lth.se` (Lund University)

ratios and less favourable combustion chamber designs [8]. However, there are few examples in the literature addressing the role heat transfer may play in this.

Speed and load both have significant effects on heat transfer. Higher engine speed results in less time for heat exchange [9], but at the same time turbulence increases and thus also convective heat transfer [10]. However, several studies confirm that load seems to be more influential than speed [11, 12, 13, 14].

High temperature and pressure, long combustion duration and flame- wall interaction has been found to cause high heat transfer losses [14]. Another research team found that the heat transfer coefficient varies significantly between different locations in the combustion chamber depending on whether the wall is in contact with the flame or not [11]. This conclusion is also supported by other researchers [15]. Another way of reducing heat flux is later combustion timing [16] which has also been proven to reduce peak radiation [17], although this could have negative effects on heat losses in some parts of the engine.

Several studies concern the heat transfer characteristics of different bowl geometries. A stepped-bowl piston with low surface-to-volume ratio was found to reduce wall heat transfer [18]. Another research group optimised a chamfered, re-entrant bowl with low swirl and an 8-hole nozzle [19]. This system provided a more uniform equivalence ratio field than the wide re-entrant bowl it was compared to, except along the cylinder liner where a lean region was found to prevent heat loss to the coolant. Fridriksson *et al.* found that the conventional re- entrant diesel geometry in their study had lower thermodynamic efficiency and higher heat losses than more shallow and open geometries, such as stepped-bowl and a tapered, lipless piston [20]. At high load the shallow, open piston bowls displayed more heat transfer in the bowl, while the conventional types showed more bowl-lip heat transfer. This was found to coincide with the location of the hot gases. A low surface-to-volume ratio, often assumed to reduce heat transfer, was only found to directly influence heat transfer before the start of spray-driven combustion. After that, other combustion parameters and turbulence were more influential [20]. The study by Fridriksson *et al.* included the geometries used in a previously published research by the authors of this paper, which forms the baseline to which the present stepped-bowl results are compared [21, 22].

The injector nozzle-hole orientation and number of holes have a documented effect on wall heat transfer [23]. These parameters require optimisation with a specific combustion chamber geometry. Reduced injection duration can be achieved with larger hole size, which increases the rate of heat release (RoHR). This generally improves efficiency, but the effect can be offset by increased heat transfer losses [23] and soot. At some distance from the nozzle the spray will reach a stagnation point. Where this occurs depends on ambient density and the state of the spray [24, 25]. At lower in-cylinder density the spray arrived at the stagnation point sooner than at higher density. A combusting spray was also found to arrive sooner than an evaporating spray. Low injection pressure and ambient density resulted in combustion starting after the spray impinged on the wall. At increased ambient density, combustion started before impingement due to lower spray velocity and shorter ignition delay. When increasing injection pressure combustion again started at impingement [24]. It has been established that spray penetration is affected by swirl, as greater air entrainment into the jet due to swirl would reduce radial penetration [26]. Increased impact area and greater spray jet momentum led to significantly increased wall heat transfer, mixture stratification, and delayed ignition timing [26]. Experiments with multi-orifice nozzles with very small orifices have been tested in conventional diesel combustion [27]. They were proven to produce a highly dispersed spray which can promote air entrainment under low swirl conditions. The nozzles had weak spray penetration, which led to decreased overall load performance. With this highly dispersed spray, the high temperature area causing cooling losses is along the side walls of the piston cavity. However, this area is reduced compared to conventional sprays [27].

The most thoroughly investigated gas flow pattern affecting heat transfer is swirl. In general, low swirl levels seem to produce low heat loss [20]. However, different geometries show dissimilar responses to swirl ratio changes, which may be due to different velocity fields. Convective heat flux is related to rotational gas motion, which was mainly found to increase close to the outer walls. Low swirl was found to reduce heat loss for conventional diesel combustion chamber (CDCC) geometries, while the more open piston geometries experienced increased heat losses as near-wall fluid velocity increased when swirl level decreased [20]. Another CFD study found that high swirl ratios significantly increased wall heat transfer and delayed the ignition timing [26]. An experimental CDC study showed that the mean piston surface temperature increased with higher swirl, suggesting an increased steady state heat transfer component [16]. Eiglmeier *et al.* [28] found that heat flux peaks increased with turbocharging, which was explained by intensified turbulence. The convective heat transfer was also found to increase [28].

EGR has a documented effect on heat transfer. Theoretically, the heat transfer coefficient is proportional to pressure and inversely proportional to temperature. This was also confirmed experimentally by Fathi *et al.* [29]. However, the heat transfer coefficient does not vary significantly with EGR, since increased EGR rates reduce both charge temperature and pressure. Convective heat transfer reduces as a result of the reduced temperature difference between charge and wall [29]. Das *et al.* [23] also obtained significant heat loss reduction with increased EGR, which was explained by the increased charge mass requiring more heat to increase charge temperature.

Although spray-swirl interactions could significantly affect the heat losses they have not been widely studied. As shown in Figure 1, before fuel injection a swirl-supported combustion system places the gas with the highest tangential velocity at the outer bowl wall, maximising the convective heat losses in this region. After fuel injection, however, the spray has entrained gas with low tangential velocity at the central bowl region and transported it to the wall. This transport sets up a vertical vortex at the wall, which displaces the high velocity gas towards the centre (Figure 1). The vortex thereby decreases the convective heat transfer to the wall during combustion. The radial location of the gas with highest tangential velocity is determined by a balance between its centrifugal force and the inward force exerted by the spray-induced vortex. The centrifugal force is determined by the swirl ratio, whereas the inward force is determined by the injection pressure.

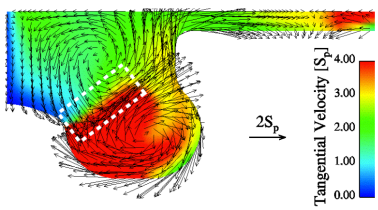

Figure 1: The fuel injection event limits the convective heat transfer to the outer bowl wall by displacing gas with high tangential velocity towards the centre (adapted from [30]).

Table 1: ENGINE SPECIFICATIONS

Displaced volume [l]	2.0
Stroke [mm]	93.2
Bore [mm]	82
Connecting rod [mm]	147
Compression ratio [-]	15.8:1
Number of valves	4
No. of injector holes	6, 8 and 10
Fuel	Diesel

2. Material and methods

2.1. Experimental setup

Experiments were performed in a 4-cylinder light-duty diesel engine with Denso injectors. Engine specifications are presented in Table 1. Three injector geometries were tested, the baseline 8-hole injectors and two sets with 6 and 10 holes, respectively. The injectors were manufactured with the same umbrella angle and total hole area as the original injectors. To set up the engine energy balance, temperature and mass flow measurements were needed. All cylinders were instrumented with thermocouples for measuring temperature differences in the cooling system.

Measurements of the cooling water temperature difference over the cylinder head were performed to calculate heat losses to the cylinder head. The cooling water flows up from the engine block to the cylinder head through channels on the inlet side, and returns to the engine block through channels on the exhaust side. The cylinder head was equipped with T-type thermocouples in all cooling channels for cylinder 3 and 4, while the other cylinders only had one on the inlet and one on the exhaust side (marked with white arrows in Figure 2). Except for the thermocouples in the middle channels on the exhaust side of cylinder 3 and 4, the thermocouples on the exhaust side were connected in pairs to the corresponding ones on the inlet side to measure the cooling water temperature difference over the cylinder head with as little measurement error as possible. The thermocouples in the middle channels were used to measure the absolute temperature in the cooling water leaving the cylinder head.

One K-type thermocouple was fitted in the feed line to the piston cooling oil rail, and two were fitted in funnel-shaped structures below the pistons to measure the oil return flow temperatures from cylinder 2 and 3.

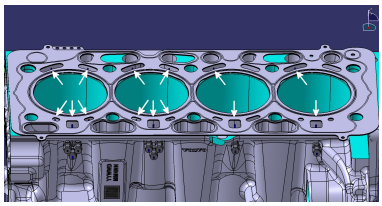

Figure 2: Thermocouple positions in cylinder head cooling channels, exhaust side view.

These two were assumed representative for all cylinders. One of these is shown in Figure 3, where the structure and the pipe guiding oil from the piston outlet to the funnel can be seen from below.

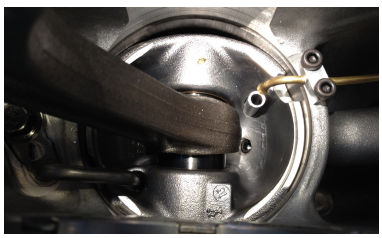

Figure 3: Position of thermocouple measuring piston oil return flow temperature.

All cylinders were fitted with Kistler pressure sensors to measure in- cylinder pressure used for the heat release analysis. Exhaust oxygen concentration was measured using an Etas lambda meter. Engine out soot emissions were measured using an AVL soot meter, all other emissions using a Horiba system.

The mass flow of cooling water over the cylinder head was measured using a GL Flow turbine flow meter, mass flow of air fed to the engine was measured using a Bronkhorst In-Flow meter, and oil mass flow to the piston cooling was measured with a Macnaught oval meter. Fuel flow was measured using a Sartorius balance.

2.2. Experimental methodology

Heat transfer to the cooling media was measured at various engine conditions. One speed-load test was performed, and during additional tests the following four parameters were swept: rail pressure, swirl, EGR and λ. All of the experimental work was performed at 1500 rpm and approximately 10.5 bar $IMEP_g$, except in the speed-load test where case 1 was performed at 2000 rpm and case 3 at 5.5 bar $IMEP_g$. The fuel flow was kept constant during all parameter sweeps, but varied between the different cases in the speed-load test. The same injection strategy was used throughout this work, and consisted of two pilot injections, main injection and one post-injection. All data points were repeated three times and the tests were randomised to exclude any background variables affecting the results.

Table 2: Speed and load combinations

Case	Speed [rpm]	$IMEP_g$ [bar]	p_{in} [bar]	EGR [%]
1	2000	10.5	1.8	17 %
2	1500	10.5	1.6	15 %
3	1500	5.0	1.1	38 %

Speed and load test. Three different combinations of two engine speeds and two load cases were performed with three randomised repetitions of each combination, each repetition containing 300 consecutive cycles. The three combinations, case 1-3, are described in Table 2. All cases were performed at 1250 bar rail pressure.

Rail pressure sweep. Rail pressure has a significant impact on heat transfer, which was confirmed by the previously published studies [21, 22]. Higher pressure reduces injection duration, and thereby also combustion duration. The rail pressure sweep was based on speed and load case 2, to which CA50 and heat release were matched. Inlet pressure was kept constant at 1.6 bar, and the EGR level was approximately 25 %. Table 3 shows the five rail pressures between 500 and 2000 bar which were included in the sweep, as well as the settings for the variables in the other sweeps. All sweeps were performed with all variables kept as constant as possible except for the one that was swept.

Swirl sweep. Several studies have found increased wall heat losses at higher swirl levels. During the swirl sweep the inlet pressure and EGR level were kept constant at the same values as during the rail pressure sweep, and the rail pressure was set to 1250 bar. As stated in Table 3, the swirl valves were set in 11 different positions between 0 and 100 % closed, representing minimum to maximum swirl level, respectively.

Table 3: Test conditions during sweeps

Rail pressure [bar]	500, 1000, 1250, 1500, 2000
Swirl valve % closed	0, 10, 20, 30, 40, 50, 60, 70, 80, 90, 100
EGR [%]	0, 12, 25
p_{in}, all except λ sweep [bar]	1.6

In a previous experiment [21] the swirl sweep was repeated at 500 bar rail pressure to find out if a lower rail pressure would result in different spray-swirl interaction effects. The conclusion was that the results were similar to the 1250 bar case.

EGR sweep. The EGR sweep was performed with constant inlet and rail pressure, the same levels as described for the swirl sweep. The EGR levels were set to approximately 0, 12 and 25 %. Both the middle and highest EGR levels differed slightly between the sweeps performed with the different injectors, with a somewhat lower level for the baseline 8-hole injectors. However, the differences were small enough to be assumed to not have any significant effect on the results. EGR serves as inert gas, which absorbs energy when heated and, thus, reduces in-cylinder temperatures. This is expected to also reduce heat losses.

Lambda sweep. During the λ sweep the rail pressure was set to 1250 bar and the EGR level was 25 %. The fuel flow was kept constant while inlet pressure was varied, resulting in λ values between 1.0 and 2.0. Higher values required higher inlet manifold pressures, which could not be reached due to safety reasons. The test effectively showed the effect on heat transfer of varying the in-cylinder pressure. High pressure normally increases temperature. On the other hand, the excess air serves as an inert gas, absorbing energy when heated and thus reducing the in-cylinder temperature. This should also have some effect on heat losses.

3. Theory

The rate of heat release (RoHR), $dQ/d\theta$, was calculated from the pressure trace for all 3x300 engine cycles using Eqn. (1) [31]. The specific heat ratio is represented by γ, p is the cylinder pressure and V is the cylinder volume.

$$\frac{dQ}{d\theta} = \frac{\gamma}{\gamma - 1} p \frac{dV}{d\theta} + \frac{1}{\gamma - 1} V \frac{dp}{d\theta} + \frac{dQ_{ht}}{d\theta} \quad (1)$$

Q_{ht} represents the heat transfer losses and is calculated using the Woschni heat transfer model described by Eqn. (2) [32], where h_c is the heat transfer coefficient, C is a constant adapting the model to a specific engine, B is the engine bore, T denotes temperature and w is the local average in-cylinder gas velocity.

$$h_c = C B^{-0.2} p^{0.8} T^{-0.53} w^{0.8} \quad (2)$$

The measured temperature differences in the cooling media and exhaust gas were used to calculate energy losses, ΔQ_{medium}, using Eqn. (3), where $\dot{m}_{medium}$ is the mass flow of the respective medium (air, cylinder head cooling water, and oil), $C_{p,low}$ and $C_{p,high}$ are the specific heats of the medium at the low and high temperature, respectively. ΔT_{medium} is the measured temperature difference in the medium between the low and high temperature measurement.

$$\Delta E_{medium} = \dot{m}_{medium} \frac{\left(C_{p,low} + C_{p,high}\right)}{2} \Delta T_{medium} \quad (3)$$

4. Results and Discussion

4.1. Speed and load test

The heat losses to exhaust, cylinder head cooling and piston cooling for the three different speed and load combinations, case 1-3, are presented in Figure 4 for all three injector sets. Error bars represent one standard deviation calculated from the three replicates combined, 900 measurements in total. All of these losses follow the same trends with the different injectors. However, losses to exhaust and piston cooling are slightly lower with the 8-hole injectors. The cylinder head losses are very similar for all injectors, but differ more for case 1 characterised by both higher load and speed. The 8-hole injectors show somewhat higher cylinder head loss than the others, with the 6-hole injectors resulting in least loss in the high load cases. The 10-hole injectors give the least cylinder head loss for case 3 with low speed and load.

The rate of heat release may show similarities and differences that could explain the trends, and it is shown in Figure 5. Each part of the figure shows one speed-load case with the RoHR for every injector configuration. For all cases the RoHR is lower with the 10-hole injectors, while the other two are relatively similar in height.

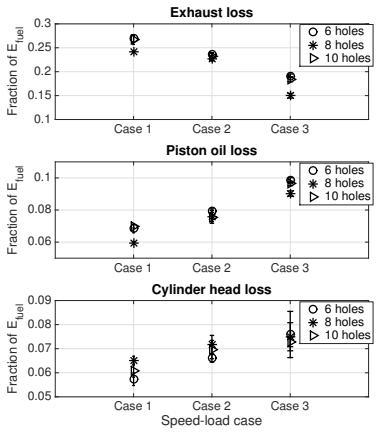

Figure 4: Fraction of fuel energy lost to cylinder head coolant, piston oil cooling and exhaust at different speed and load conditions.

Combustion also seems to be slower with the 10-hole injectors, except for case 3 where the main combustion peak is significantly narrower. The later part of the combustion is relatively similar to the 8-hole injector. In this case the 6-hole injectors clearly reduce the combustion duration with a both taller and narrower RoHR. Case 1 also presents slow combustion using the 10-hole injectors. The later part of the combustion is significantly slower than with the other injectors.

The heat release behaviour of the injectors is reflected in the combustion phasing and duration shown in the left and right part of Figure 6, respectively. The flow characteristics were supposed to be the same for all injectors, but both the 6- and 10-hole injectors required longer injection durations to maintain the same fuel flow as the 8-hole injectors. This affected the combustion phasing, making it somewhat difficult to keep it constant. This was especially true for case 3, with low speed and load. This could be because of the shorter injection durations. The shorter duration, the less time for the fuel flow to stabilise. The phasing was constantly later with the 6-hole injectors and mostly earlier with the 8-hole injectors. The only exception is case 2, where the 10-hole injectors had the earliest phasing.

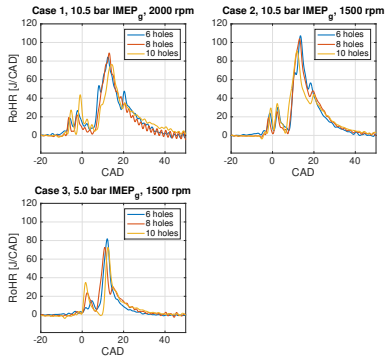

Figure 5: Rate of heat release at different speed and load conditions cases.

The combustion durations presented in the right part of Figure 6 reflect the behaviour of the injection durations. The 8-hole injectors had shortest injection duration in the high load cases, but for case 3 both main injection and combustion duration are shortest with the 6-hole injectors.

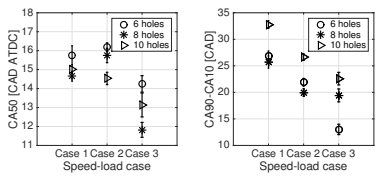

Figure 6: Combustion phasing (left) and duration (right) at different speed and load conditions.

The engine energy balance was set up as described in section 2.2, and is presented in Figure 7. For the high load cases the net indicated work is similar for all injectors, with a slight increase for the 10-hole injectors. In general, the 8-hole injectors present less total heat loss than the others. An interesting observation is the the clear difference in indicated work between the injectors for case 3, with low speed and load. For case 2 all parts

are relatively equal for all versions, and for case 1 the 6- and 10-hole injectors show less cylinder head cooling losses but larger piston and exhaust losses. Thus, it is the more extreme speed- and load points that differ the most. Case 1 with both high speed and load shows an effect on heat transfer to exhaust and cooling media, whereas the low speed and load case 3 mainly shows an effect on indicated work.

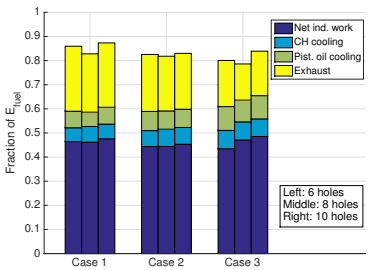

Figure 7: Engine energy balance at different speed and load conditions.

In the high load cases (1 and 2) the temperature is lower with the 6-hole injectors, in case 3 the 6- and 10-hole injectors give similar temperatures. Emissions of NO_x and soot are similar with all three injectors in case 3, but in case 1 and 2 the 6-hole injectors give much less soot and higher NO_x than the 10-hole injectors. The 8-hole injectors show even higher NO_x levels, but soot data is unfortunately not available. The high NO_x level with the 8-hole injectors can be explained by the faster combustion causing higher temperature. Faster combustion could be the answer for the 6-hole injectors as well, even though it did not show on the calculated temperature. The 10-hole injectors in general had slower combustion with a longer mixing controlled part, which is known to result in more soot. The 6-hole injectors had a larger part of premixed combustion, and thus more NO_x and less soot. Both the 6- and 10-hole injectors burned later in the cycle, which could also explain their higher exhaust losses.

4.2. Rail pressure sweep

The two previous studies [21, 22] showed that rail pressure has an effect on heat transfer to cooling media and exhaust. The injection durations had to be adjusted to achieve the same fuel flow for every set of injectors. In general the 6-hole injectors required the longest injections and the 8-hole injectors the shortest. Only the 500 bar rail pressure case differed, then the 10-hole injectors needed the longest injection duration. The observed heat losses are presented in Figure 8. The same trends observed in the previous studies can also be seen here: Exhaust losses decrease with increasing rail pressure, while losses to piston and cylinder head cooling tend to increase. Comparing the different injectors it can be seen that the 8-hole injectors give the least exhaust losses, which is consistent with their shorter combustion duration. However, short combustion duration is often a result of a larger premixed combustion part which in turn increases piston cooling losses. In Figure 8 it is clearly the 6-hole injectors that have the highest piston cooling losses. As proposed by previous research [24, 25] this could also be an effect of different penetration length. The larger holes of the 6-hole injectors could give a longer penetration so a larger bowl area gets in contact with the burning spray, giving rise to higher piston cooling losses.

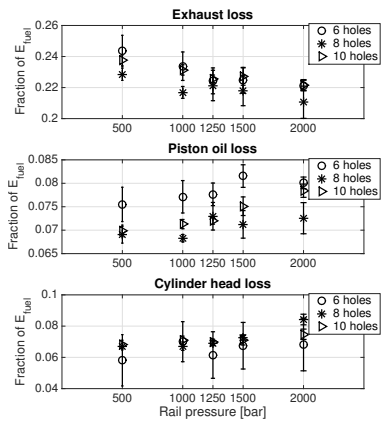

Figure 8: Fraction of fuel energy lost to cylinder head coolant, piston oil cooling and exhaust at different rail pressures.

The rates of heat release (RoHR) for three of the rail pressures, 500, 1250 and 2000 bar, are presented in Fig-

ure 9. For the two lower pressures the 6-hole injectors give the tallest main peak and shortest mixing controlled tail. For the highest rail pressure the 8-hole injectors give the tallest peak, but it is still the 6-hole injectors that give the shortest later part of combustion. The 6-hole injectors also show a steeper rising edge, and the 10-hole injectors a longer combustion.

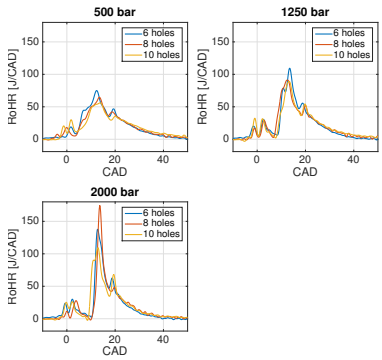

Figure 9: Rate of heat release at different rail pressures.

The combustion phasing shown in the left part of Figure 10 had a tendency to occur earlier with higher rail pressure, because of the shorter injection duration. This could be adjusted to some extent by injecting later. The right part of the figure shows the combustion duration. The 10-hole injectors consistently results in slower combustion than the others. At lower rail pressure the 6-hole injectors are by far the fastest burning alternative, but from 1250 bar rail pressure and up the 6- and 8-hole injectors give similar results. Again, looking at the RoHR in Figure 9, the main peak is taller for the 6-hole injectors than for the others. This and the shorter later part could explain the faster combustion.

The engine energy balance showed that the main difference between the injectors was the indicated work at low rail pressure, where the 6-hole injectors show best performance. This could be expected by the faster combustion discussed above. However, the slower combustion with the 10-hole injectors does not seem to influence the extracted work significantly. It remains at the same level as with the 8-hole injectors.

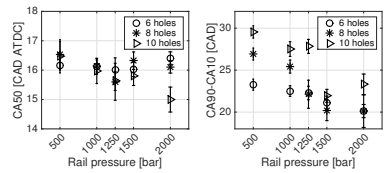

Figure 10: Combustion phasing (left) and duration (right) at different rail pressures.

Engine out emissions are presented in Figure 11. The 6-hole injectors consistently give rise to the highest NO_x emissions. This is probably connected to the fast and more premixed combustion that was demonstrated by the RoHR in Figure 9 and combustion duration in Figure 10. The 8- and 10-hole injectors give very similar results for all rail pressures except at 1250 bar, where the NO_x level is increased for the 8-hole injectors. This is also where the combustion duration differs the most between the injectors, with a much longer duration for the 10-hole injectors.

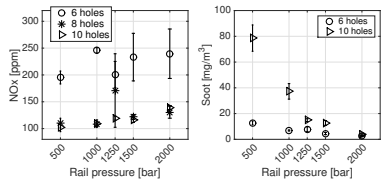

Figure 11: Engine out NO_x (left) and soot (right) at different rail pressures.

The right part of the figure shows soot emissions. As described for the speed-load test before, the soot meter was not installed when the 8-hole injectors were tested so unfortunately there are no soot measurements for them. However, there is a significant difference between the 6- and 10-hole injectors. At low rail pressures the 10-hole injectors have significantly higher soot emissions than the 6-hole injectors. This is most likely related to poor mixing with the 10-hole injectors. Small holes and low injection pressure combined is likely to impair mixing. As seen in Figure 9, the 10-hole injectors had a smaller main peak and longer mixing controlled combustion. Slow combustion often produces

more soot than fast combustion.

4.3. Swirl sweep

The losses to the different media during the swirl sweep are presented in Figure 12. The 0 on the x axis means that the swirl valve was fully open (low swirl), and 100 means fully closed (high swirl). Exhaust losses rarely seem to be affected by the swirl level at all, which is consistent with previous findings [21, 22]. The 6-hole injectors give rise to less exhaust loss than the other two, which are both on similar levels. This implies that exhaust gases were hotter in the latter cases. Heat losses to the piston oil cooling were similar for the 6- and 10-hole injectors, with higher loss for the 8-hole injectors. All injectors follow a trend of somewhat larger piston cooling losses at high swirl levels, which could be due to faster combustion mostly taking place inside the bowl. The cylinder head loss follows the same trend, even if the differences are small. This could be due to higher in-cylinder temperature at higher swirl levels. Again the 6-hole injectors show less loss, and the 10-hole injectors mostly higher loss.

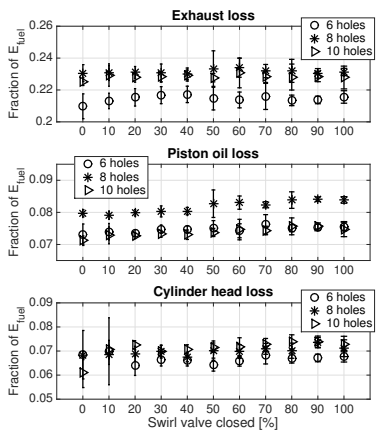

Figure 12: Fraction of fuel energy lost to cylinder head coolant, piston oil cooling and exhaust at different swirl levels.

Comparing the combustion phasing and durations in the left and right parts of Figure 13, respectively, it can be seen that the phasing was not greatly affected by the swirl level. The first point of the sweep with the 8-hole injectors differs from the others, but otherwise a slight trend towards later phasing with higher swirl can be distinguished. The 6-hole injectors show the opposite trend with slightly earlier phasing at higher swirl levels, but the difference is very small compared to the error bars. The combustion duration was reduced at higher swirl levels for all injectors, but to a varying extent. The 8-hole injectors had the shortest combustion duration, but falls between the other two in phasing. The 10-hole injectors had the earliest phasing, but as during the previously discussed tests they also had the longest combustion duration. The 8- and 10-hole injectors showed the same level of exhaust losses, which is contradictory to the finding regarding combustion duration. Slower combustion often results in higher exhaust temperatures. However, the later part of combustion trails off slightly faster with the 8-hole injectors, while the 10-hole injectors have a narrower main peak.

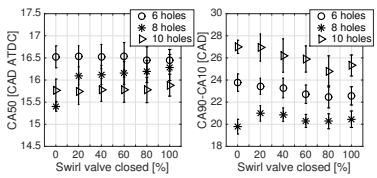

Figure 13: Combustion phasing and duration at different swirl levels.

The energy balance is similar for all swirl levels. The 8-hole injectors show slightly higher net indicated work, but also higher losses, especially compared to the 6-hole injectors.

The NO_x and soot emissions are presented in the left and right part of Figure 14. The NO_x emissions follow the same trend for all injectors, with more NO_x at higher swirl levels. The 6- and 10 hole injectors give similar levels, while the 8-hole injectors give higher levels. This could be explained by their shorter combustion duration, which temporarily significantly increases temperature and, thus, promotes NO_x formation. The soot levels in the right part of the figure look very different for the three injector geometries. All are reduced at higher swirl levels, but the 10-hole injectors are affected to a much higher degree than the other configurations. The 8-hole injectors give much less soot than the 6-hole injectors. The 10-hole injectors start at the same level as the 6-hole injectors, but with increasing swirl level

the soot level decreases and ends up at the same level as the 8-hole injectors at the highest swirl levels. This confirms that the 10-hole injectors have difficulties mixing fuel and air, and are thus helped significantly by high swirl.

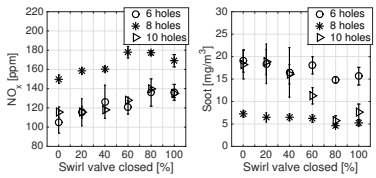

Figure 14: NO_x (left) and soot (right) emissions at different swirl levels.

4.4. EGR sweep

The EGR sweeps with the tree injector geometries were performed in the same way, but still the middle point differed between 11 and 13 % EGR, and the last point between 23 and 26 %. These differences were considered small enough to not have any significant effect on the result. The heat losses for the three EGR sweeps are presented in Figure 15. The 8-hole injectors give the least exhaust losses at all EGR levels, while the other two give similar loss levels. Piston cooling losses are highest with the 6-hole injectors, which also provide the least cylinder head losses in both cases with EGR. The highest cylinder head losses are given by the 8-hole injectors, but the 10-hole injectors are the ones that increase those losses the most at higher EGR levels. This is probably an effect of longer combustion duration.

The RoHR follows the same pattern as before for the different injectors. The 6-hole injectors still promote faster combustion, which is even more clear at higher EGR levels. The main peak looks similar for all injectors at all EGR levels, the main difference is in the later part of the combustion. This could explain why the cylinder head losses increase with EGR level for the 10-hole injectors. As combustion duration is increased, more of the combustion reaches the top part of the cylinder, which then gets hotter and in turn heats up the cooling water.

Figure 16 shows the combustion phasing to the left and the combustion duration to the right. The phasing was later at higher EGR values, which can be explained by the slower combustion seen to the right. It also clearly shows that the 6-hole injectors gave the

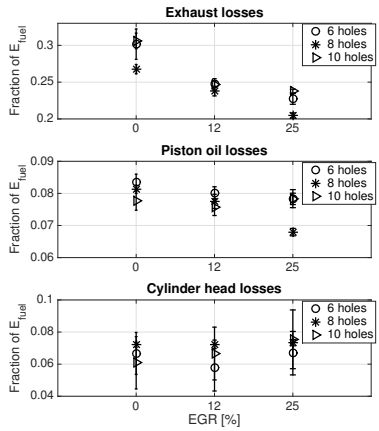

Figure 15: Fraction of fuel energy lost to cylinder head coolant, piston oil cooling and exhaust at different EGR levels.

fastest combustion and the 10-hole injectors the slowest. With the 8-hole injectors, phasing was delayed more with EGR than with the other injectors. This resulted in even slower combustion.

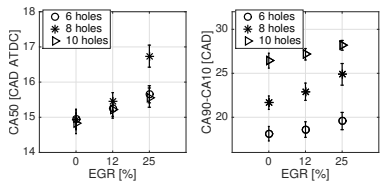

Figure 16: Combustion phasing (left) and duration (right) at different EGR levels.

Despite the slow combustion with the 10-hole injectors, these gave the highest indicated work, which is evident in Figure 17. The trend is the same at all tested EGR levels, which is consistent with the speed-load test but somewhat different from the other parameter

sweeps.

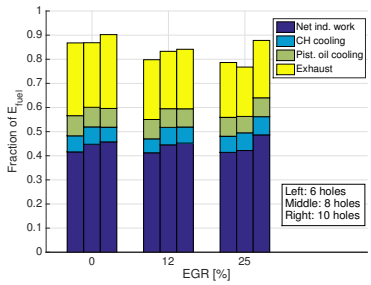

Figure 17: Engine energy balance at different EGR levels.

4.5. Lambda sweep

During the λ sweep the exhaust losses were found to increase at higher λ values for all injectors, which is demonstrated in Figure 18. This is likely due to higher temperatures following the increased intake pressure. The 10-hole injectors show the highest exhaust losses and the 8-hole injectors the lowest. Piston cooling losses were highest with the 6-hole injectors, but decreased at the highest λ values. As described for the previous sweeps, high piston cooling losses implies fast combustion but also flame impingement. This could explain why the piston cooling losses decrease at higher λ values. Higher pressure decreases spray penetration length, and should thus also reduce impingement on combustion chamber walls. With the 8-hole injectors piston cooling losses increased somewhat with λ, while with the 10-hole injectors they were unaffected. Cylinder head losses were decreasing with higher λ values for all injectors. They are relatively similar, but generally lowest with the 8-hole injectors.

The RoHR calculations again clearly demonstrate that, as before, the 6-hole injectors have a shorter combustion duration. Combustion also often starts earlier with the 6-hole injectors. The 10-hole injectors consistently show a lower main peak. Maybe the smaller hole size caused the spray to break up earlier, thus penetrating a smaller volume and mix more slowly with the air as well as burn at a lower turbulence level.

Figure 19 shows the combustion phasing to the left and the combustion duration to the right. Higher λ values result in earlier phasing, but the 8-hole injectors are

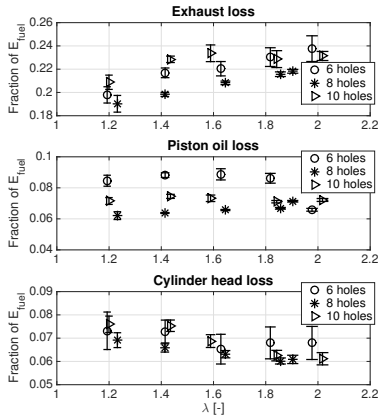

Figure 18: Fraction of fuel energy lost to cylinder head coolant, piston oil cooling and exhaust at different λ values.

affected the most. Combustion duration is shorter with the 6-hole injectors and slower with the 10-hole injectors, and it is generally shorter at higher λ values. With higher λ the pressure is increased, which could increase the turbulence level and speed up combustion.

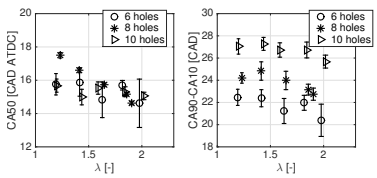

Figure 19: Combustion phasing and duration at different λ values.

Net indicated work increases with λ according to the energy balance. This could be expected considering the higher air fraction in the cylinder, which increases the ratio of specific heats, γ, and thus the efficiency. The extracted work is relatively similar for all injectors, but in most cases slightly lower with the 10-hole injectors.

One reason could be the slower combustion, but on the other hand the trend was the opposite during the EGR sweep. Then the 10-hole injectors had the highest net indicated work.

The NO_x and soot emissions are presented in the left and right part of Figure 20, respectively. The NO_x level increases with λ for all injector geometries, which could be expected because of the faster combustion and higher temperatures. At higher λ values the levels reach a plateau. Excess air acts as a heat sink, and counteracts the temperature rise caused by the higher pressure. High NO_x usually corresponds to low soot emissions, which can be seen in the right part of Figure 20. At lower λ values than 1.3 soot emissions were too high for the measurement equipment to handle. High temperatures and excess air helps soot oxidation.

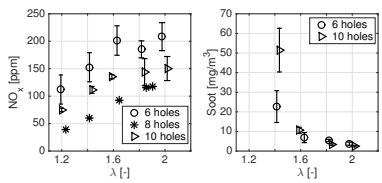

Figure 20: NO_x (left) and soot (right) emissions at different λ levels.

5. Conclusions

A parametric study of the injector geometry effects on heat losses in a multi-cylinder, conventional LD diesel engine operated in CDC mode was performed. The heat losses were quantified and compared using heat release analysis and energy balance calculations.

1. The speed and load test showed that the 8-hole injectors gave the lowest exhaust and piston cooling losses, and highest cylinder head losses. The other geometries were similar, but the 6-hole injectors gave lower cylinder head losses at high load. At low load injectors with larger hole number gave higher indicated work. At high load the 6-hole injectors gave little soot and the highest NO_x emissions.
2. During the rail pressure sweep the 6- and 10-hole injectors gave highest exhaust and piston cooling losses. The 6-hole injectors had the lowest cylinder head losses. The 10-hole injectors had the longest combustion duration. The 6-hole injectors gave the highest NO_x levels and low soot. They also gave highest work at low rail pressure.
3. During the swirl sweep the 6-hole injectors gave the least exhaust and cylinder head losses, while the other geometries were similar. The 10-hole injectors had longest combustion duration, and the 8-hole injectors the shortest. Higher swirl levels significantly reduced soot with for the 10-hole injectors. Over all the 6-hole injectors gave higher soot levels.
4. The EGR sweep showed that the 8-hole injectors had the least exhaust losses, and highest cylinder head losses. The highest exhaust losses were found with the 10-hole injectors.The 6-hole injectors had the highest piston cooling losses. Injectors with 6-holes gave the fastest combustion, and with 10-holes the slowest. The 10-hole injectors gave the highest work.
5. At all λ levels the 8-hole injectors gave the lowest and the 10-hole injectors the highest exhaust losses. The 6-hole injectors had the highest piston cooling losses. The net indicated work increased with λ. The 6-hole injectors had the fastest combustion, and 10-hole injectors the slowest. The 6-hole injectors gave the highest NO_x levels, but both 6- and 10-hole injectors gave low soot emissions at higher λ levels.

The general observations were that injectors with less holes gave shorter combustion duration, higher piston cooling losses and less exhaust losses. Larger number of holes resulted in longer combustion duration and more exhaust losses, which can be used in waste heat recovery systems and help exhaust after treatment systems reach sufficient operating temperatures.

6. References

[1] T. Hejwowski, A. Weronski, The effect of thermal barrier coatings on diesel engine performance, Vacuum 65 (3-4) (2002) 427–432.

[2] M. Abedin, H. Masjuki, M. Kalam, A. Sanjid, S. Rahman, B. Masum, Energy balance of internal combustion engines using alternative fuels, Renewable and Sustainable Energy Reviews 26 (2013) 20–33.

[3] A. Uzun, I. Çevik, M. Akçil, Effects of thermal barrier coating on a turbocharged diesel engine performance, Surface and Coatings Technology 116-119 (1999) 505–507.

[4] I. Taymaz, The effect of thermal barrier coatings on diesel engine performance, Surface and Coatings Technology 201 (9-11 SPEC. ISS.) (2007) 5249–5252.

[5] S. Chan, K. Khor, Effect of thermal barrier coated piston crown on engine characteristics, Journal of Materials Engineering and Performance 9 (1) (2000) 103–109.

[6] A. Modi, D. Gosai, Experimental study on thermal barrier coated diesel engine performance with blends of diesel and palm biodiesel, SAE International Journal of Fuels and Lubricants 3 (2) (2010) 246–259.

[7] I. Sher, D. Levinzon-Sher, E. Sher, Miniaturization limitations of HCCI internal combustion engines, Applied Thermal Engineering 29 (2-3) (2009) 400–411.

[8] S. Kokjohn, R. Hanson, D. Splitter, J. Kaddatz, R. Reitz, Fuel reactivity controlled compression ignition (RCCI) combustion in light- and heavy-duty engines, SAE International Journal of Engines 4 (1) (2011) 360–374.

[9] F. Payri, X. Margot, A. Gil, J. Martin, Computational study of heat transfer to the walls of a DI diesel engine, SAE Technical Papers.

[10] O. Andersson, P. C. Miles, Diesel and Diesel LTC Combustion, John Wiley & Sons, Ltd, 2014. doi:10.1002/9781118354179.auto120.
URL http://dx.doi.org/10.1002/9781118354179.auto120

[11] G. Mavropoulos, C. Rakopoulos, D. Hountalas, Experimental investigation of instantaneous cyclic heat transfer in the combustion chamber and exhaust manifold of a DI diesel engine under transient operating conditions, SAE Technical Papers.

[12] A. Sharief, T. Chandrashekar, A. Antony, B. Samaga, Study on heat transfer correlation in IC engines, SAE Technical Papers.

[13] Y. Najjar, Protection of the environment by using innovative greening technologies in land transport, Renewable and Sustainable Energy Reviews 26 (2013) 480–491.

[14] J. Sun, J. Bittle, T. Jacobs, Influencing parameters of brake fuel conversion efficiency with diesel / gasoline operation in a medium-duty diesel engine, SAE Technical Papers 2.

[15] A. Kleemann, A. Gosman, Heat transfer sensitivity study for an advanced diesel engine, SAE Technical Papers.

[16] E. Gingrich, J. Ghandhi, R. Reitz, Experimental investigation of piston heat transfer in a light duty engine under conventional diesel, homogeneous charge compression ignition, and reactivity controlled compression ignition combustion regimes, SAE International Journal of Engines 7 (1) (2014) 375–386.

[17] M. Said, D. Buttsworth, T. Yusaf, A review of radiation heat transfer measurement for diesel engines using the two-colour method, 2009, pp. 202–207.

[18] J. Dolak, Y. Shi, R. Reitz, A computational investigation of stepped-bowl piston geometry for a light duty engine operating at low load, SAE Technical Papers.

[19] J. Styron, B. Baldwin, B. Fulton, D. Ives, S. Ramanathan, Ford 2011 6.7l power stroke®diesel engine combustion system development, SAE Technical Papers.

[20] H. Fridriksson, M. Tuner, O. Andersson, B. Sunden, H. Persson, M. Ljungqvist, Effect of piston bowl shape and swirl ratio on engine heat transfer in a light-duty diesel engine, SAE Technical Papers 1.

[21] J. Dahlström, O. Andersson, M. Tunér, H. Persson, Effects of spray-swirl interactions on heat losses in a light duty diesel engine, ASME Proceedings (2015) V08AT10A062doi:10.1115/IMECE2015-53606.
URL http://proceedings.asmedigitalcollection.asme.org/proceeding.aspx?articleid=2501068

[22] J. Dahlström, O. Andersson, M. Tunér, H. Persson, Experimental comparison of heat losses in stepped-bowl and re-entrant combustion chambers in a light duty diesel engine, SAE Technical Papersdoi:2016-01-0732.
URL http://papers.sae.org/2016-01-0732/

[23] S. Das, C. E. Roberts, Factors affecting heat transfer in a diesel engine: Low heat rejection engine revisitedDoi: 10.4271/2013-01-0875.

[24] C. Weingartz, C. Anderson, S. Miers, Determination of heat transfer augmentation due to fuel spray impingement in a high-speed diesel engine, SAE Technical Papersdoi:10.4271/2009-01-0843.

[25] H. Osada, N. Uchida, K. Shimada, Y. Aoyagi, Reexamination of multiple fuel injections for improving the thermal efficiency of a heavy-duty diesel engine, SAE Technical Papers 2.

[26] F. Perini, A. Dempsey, R. Reitz, D. Sahoo, et al., A computational investigation of the effects of swirl ratio and injection pressure on mixture preparation and wall heat transfer in a light-duty diesel engine, SAE Technical Papers.

[27] M. Kono, M. Basaki, M. Ito, T. Hashizume, S. Ishiyama, K. Inagaki, Cooling loss reduction of highly dispersed spray combustion with restricted in-cylinder swirl and squish flow in diesel engine, SAE Technical Papers.

[28] C. Eiglmeier, H. Lettmann, G. Stiesch, G. Merker, A detailed phenomenological model for wall heat transfer prediction in diesel engines, SAE Technical Papers.

[29] M. Fathi, R. Saray, M. Checkel, The influence of exhaust gas recirculation (egr) on combustion and emissions of n-heptane/natural gas fueled homogeneous charge compression ignition (HCCI) engines, Applied Energy 88 (12) (2011) 4719–4724.

[30] P. Miles, B. Rempelewert, R. Reitz, Squish- swirl and injection-swirl interaction in direct-injection diesel engines., ICE 2003: 6th International Conference on Engines for Automobiles.

[31] J. B. Heywood, Internal Combustion Engine Fundamentals, McGraw-Hill, Inc., 1988.

[32] G. Woschni, Determination of local heat transfer coefficients at the piston of a high speed diesel engine by evaluation of measured temperature distributionSAE paper 790834.